



People's Democratic Republic of Algeria  
Ministry of Higher Education and Scientific Research

University Med Khider Biskra

Faculty of Exact Sciences and Sciences of Nature and Life

Department of Matter Sciences



Thesis presented to obtain the degree of

**Doctorate**

Speciality: Physics of thin films

*Thesis entitled:*

*The effect of doping on the properties of thin films of Indium oxide  
( $In_2O_3$ ) deposited by ultrasonic spray for optoelectronic application.*

*Presented by :*

***Rahil AZIZI***

**The Jury :**

<b>M<sup>r</sup>. H. Ben Temam</b>	<b>Professor</b>	<b>University of Biskra</b>	<b>President</b>
<b>M<sup>r</sup>. A. Attaf</b>	<b>Professor</b>	<b>University of Biskra</b>	<b>Supervisor</b>
<b>M<sup>me</sup>. H. Saidi</b>	<b>Professor</b>	<b>University of Biskra</b>	<b>Co-supervisor</b>
<b>M<sup>r</sup>. A. Gueddim</b>	<b>Professor</b>	<b>University of Djelfa</b>	<b>Examiner</b>
<b>M<sup>me</sup>. M. Nouadji</b>	<b>MCA</b>	<b>University of Biskra</b>	<b>Examiner</b>

Academic Year: 2019/2020

# Table of contents

## ACKNOWLEDGEMENTS

### General introduction

### Reference

**The first part:** The general concepts on thin films, Ultrasonic spray elaboration and characterization techniques for indium oxide thin films

## CHAPTER I: GENERAL CONCEPTS ON THIN FILMS, INDIUM OXIDE AND THE DIFFERENT DEPOSITION TECHNIQUES

I.1 Introduction.....	1
I.2 Thin films:.....	1
I.2.1 Definition of a thin film:.....	1
I.2.2 Steps of the formation and growth of thin film.....	2
I.2.3 Classification of growth patterns.....	4
I.2.4 Applications of thin layers.....	6
I.3 Transparent Conductive Oxides (TCO).....	7
I.4 Presentation of the TCO studied [Indium Oxide ( $\text{In}_2\text{O}_3$ )].....	9
I.4.1 Properties of indium oxide ( $\text{In}_2\text{O}_3$ ):.....	9
I.4.1.1 Crystallographic properties.....	9
I.4.1.2 Optical properties:.....	11
I.4.1.3 Electrical properties :.....	11
I.4.2 Applications of indium oxide.....	12
I.5 Some methods of depositing thin films:.....	13
I.5.1 Physical vapor deposition (PVD).....	14
I.5.2 Chemical vapor deposition (CVD) .....	14
I.6 Ultrasonic pyrolysis spray.....	16
I.6.1 The pyrolysis spray.....	16
I.6.1.1 Deposit solution (source).....	17

I.6.1 .2 Generation of droplets (transport).....	18
I.6.1 .3 Chemical reaction on the substrate (deposit).....	18
Reference.....	19

## **CHAPTER II: ULTRASONIC SPRAY ELABORATION AND CHARACTERIZATION TECHNIQUES FOR INDIUM OXIDE FILMS**

II.1 Introduction:.....	22
II.2 Elaboration of thin layers of In <sub>2</sub> O <sub>3</sub> by ultrasonic spray: .....	22
II.2.1 Experimental montage used: .....	22
II.2.2.Experimental procedure: .....	25
II.2.2.1 Experimental conditions: .....	25
II.2.2.2 Choice of the deposit substrate:.....	26
II.2.2.3 Cleaning of substrates:.....	27
II.2.2.4 Adhesion Test.....	27
II.2.2.5 Film thickness .....	28
II.3 Characterization Techniques:.....	28
II.3.1 Structural characterization methods:.....	28
II.3.1.1. X-ray diffraction:.....	28
II.3.1.2 Scanning electron microscopy (SEM):.....	32
II.3.2 Optical characterization method:.....	35
II.3.2.1 UV-Visible spectroscopy:.....	35
II.3.2.2 Photoluminescence spectroscopy.....	39
II.3.3 Infrared Spectroscopy:.....	40
II.3.3 Electrical characterization:.....	42
Reference.....	44

**The second part:** The results and discussion

## **CHAPTER III: GROWTH RATE INFLUENCE ON INDIUM**

### **OXIDE THIN FILMS**

III.1 Introduction:.....	46
III.2. Growth rate:.....	46

III .3 Structural properties:.....	47
III.4 Surface morphology:.....	52
III.5. Optical properties.....	54
III.6. Electrical properties.....	58
III.7 . Conclusions:.....	59
References.....	60

## **CHAPTER IV: INFLUENCE OF INDIUM ACETATE ON PROPERTIES OF INDIUM OXIDE THIN FILMS**

IV .1 Introduction:.....	63
IV.2. Growth rate:.....	63
IV .3 XRD Analysis :.....	64
IV.4 UV-VIS transmittance Analysis:.....	67
IV.5. Reflectance Analysis :.....	70
IV.6. FTIR Analysis:.....	72
IV.7 Electrical study:.....	73
IV.8.Conclusion:.....	75
References.....	76

## **CHAPTER V: INFLUENCE OF THE SUBSTRATES ON PROPERTIES OF INDIUM OXIDE THIN FILMS**

V.1 Introduction:.....	81
V.2 Growth rate:.....	81
V .3 Structural properties:.....	83
V .4 Optical properties:.....	88
V .5 Electrical properties:.....	90
V .6 Conclusion:.....	90
Reference.....	92

## **CHAPTER VI: EFFECT OF DOPING (Sb and Mo) ON PROPERTIES OF INDIUM OXIDE THIN FILMS**

VI .1 Introduction: .....	94
VI.2. Antimony doping (Sb).....	95

VI .2.1 Structural properties :	95
VI .2.2 Surface morphology	98
VI .2.3 Optical properties:	100
VI .2.4 FTIR Analysis :	103
VI .2.5 Photoluminescence properties:	104
VI .2.6 Electrical properties:	106
VI. 3. Molybdenum doping (Mo)	105
VI .3.1 Structural properties:	105
VI .3.2 Surface morphology:	110
VI .3.3 Transmittance Analysis:	112
VI .3.4 The resistivity	114
VI .4 Conclusion:	115
References	<b>Err</b>
	<b>eur ! Signet non défini.</b>

General conclusion

# List of Figures

## CHAPTER I

Figure.I.1 : Diagram of the steps of the thin film manufacturing process.....	2
Figure.I.2 Nucleation , coalescence and growth of thin films .....	4
Figure.I.3 : The three growth models of a thin layer .....	5
Figure.I.4 : Some applications of TCO .....	8
Figure.I.5: Crystallographic structure , Cubic bixbyite structure (1/16 of the units) .....	10
Figure.I.6 : Principle scheme of chemical vapor deposition (hot wall furnace).....	15

## CHAPTER II

Figure II.1: The complete device of the Ultrasonic Spray technique from the University of Biskra.....	23
Figure II.2: Cut glass substrates using a sharp pen.....	27
Figure II.3: Principle of two-circle diffraction .....	29
Figure II.4: Bragg's law giving the directions where the interferences are construction.....	29
Figure II.5: Illustration showing the definition of grain size from the X-ray diffraction curve .....	31
Figure II.6: Schematic of the electron optics constituting the SEM .....	33
Figure II.7 Scattering pear .....	34
Figure II.8: Direct measurement of the thickness of the $\text{In}_2\text{O}_3$ layer from the image obtained by SEM.....	34
Figure II.9: Schematic representation of the UV-Visible spectrophotometer.....	36
Figure II. 10 : Determination of the optical gap according to the Tauc method for a thin layer of $\text{In}_2\text{O}_3$ .....	37
Figure II.11: Function of distribution of the energy states in the bands.....	37
Figure II.12: Determination of Urbach energy .....	38
Figure II. 13: Schematic of PL from the standpoint of semiconductor or crystalline systems and molecular systems.....	39
Figure II. 14: Diagram of a Fourier Transform Spectrometer.....	41
Figure II. 15: Interferogram at the output of the detector and example of infrared spectrum of an one of the films .....	42

Figure II.16: Four-point method .....	43
---------------------------------------	----

## CHAPTER III

Figure III. 1. Growth rate as a function of solution flow rate and inset shows the film thickness dependence on solution flow rate.....	47
Figure III. 2 XRD pattern of In <sub>2</sub> O <sub>3</sub> thin films deposited with different growth rates.....	49
Figure III. 3 The Influence of the solution flow rate on the film growth rate.....	50
Figure III. 4. Microstraine as a function of growth rate.....	51
Figure III. 5. SEM surface images of the In <sub>2</sub> O <sub>3</sub> thin films deposited at various growth rate...53	
Figure III. 6 SEM micrographs of the cross section of In <sub>2</sub> O <sub>3</sub> as a function growth rate (a) 1.728 nm/s ,(b) 2.801 nm/s.....	53
Figure III. 7. EDS analysis of the In <sub>2</sub> O <sub>3</sub> thin film deposited at 2.554 nm/s.....	54
Figure.III .8. Optical transmittance spectra of In <sub>2</sub> O <sub>3</sub> thin films as a function of growth rate...54	
Figure III.9. Typical variation of the quantity $(\alpha hv)^2$ as a function of photon energy, inset shows optical band gap energy with various growth rates.....	56
Figure III .10. Variations of the optical band gap and disorder in thin films as a function of the growth rate. Inset figure is a schematic drawn of energy band diagram.....	57
Figure III. 11. Electrical resistivity of In <sub>2</sub> O <sub>3</sub> thin film with various growth rates.....	58

## CHAPTER IV

Figure IV. 1. Variation of growth rate as a function of solution concentration and inset shows film thickness dependence on solution concentration.....	64
Figure IV 2. XRD pattern of In <sub>2</sub> O <sub>3</sub> thin films deposited with different molar concentration .....	65
Figure IV. 3. The variations of the crystallite size, the microstrain and dislocation density in the films as a function of molar concentration.....	66
Figure IV.4. Optical transmittance spectra of In <sub>2</sub> O <sub>3</sub> thin films as a function of molar concentration.....	68
Figure IV.5. Typical variation of the quantity $(\alpha hv)^2$ as a function of photon energy with various solution concentration .....	69
Figure IV. 6. Variation of the optical band gap and disorder in thin film as a function of solution concentration .....	70
Figure IV.7 variation of refractive index (n) as a function of the wavelength with various solution concentration.....	71
Figure IV.8. Variation of extinction coefficient (K) as a function of the wavelength with various solution concentration.....	72
Figure IV.9. Fourier transform infrared (FTIR) spectrum of In <sub>2</sub> O <sub>3</sub> films with various solution concentration.....	73

Figure IV. 10 The electrical resistivity and the conductivity as a function of the concentration of solution.....	74
---	----

## CHAPTER V

Figure V.1: The growth rate of $\text{In}_2\text{O}_3$ films on different substrates.....	83
Figure V.2: Anatase nuclei $\text{TiO}_2$ formed on Si (left) and glass (right) substrates .....	83
Figure V.3 : XRD pattern of $\text{In}_2\text{O}_3$ thin films deposited on a different substrates.....	85
Figure V.4 : The preferential orientation (222) and (400) of growth with various substrates type .....	86
Figure V.5: The crystallite size of the $\text{In}_2\text{O}_3$ thin films deposited on various substrates.....	87
Figure V.6: Optical transmittance spectra of $\text{In}_2\text{O}_3$ thin films as a function of different substrates .....	89
Figure V.7: different substrates the variation of gap energy.....	89

## CHAPTER VI

Figure VI. 1: XRD pattern of pure $\text{In}_2\text{O}_3$ and $\text{Sb-In}_2\text{O}_3$ with various Sb concentration (2,4,6 and 8 wt.% ).....	96
Figure VI. 2: The crystallite sizes of the two strongest peaks (2 2 2) and (4 0 0) of pure $\text{In}_2\text{O}_3$ and $\text{Sb-In}_2\text{O}_3$ .....	97
Figure VI.3: The micrograph of SEM $\text{Sb-In}_2\text{O}_3$ films (A: un-doped /B: 2 Wt% Sb / C: 4 Wt% Sb / D : 6 Wt% Sb / E: 8 Wt% Sb ).....	98
Figure VI. 4 The EDS spectra of $\text{Sb-In}_2\text{O}_3$ films (2 wt% Sb).....	99
Figure VI.5 :Optical transmittance and reflectance spectra of undoped and antimony doped indium oxide films.....	100
Figure VI.6: The band gap as function of Sb dopant concentration .....	102
Figure VI.7 :The Fourier transform infrared (FTIR) spectrum of undoped and antimony doped indium oxide films deposited on glass substrate.....	103
Figure VI.8 :Photoluminescence spectra of undoped and antimony doped indium oxide films deposited on glass substrate.....	105
Figure VI. 9: XRD pattern of pure $\text{In}_2\text{O}_3$ and $\text{Mo-In}_2\text{O}_3$ with various Mo concentration (1,2,3 and 4wt.% ).....	108
Figure VI. 10: The crystallite sizes and microstrain of un-doped $\text{In}_2\text{O}_3$ and $\text{Mo-In}_2\text{O}_3$ .....	109
Figure VI.11: The micrograph of SEM of $\text{Mo-In}_2\text{O}_3$ .....	110
Figure VI.12 : The micrograph of SEM $\text{Mo-In}_2\text{O}_3$ films (1 Wt% Mo ).....	111
Figure VI.13 : EDS spectra of $\text{Mo-In}_2\text{O}_3$ films .....	112
Figure VI.14 :Optical transmittance and reflectance spectra of undoped and antimony doped indium oxide films.....	113

# List of Tables

## CHAPTER I

Table I.1: shows the number and positions of the 80 atoms forming the elemental cell of indium oxide.....	10
Table I.2: Shows general methods for depositing a thin films.....	13

## CHAPTER II

Table II.1: Elements of the assembly.....	24
---	----

## CHAPTER III

Table III. 1. Grain size, lattice parameter, optical band gap and disorder energy of $\text{In}_2\text{O}_3$ thin films as a function of the growth rate.....	52
---	----

## CHAPTER V

Table V.1: Electrical properties of layers in different substrates. ....	90
--	----

## CHAPTER VI

Table VI. 1: The lattice parameters, the electrical resistivity ( $\rho$ ), Hall mobility ( $\mu$ ) and carrier concentration ( $n$ ) of un-doped and Sb-doped $\text{In}_2\text{O}_3$ .....	95
Table VI. 2 The structural parameters of $\text{In}_2\text{O}_3$ :Mo films .....	109
Table VI. 3: The electrical and optical parameters values $\text{In}_2\text{O}_3$ thin films doped with various Mo concentration.....	114

## *Dedication*

*I dedicate this thesis to:*

*My dear parents :*

*My father (Noureddine)*

*My mother (Salima)*

*My dear husband and his parents*

*My lovely daughter (Alaa Al -Rahmane)*

*My dear sisters (Wissel - Oumniya)*

*My dear brothers (Maroune -Moncef)*

*All my big family members*

*All my dear friends*

**RAHIL**

# Acknowledgements

First, I thank **Allah** Almighty for giving me the will and courage to do my job and achieve my goal. I also express my deep gratitude to my parents and my husband for their encouragement, support and sacrifices.

A big thank you to the supervisor **M<sup>r</sup>. A. ATTAF**, Professor at the University of Biskra, for his acceptance to take charge of my work and for the time spent in this work, I really thank him for his permanent support and the trust he has granted for me. Also, I thank to the Co-supervisor **M<sup>me</sup>. H. SAIDI**, Professor at University of Biskra.

It is also very pleasant to thank **M<sup>r</sup>. H. BENTAMAM** Professor at University of Biskra, who will be the head of chairing the jury of thesis.

I express my sincere thanks to **M<sup>r</sup>. A. GUEDDIM** Professor at University of Djelfa, for honoring me for being an examiner of this work.

My most grateful thanks to **M<sup>me</sup>. M. NOUADJI**, MCA at University of Biskra, who kindly agreed to be part of the jury and review my work.

Our thanks also go to all the teachers of the physics department.

I would like to thank very much :

- **M<sup>me</sup>. L. AZIZI**, teacher of English
- My colleagues: **Adel .B**, **Sihem .L**, **Youcef .B**, **Hamza.B**, **Meriem .Ch**.
- All my friends who have helped me from far or near to realize this work.

Finally, I would like to thank all people who collaborated to characterize samples.

# General Introduction

## General Introduction

Depending on the excellent optical and electrical properties for metal oxide semiconductor thin films and numerous studies have been conducted on them. The unique class of materials that depends on the metal oxides is Transparent Conducting Oxides (TCOs) which has both optical transparency and electrical conductivity . Among the most used TCO materials, indium oxide ( $\text{In}_2\text{O}_3$ ) is a versatile material with various wide applications and technologically important TCO material of n-type semiconductor [1]. It has a wide band gap with a direct band gap around 3.5 - 3.8 eV [2] and an indirect band gap of about 2.6 eV [3]. It is cubic with the lattice constant of  $a = 10.117 \text{ \AA}$  and space group (  $Ia\bar{3}$  ) [4]. High electrical conductivity and transparency to visible light is considerably used for photovoltaic devices, transparent windows, liquid crystal displays (LCD), solar cell, light emitting diode (LED), gas sensors and anti- reflecting coatings [5].

Most of undoped and doped  $\text{In}_2\text{O}_3$  thin films are prepared by variety of physical and chemical methods such as: spray pyrolysis [6], vacuum evaporation [7], magnetron sputtering [8], dc- sputtering [9], sol gel [10], electron beam evaporation [11], reactive thermal evaporation [12] and pulsed laser ablation [13]. Among these deposition methods, spray pyrolysis is a preferred technique. It is versatile to fabricate thin films , not expensive, commercially viable, easy and simple to manipulate and applicable to large area. Moreover, the variety of the precursor solutions to prepare the  $\text{In}_2\text{O}_3$  thin films; the initial materials used are usually  $\text{InCl}_3$  [14,15], sometimes  $\text{InNO}_3$  [16,17] and rarely indium acetylacetonate (In-acac) [18].

The main aim of this work is to obtain undoped and doped indium oxide films with suitable properties for optoelectronic application which can be used as transparent conductive oxide (TCO) thin films to reduce the losses during photovoltaic conversion ,through studying the effect of many parameters as it followed by evolution of the structural, optical and electrical properties of  $\text{In}_2\text{O}_3$  films has been investigated.

The thesis is organized as following:

**The first part embraces two chapters (I and II): In Chapter I,** we will present general concepts on thin films, indium oxide and the different deposition techniques. **In Chapter II** , we will present ultrasonic spray elaboration and characterization techniques for indium oxide thin films .

**The second part consists four chapters (III, IV ,V , VI ): In chapters III ,IV and V** we will present the results and discussion on the ultrasonically deposited **undoped indium oxide thin films** with the effect of many parameters as following :

- **Chapter III** : Influence growth rate (by changing the solution flow rate )
- **Chapter IV** : Influence of indium acetate (various molar concentration)
- **Chapter V** : Influence of substrates type.

**But In chapter VI:** we will present the results and discussion on the ultrasonically deposited **doped indium oxide thin films** with various concentration of antimony (Sb) and molybdenum (Mo) .

At last, We will end this manuscript with a **general conclusion** about the work which has been done and we will give some perspectives on the continuity of the research work.

## Reference

- [1] T. Koida, H. Fujiwara, M. Kondo, High-mobility hydrogen-doped  $\text{In}_2\text{O}_3$  transparent conductive oxide for a-Si: H/c-Si heterojunction solar cells, *Solar Energy Materials and Solar Cells*. Vol. 93, (2009) 851–854
- [2] A. Walsh, J. L. Da Silva, S. H. Wei, C. Körber, A. Klein, L. F. J. Piper, ... & D. J. Payne, Nature of the Band Gap of  $\text{In}_2\text{O}_3$  Revealed by First-Principles Calculations and X-Ray Spectroscopy, *Physical Review Letters*. Vol.100, (2008) 167402
- [3] A. Raza, O.P. Agnihotri, B. K. Gupta, Preparation and intrinsic absorption in the band edge in chemically sprayed  $\text{In}_2\text{O}_3$  layers., *Journal of Physics D: Applied Physics*. Vol.10, (1977)1871.
- [4] M. Morezio, Refinement of the crystal structure of  $\text{In}_2\text{O}_3$  at two wavelengths ., *Acta Crystallographica*. Vol. 20, (1966) 723
- [5] M. Girtan, H. Cachet, G. I. Rusua, On the physical properties of indium oxide thin films deposited by pyrosol in comparison with films deposited by pneumatic spray pyrolysis, *Thin Solid Films*. Vol. 427, (2003) 406-410.
- [6] J.C. Manificier; L. Szepessy, J.F. Bresse, M. Peroten, R. Stuck,  $\text{In}_2\text{O}_3:(\text{Sn})$  and  $\text{SnO}_2:(\text{F})$  films — Application to solar energy conversion; part 1 — Preparation and characterization,, *Mater. Res. Bull.* Vol. 14, (1979)109-119
- [7] K.R. Murali, V. Sambasivam, M. Jayachandran, M.J. Chockalingam, N. Rangarajan, V.K. Venkatesan, Characterization of indium tin oxide films . *Surf. Coat. Technol.* Vol.35, (1988)297
- [8] W.G. Haines, R.H. Bube, Effects of heat treatment on the optical and electrical properties of indium–tin oxide films, *J. Appl. Phys.* Vol.49, (1978) 304
- [9] Z. Qiao, R. Latz, D. Mergela, Thickness dependence of  $\text{In}_2\text{O}_3:\text{Sn}$  film growth *Thin Solid Films*. Vol. 466, (2004) 250
- [10] M.A.F. Mendoza, C.R. Perez, G.T. Delgado, J.M. Marín, O.Z. Angel, Influence of the annealing temperature on the properties of undoped indium oxide thin films obtained by the sol–gel method, *Thin Solid Films*. Vol. 517, (2008) 681

- [11] S.M.Rozati, S.Mirzapour, M.G.Takwale, B.R.Marathe,V.G.Bhide, Influence of annealing on evaporated indium oxide thin films., Mater. Chem. Phy. Vol. 36, (1994) 252
- [12] Chia-PuChu, Tsung-ShineKo, Yu-Cheng Chang,Tien-ChangLu, Hao-Chung Kuo, Shing Chung Wang, Thermally evaporated  $\text{In}_2\text{O}_3$  nanoloquats with oxygen flow-dependent optical emissions Mater. Sci. Eng. B. Vol. 147, (2008) 276
- [13] V. Marotta, S. Orlando, G.P. Parisi, A. Giardini, G. Perna, A.M. Santoro, V. Capozzi, Electrical and optical characterization of multilayered thin film based on pulsed laser deposition of metal oxides., Appl. Surf. Sci. Vol.168, (2000) 141–145
- [14] P.K. Manoj, K.G. Gopachandran, P. Koshy, V.K. Vaidyan, B. Joseph, Growth and characterization of indium oxide thin films prepared by spray pyrolysis, Opt. Mater. 28 (2006) 1405–1411
- [15] G. Korotcenkov, A. Cerneavski , V. Brinzari , A. Vasiliev , M. Ivanov , A. Cornet , J. Morante , A. Cabot , J. Arbiol ,  $\text{In}_2\text{O}_3$  films deposited by spray pyrolysis as a material for ozone gas sensors, Sensors and Actuators B. 99 (2004) 297–303
- [ 16] B.-C. Kim, J.-Y. Kim, D.-D. Lee, J.-O. Lim, J.-S. Huh, Effect of crystal structures on gas sensing properties of nanocrystalline ITO thick films, Sens. Actuators B . 89 (2003) 180–186.
- [17] J.-H. Lee, B.-O. Park, Transparent conducting  $\text{In}_2\text{O}_3$  thin films prepared by ultrasonic spray pyrolysis, Surf. Coat. Technol. 184 (2004) 102–107
- [18] M. Jothibas , C. Manoharan , S. Ramalingam , S. Dhanapandian , S. Johnson Jeyakumar , M. Bououdina , Preparation, characterization, spectroscopic (FT-IR, FT-Raman, UV and visible) studies, optical properties and Kubo gap analysis of  $\text{In}_2\text{O}_3$  thin films, Journal of Molecular Structure .1049 (2013) 239–249.

# **The first part:**

The general concepts on thin films , Ultrasonic spray elaboration and characterization techniques for indium oxide thin films

## **CHAPTER I:**

# **GENERAL CONCEPTS ON THIN FILMS, INDIUM OXIDE AND THE DIFFERENT DEPOSITION TECHNIQUES**

## **I.1 Introduction:**

Technologies based on the exploitation of the specific properties of films, called thin films, developed strongly at the end of the 20<sup>th</sup> century and became one of the most important paths. That's why we will focus on it in this chapter. We will present simple definitions of thin films and their applications, then we will mention the main properties of transparent conductive oxides (TCO) and in particular those of indium oxide ( $\text{In}_2\text{O}_3$ ), we will also note different depositions techniques which are used to grow  $\text{In}_2\text{O}_3$  films.

## **I.2 Thin films:**

### **I.2.1 Definition of a thin film:**

As a principle, the thin film of specific material is an element of this material with reduced dimensions called thickness, it is expressed in Angstrom, and this small distance between the two boundary surfaces (this quasi two- dimensional) cause a disruption of the majority of the physical properties [1]. The essential difference between the material in the massive state and the one in thin layers is that; in the massive state the role of the limits in the properties is usually neglected, whereas in a thin layer the effects are related to the predominant surface areas. It is quite obvious that the thinner of the thickness, will be the more on this two-dimensional effect that will be important. However, when the thickness will exceed a certain threshold; its effect will become minimal and the material will recover the well-known properties of the solid material [2]. The second essential characteristic of thin film is whatever the procedure used for its manufacture, the thin film is always integral with a substrate. Consequently, it will be imperative to take into account this major fact in the design, namely that the support has a very strong influence on the structural properties of the layer. Thus a thin layer of the same material, of the same thickness may have substantially different physical properties depending on whether it will be deposited on an amorphous insulating substrate such as glass, or a monocrystalline silicon substrate, for example. Consequently, the thin film is anisotropic by construction [3].

In practice, we can distinguish two main families of methods, where using of the carrier gas to move the material to the substrate and which are similar to the diffusion techniques used in the manufacture of active components, and those that involve in the reduced pressure environment whereas the material deposited by an initial pulse of thermal or mechanical nature [4].

### 1.2.2 Steps of the formation and the growth of thin film

It is distinguished by three steps :

- Synthesis or creation of the deposit species.
- Transport of these species to the substrate.
- Deposition on the substrate and growth of the layer.

The first two steps define the technique of depositions , the third involves the phenomena of generation and growth of the layer [5]. In addition to the last stage after the process of forming the thin layers called analysis which are illustrated this deposition processes in the following **Figure.I.1**:

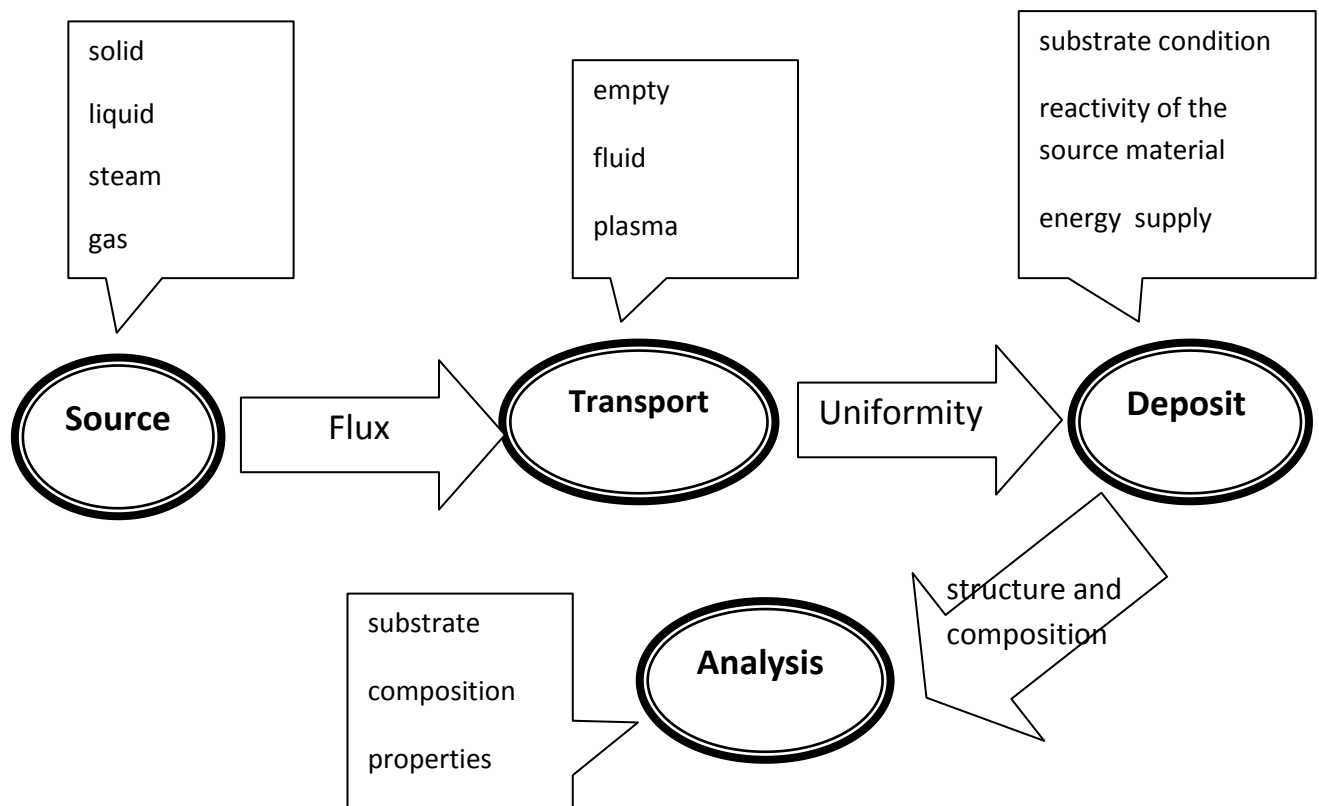


**Figure.I.1 :** Diagram of the steps of the thin film manufacturing process

The formation of thin film is achieved by a combination of nucleation and growth processes, described as follows [6]:

- The species, at the moment of the impact on the substrate, lose their displacement velocity component which are physically absorbed on the surface of the substrate
- Initially, the species absorbed are not in thermal equilibrium with the substrate, and therefore it moves on its surface. During these trips, they will interact with each other; creating clusters that will grow.
- These clusters, which are called islands or nuclei, are thermodynamically unstable and naturally tend to desorb. However, if the deposition parameters are such that the islands collide with each other, it develops dimensionally. When they reach a certain size, the Islets become thermodynamically stable. It is said that the nucleation threshold has been crossed. This step, which discuss the formation of stable islands, chemisorbed, and sufficient size, is called nucleation.
- The Islets continue to grow in number and size until a nucleation density, which called saturation, is reached. The nucleation density and the average size of the Islets depend on several parameters such as the energy of the incident species, their quantity per unit of time and surface, the energies of activation, absorption, desorption, thermal diffusion, the temperature, the topology and the chemical nature of the substrate. An island can grow parallel to the surface of the substrate by superficial diffusion of the absorbed or perpendicular spaces by direct impact of the incident species on the islands. In general, the lateral growth rate is much greater than the perpendicular growth rate.
- The next step in the process of forming the thin layer is called coalescence. The islands begin to agglomerate with one another by reducing the surface of the uncoated substrate. Coalescence can be accelerated by increasing the surface mobility of the adsorbed species, for example by increasing the temperature of the substrate. During this step, we can observe the formation of new islands on the surfaces liberated by the older island approximation.
- Islets become islands that continue to grow, leaving only holes or channels of small dimensions between them. The structure of the layer changes from the discontinuous

type to the porous type. Gradually, a continuous layer will be formed when the holes and channels fill up.

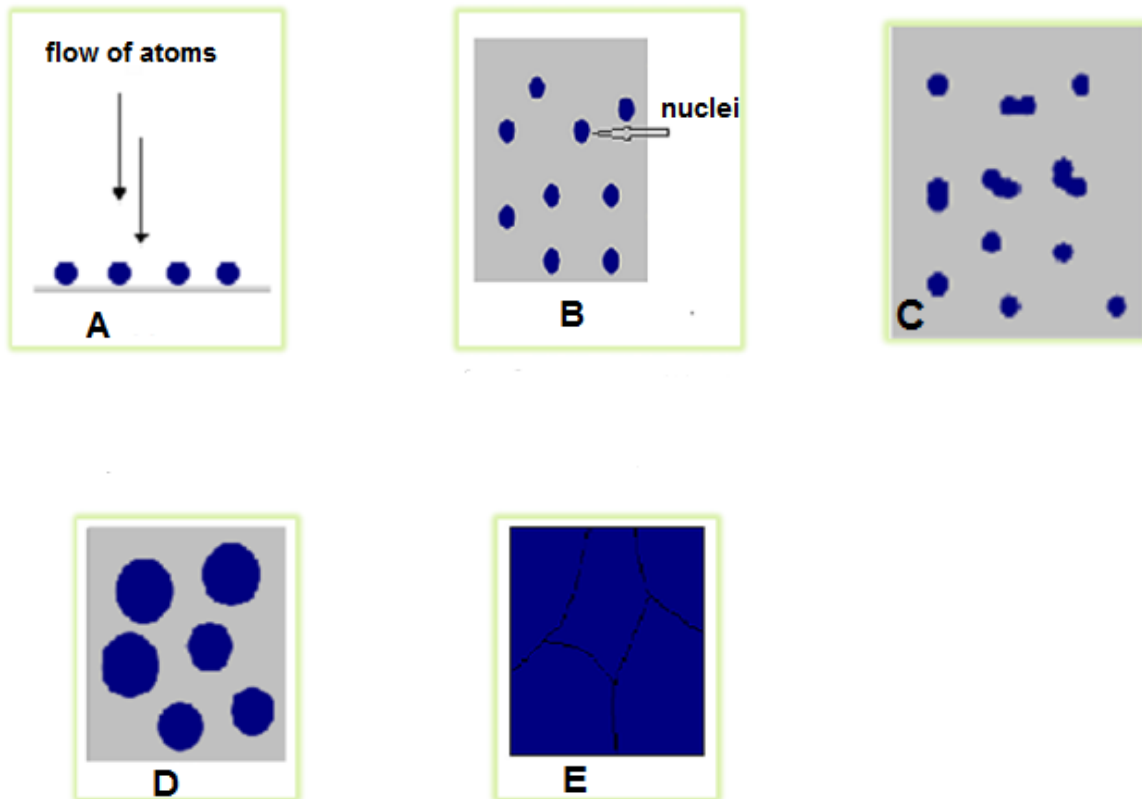


**Figure.I.2** Nucleation , coalescence and growth of thin films [7] : (A): the arrival of atoms on a substrate, (B): the morphology of the substrate, (C) : the coalescence, (D): step after coalescence, (E): growth .

### I.2.3 Classification of the growth patterns :

According to the thermodynamic parameters of the deposition and the substrate surface, the nucleation and island growth steps can be described as the following types :

#### a) Islands type (called Volmer-Weber)

In this growth mode (3D or multilayer), small clusters nucleate directly on the surface of the substrate and grow in islets on it [5]. (figure I.3.A)

**b) Layer type (called Frank-van der Merwe)**

This mode of growth occurs when the adatom-substrate interaction is very strong (2D or layer by layer), which induces the condensation of the species, then the formation of a monolayer [8]. (Figure I.3.B)

**c) Mixed type (called Stranski-Krastanov)**

This mode of growth is an intermediate case between the two preceding types [8]. (Figure I.3.C).

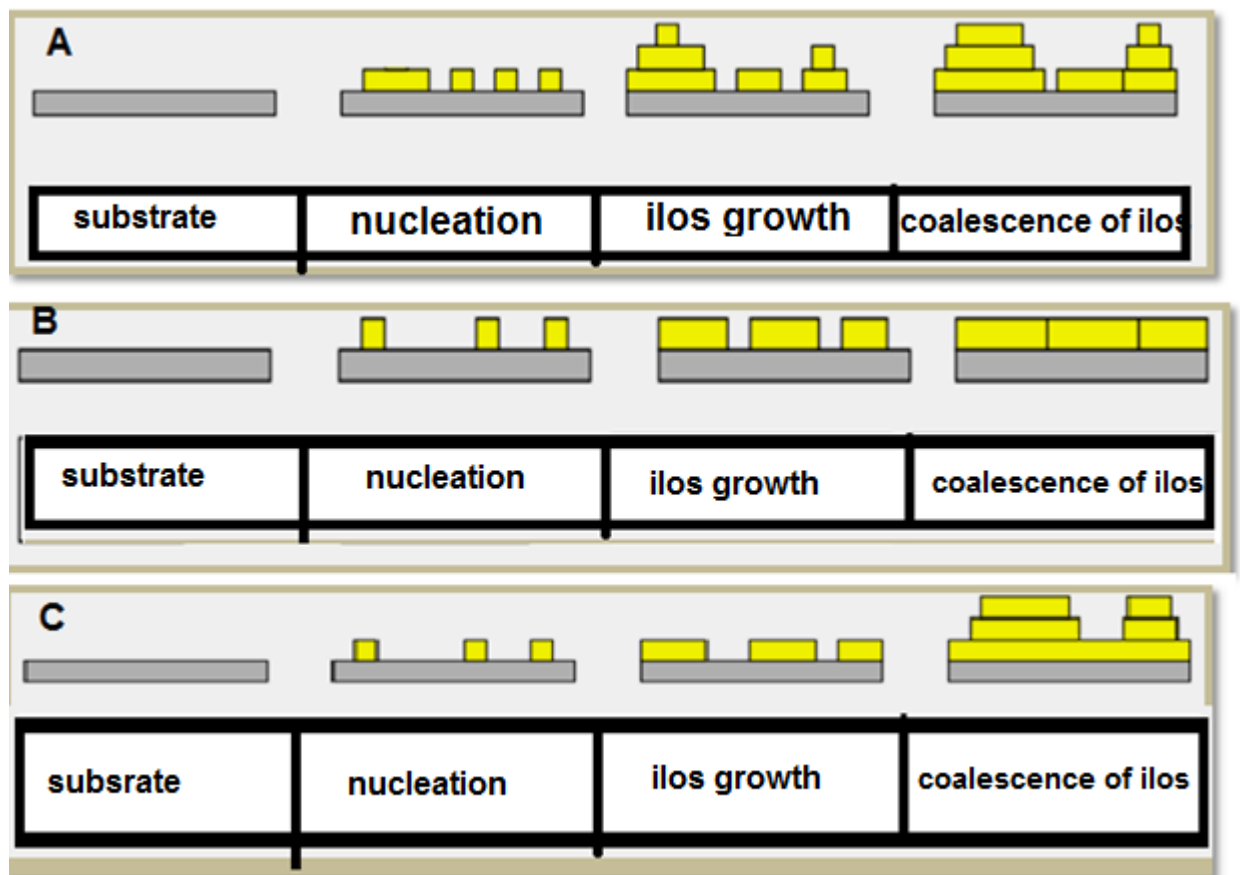


**Figure.I.3** : The three growth models of a thin layer [9].

A) Multilayer growth mode, or Volmer-Weber

B) Mode of growth layer by layer, or Franck-Van den Merwe ; C) Growth mode Stranski-Krastanov

### 1.2.4 Applications of thin layers:

Thin films are a technology of the future for many fields especially in micro and nanoelectronics . Their advantages are among others, a cost of manufacture few and deposit possibilities on different types of substrate (rigid, flexible ...) [10]. During the twentieth century, more advanced applications have diversified in the following areas [9]:

**Microelectronics:** these was developed in the 1960s ; thanks to the implementation of thin conductive or insulating layers increasingly which can be found under passivative layer types (electronic contact), PN junction, diode, transistor , piezoelectric material, LED lamp, superconductor,

**Optics:** while maintaining aesthetic applications, the optical applications of the layers have made it possible to develop more efficient radiation sensors, such as anti-reflection layers in solar cells, mirror tain, anti-reflection treatment of camera lenses , photodetection, flat panel displays, ophthalmic applications, optical guides (energy controls - architecture, vehicles, energy conversion ...)

**Mechanical:** tribological coatings (dry lubrication, resistance to wear, erosion, abrasion, diffusion barriers) ...

**Chemistry:** the main applications of surface coatings are oriented toward a better resistance to corrosion by the creation of a waterproof film (resistance to corrosion), gas sensor, catalytic coatings, protective layers.

**Thermal:** the use of a thermal barrier layer decreases the surface temperature of the metal of the reactors fins. Thus, making it possible to improve the performance of the reactors (increase of the internal temperature).

**Biology:** such as micro biological sensors, biochips, biocompatible materials ..

**Micro and nanotechnologies:** mechanical and chemical sensors, micro fluidics, actuators, detectors, adaptive optics, nano photonics ...

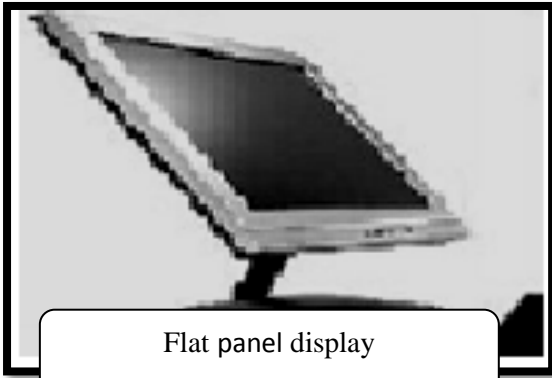
**Magnetic:** such as information storage (computer memory), security devices sensors.

**Decoration:** such as watches, glasses, jewelery, home furnishings.

### **I.3 Transparent Conductive Oxides (TCO):**

Transparent and conductive oxides are promising materials. Since the discovery at the beginning of the century of the double property of electrical conductivity and transparency in the visible domain. Historically, the first coexistence of electrical conductivity and optical transparency in the visible was observed in 1957 on thin films of CdO cadmium oxides. From the industrial point of view, tin-doped indium oxide (ITO) is the most widely used material. According to NanoMarkets, the ITO with its flaws and shortcomings will continue to dominate the transparent and conductive oxide industry in the near future [11]. An excellent TCO is defined by high electrical conductivity combined with low visible absorption. In general, these two characteristics are related to the thickness of the deposited layer. For example, they depend on the size of the grains, which usually increases with the thickness of the film. The most known TCOs are the oxides of indium, cadmium, tin, zinc and gallium. Commonly the oxides are doped with a metal. However, this metallic dopant is active only when it replaces the primary metal. The conduction band is then strongly disturbed by each doping atom, the diffusion of the conduction electrons is then increased, and the mobility and consequently the conduction falls. This is why some oxides are doped with fluorine when it is substituted for oxygen, causes a disturbance of the valence band, which minimizes the diffusion of conduction electrons [12]. The properties of TCOs in particular highlighted above allow to consider their use in many applications. Such as : windows at a low radiative heat loss [13,14 ], flat panel displays [13].

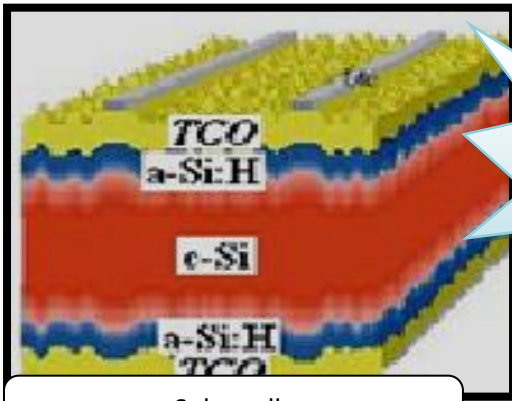
In the following **Figure.I.4**, we will present the main applications of TCO materials :



Flat panel display



Organic diodes OLED

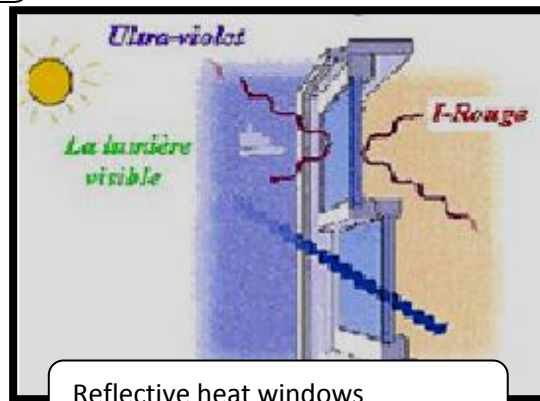


Solar cells

Some applications of TCO



Smart windows



Reflective heat windows

**Figure.I.4:** Some applications of TCO [5].

## I.4 Presentation of the TCO studied [Indium Oxide ( $\text{In}_2\text{O}_3$ )]:

Due to its distinctive optical, chemical, and electronic properties, indium oxide is gaining the increasing attention in applications ranging from optoelectronic devices to chemical probes. Its chemical probes can detect several toxic and non-toxic gases such as:  $\text{O}_3$ ,  $\text{CO}$ ,  $\text{H}_2$ ,  $\text{NH}_3$ ,  $\text{NO}_2$ , and  $\text{Cl}_2$  [5, 15]. Indium oxide ( $\text{In}_2\text{O}_3$ ) is an important n-type semiconductor with a wide direct band gap of 3.5-3.8 eV [16]. It has interesting properties such as high transparency to visible light [17], excellent substrate adhesion [18], good chemical stability [19], high electrical conductivity [20], hardness and chemical inertia and the strong interaction between some toxic gas molecules and its surfaces. These properties make it an attractive material for a variety of applications, including solar cells, panel displays, organic light emitting diodes, photocatalysts, architectural glasses. Moreover,  $\text{In}_2\text{O}_3$  is an important material for semiconductor gas sensors [21].

### I.4.1 Properties of indium oxide ( $\text{In}_2\text{O}_3$ ):

#### I.4.1.1 Crystallographic properties:

The solid indium oxide ( $\text{In}_2\text{O}_3$ ) (crystalline solid) is yellow color and has a melting point on 1913 ° C. The density of  $\text{In}_2\text{O}_3$  is 7.12 g / cm<sup>3</sup> can crystallize in two different structures as a cubic centered and hexagonal body [21]:

a) **Centered cubic structure:** It is an identical structure to that of the bixbyite  $\text{Mn}_2\text{O}_3$  (called C-type rare earth oxide structure) whose mesh contains 80 atoms, or 16 formula units. The space group is  $Ia_3$  and the mesh parameter is  $a = 1.012$  nm. Among the 32 In atoms, 1/4 of the In atoms (In1) occupy the centers of the trigonally distorted octahedra (8b position) and 3/4 of In atoms (In2) occupy the centers of tetragonally distorted octahedra ( 24d position) that ensure a good packing ratio [22 ]. The ratio  $\text{In1} / \text{In2} = 1: 3$  , whereas the 8 b cations are coordinated to six oxygen anions and to 2 oxygen interstitial positions but the 24 d cations are coordinated to six oxygen anions at three distances and to 2 oxygen interstitial sites. The 48 oxygen anions are coordinated to four cations [ 23]

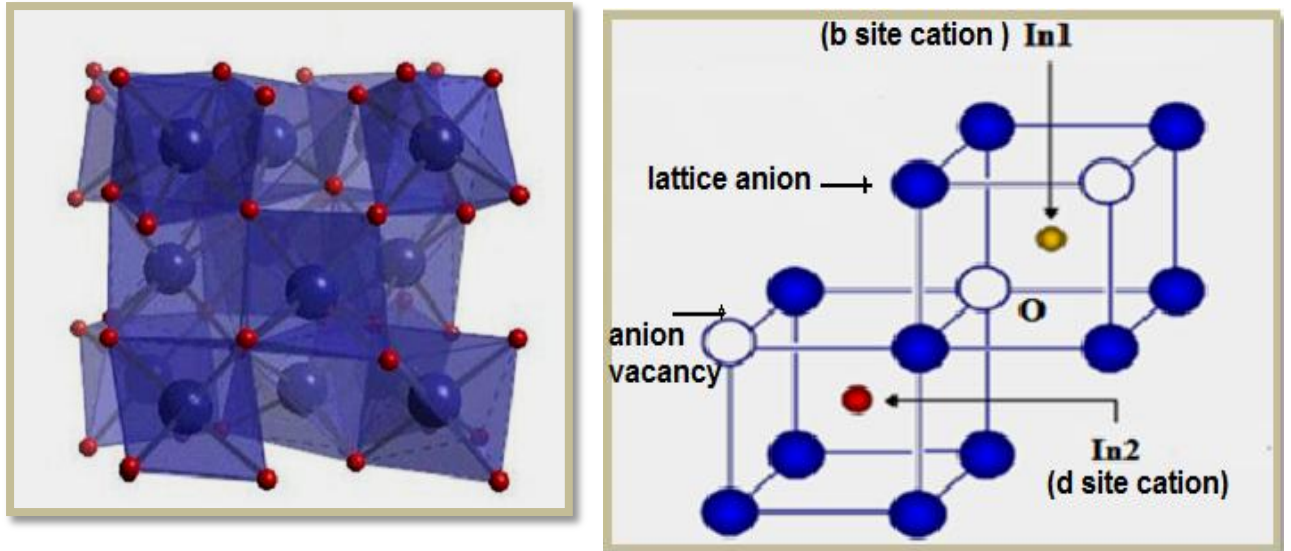


**Figure.I.5:** Crystallographic structure , Cubic bixbyite structure (1/16 of the units) [21,23].

In case of doping, 1/4 of the doping atoms are on the In1 sites and 3/4 on the In2 sites.

**Table I.1:** shows the number and positions of the 80 atoms forming the elemental cell of indium oxide [21].

Number	atome	X	Y	Z
8	$\text{In}^{3+}$ (In1)	1/4	1/4	1/4
24	$\text{In}^{3+}$ (In2)	0,4668	0	1/4
48	$\text{O}^{2-}$	0,3905	0,1529	0,3832

b) **Hexagonal structure:** it is identical to that of  $\alpha$ -alumina (corundum). It is obtained either by adding metal dopants or by elaborating under high pressure (for example 65 kbar and 1000 ° C.). The network parameters are:  $a = 5.484\text{\AA}$  and  $c = 14.508\text{\AA}$  [24].

### I.4.1.2 Optical properties:

The interaction of light (electromagnetic wave) with  $\text{In}_2\text{O}_3$  films (electrons of the valence band) can clearly explain these optical properties. If the energy associated with the electromagnetic wave which is capable of transferring electrons from the valence band to the conduction band, an electromagnetic wave interacting with these films will be completely absorbed by it, i.e. this energy is at least equal to 3.55 eV (the width of the forbidden band of  $\text{In}_2\text{O}_3$ ).

Pan and Ma, found an optical transmittance (T) in the visible region and I-Red of the order of 90% for pure films of  $\text{In}_2\text{O}_3$  deposited by the thermal evaporation of a mixture of  $\text{SnO}_2$ -10% In in ambient oxygen at 340 ° C. This is the best value obtained for any undoped transparent conductor which rivals those for the ITO system very closely.

The refractive index in the visible region ranges between 1.9 and 2.08. Muller reported an effective mass  $m^* = 0.3m_e$  for conduction electrons [5,21].

### I.4.1.3 Electrical properties:

It is recalled that the electronic band structures of oxygen and indium are:



The 2P states of oxygen forms the valence band and the indium S states constitutes the conduction zone of the semiconductor of  $\text{In}_2\text{O}_3$ .

$\text{In}_2\text{O}_3$  has single free electron-like band of s-character forming the bottom of the conduction band hybridized with a highly dispersed O 2s states. The valence band edge arises from the O 2p states hybridized with  $\text{In}_2$  5d. This intriguing band structure results in uniform distribution of the charge that reduces the scattering to a minimum. Moreover, the high electrical conductivity due to mobility enhancement and Burstein–Moss shift can also be explained on the basis of dispersion of these bands [22].

Indium oxide is an n-type semiconductor with a direct gap. The high conductivity of the pure oxide layers is due to the high free carrier concentration (electrons).

The latter is attributed to the deviation from stoichiometry (or intrinsic defects in the structure). There is a big difference in the gap energy, literature reported by the references. At room temperature, it varies between 3.55 and 3.75 eV.  $\text{In}_2\text{O}_3$  as a transparent conductor has a higher mobility which varies in the range  $10\text{-}75\text{ cm V}^{-1}\text{s}^{-1}$ , with an electron concentration  $N \approx 10^{19}\text{-}10^{20}\text{ cm}^{-3}$ , and a resistivity  $\rho \geq 10^{-3}\text{ }\Omega\text{cm}$ . the best results are obtained after reducing heat treatment which improves the conductivity. On the other hand, it has been found that a thermal oxidation treatment results in a reduction of the conductivity [5].

#### **I.4.2 Applications of indium oxide:**

The transparent and conductive oxides (OTC),  $\text{In}_2\text{O}_3$  is physically stable and chemically inert. As a transparent conductor, it shows features similar to  $\text{SnO}_2$  which is important for applications in many aspects. Indium oxide can be used as OTC material in :

➤ **optoelectronic devices, including solar cells**

TCOs in solar cells are used as transparent electrodes. They must necessarily have a high optical transmission in order to allow efficient transport of photons to the active layer and also a good electrical conductivity which is required to obtain the least losses of photogenerated transport charge [21].

➤ **Gas sensors**

- Gas sensors play a vital role in detecting, monitoring and controlling the presence of dangerous and toxic gases such as ammonia, ozone in the atmosphere at very low concentrations.
- Semiconductor gas sensors in the form of thin films are highly sensitive and reliable, having a performance or price ratio comparable to that of microelectronic components [25].

➤ **Humidity sensors**

Moisture is a constant environmental factor, so its precise measurement and control are very important. Moisture sensors are generally required in the areas of home

appliances, the medical industry, the agricultural industry and the automobile industry. [26]

Other applications include electroluminescent devices, anti-reflection coatings, electroluminescent liquid, crystal liquid, crystal displays, electrochromic devices, photothermal devices, and light-emitting diodes. Since  $\text{In}_2\text{O}_3$  is mostly used in film form, it is generally characterized in terms of the properties of thin films [22].

### I.5 Some methods of depositing thin films:

Several methods are used to develop the growth of thin films. These methods are generally classified into two main families: chemical development methods and physical treatment methods. Chemical methods include: chemical vapor deposition (CVD), sol-gel process and interactive chemical technology. For physical methods, the most common are vacuum evaporation, spraying and laser ablation. We will find all families of layers deposits below. The methods are listed in the Table I.2.

**Table I.2:** Shows general methods for depositing a thin films.

General methods for depositing a thin films			
Physical process (PVD)		Chemical process (CVD)	
In empty environment	In plasma medium	In the solution	In the vapor phase
-Evaporation -Reactive evaporation - Magnetron DC -Laser ablation	-Cathodic spray -Reactive spray - Radio spray Frequency	-Sol gel -Spray -Electron depositions	-CVD -LACVD -PECVD -MOCVD

### **I.5.1 Physical vapor deposition (PVD) :**

Physical vapor deposition consists of using vapors from the material to be deposited to deposit on any substrate [27]. The transport of the vapors from the target to the substrate requires a fairly high vacuum ( $10^{-5}$  to  $10^{-10}$  Pa) to transport the atoms of the target to the substrate, avoiding the formation of powder bound to condensation in the homogeneous phase.

Physical vapor deposition (PVD) has many advantages over chemical vapor deposition, such as:

- The films are dense.
- The process is easy to control without any pollution.

### **I.5.2 Chemical vapor deposition (CVD) :**

Chemical Vapor Deposition (CVD) is a method in which the constituents of a gas phase react to form a solid film deposited on a heated substrate. The volatile compounds of the material which will be deposited are optionally diluted in a carrier gas and introduced into an enclosure where the substrates are placed. The CVD is an interdisciplinary field, it includes a set of chemical reactions, a thermodynamic and kinetic process, a phenomenon of transport. The chemical reaction is central to these disciplines: it determines the nature, the type and species presented.

The most used synthetic methods are:

- LPCVD (Low Pressure Chemical Vapor Deposition); it is the case of hot wall reactor that is heated directly.
- PECVD (Plasma Enhanced Chemical Vapor Deposition) or PACVD (Plasma Assisted Chemical Vapor Deposition). Consists of the assistance of a plasma to obtain the deposits at lower temperatures.
- The assistance of a laser makes it possible to locate on parts , the different areas , the use of OMCVD organometallic method which compounds considerably lowering the temperature for obtaining the deposit.

The principle of the CVD technique, in the case of the hot wall, is presented in Figure I.6 [ 28].

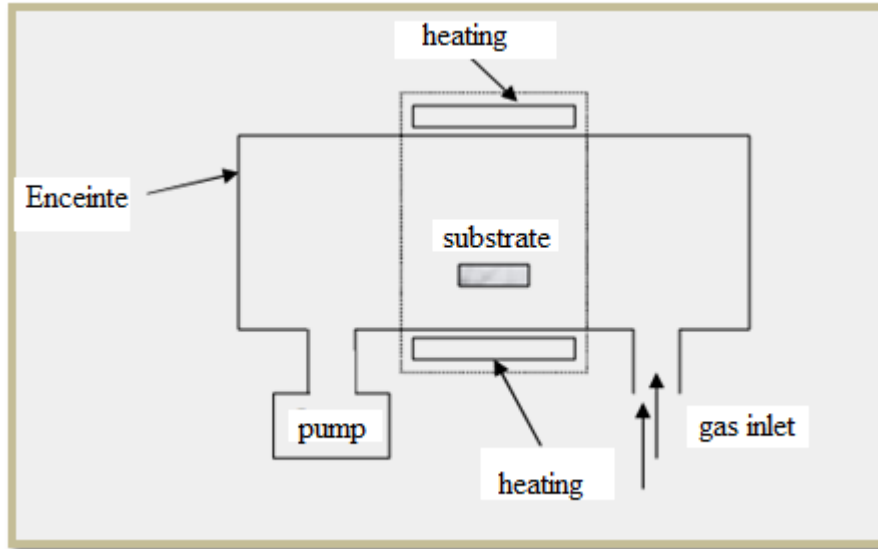


**Figure.I.6 :** Principle scheme of chemical vapor deposition (hot wall furnace) [28].

The kinetics of the process depends on the following steps [29]:

- 1) Convection of the gaseous reagent (dynamic flow).
- (2) Dissemination of the reagent to the substrate.
- (3) Adsorption of the reagent on the substrate.
- (4) Chemical reaction of the adsorbed species.
- (5) Desorption of products gaseous reaction.
- (6) Diffusion of its products through the boundary layer.
- (7) Evacuation of the gases from the system.

The main advantages of these techniques are to allow the crystallization of films without the use of annealing, to be able to control the composition during the

deposition, and to produce a deposit of uniform thickness and composition which also has excellent adhesion. However, these techniques have the disadvantage of giving films contaminated by the precursor residues and that of having an often high reaction temperature [12].

We choose in this work, ultrasonic spray as a method from the above methods because the pyrolysis spray is a deposition technique used to prepare thin and thick films. Unlike many other film deposition techniques, it represents a very simple method which does not require high quality chemicals. This method was used for depositing dense and porous films. Even multilayer films can be easily prepared using this technique. The typical equipment of the pyrolysis spray consists of an atomizer, a precursor solution, a substrate heater and a temperature controller. Ultrasonic atomizers are used in the technique of pyrolysis spray. In an ultrasonic atomizer the ultrasonic frequencies produce the shortwave required for fine atomization which is a very inexpensive and economical technique, it is also industrializable. It is described as below:

## **I.6 Ultrasonic pyrolysis spray:**

### **I.6.1 The pyrolysis spray:**

The spray technique was first introduced by Chamberlin and Skarman in 1963. It was used successfully for CdS films. It was then adapted for the preparation of several materials such as Cd, Zn, Sn,  $\text{CuInS}_2$ ,  $\text{FeS}_2$ , etc. As well as for obtaining thin films of transparent and conductive oxides ( $\text{SnO}_2$ ,  $\text{ZnO}$ ,  $\text{In}_2\text{O}_3$  ...) [30].

"Pyrolysis Spray" is the most common name given to this technique. It consists of: pyrolysis and spray.

- **Pyrolysis:** comes from pyrolytic and indicates the heating of the substrate. There is a thermal decomposition of a source to release a metal or a compound. The temperature of the substrate provides the necessary energy, called activation energy, to trigger the chemical reaction between the compounds. The experiment can be performed in air, and can be prepared in a chamber under a vacuum of about 50 torr.

- **Spray:** it indicates the jet of a liquid in fine droplets, launched by a sprayer.

Typically, the equipment used in the pyrolysis spray consists of an atomizer, solution precursor, heated substrate and temperature controller. In general, the atomizers used to produce a spray jet fall into two categories:

*Technique of a pneumatic spray:* in this case, it is the effect of the pressure of the carrier gas which causes the liquid to be sprayed into fine droplets.

*Technique of an ultrasonic spray:* in this case, the atomization of the liquid is produced by ultrasonic waves.

In the first case, the jet comes out of the nozzle with an initial speed depending on the values of the pressure and the diameter of the nozzle, but it has disadvantage which led the sizes of the drops are not homogeneous. Where as, in the second process the outlet velocity of the beak is zero but the size of the droplets is very fine and homogeneous [31], it is containing sprayed by a 50 KHz ultrasonic generator which will be converted at the level of the atomizer into a jet of very fine droplets onto substrates that are arranged on a substrate carrier heated to a temperature that allows the activation of the chemical reaction between the compounds. The experiment can be performed in air, and can be prepared in an enclosure (or in a reaction chamber) under a vacuum of about 50 Torr [15, 30].

The description of the films formation by the pyrolysis spray method can be summarized as follows [30]:

- Formation of the droplets at the exit of the beak.
- Decomposition of the precursor solution on the substrate surface by pyrolysis reaction.

#### **1.6.1.1 Deposit solution (source):**

The composition of the final solution is determined by the reagents dissolved in the solvent (starting solution) according to the predetermined stoichiometric ratio. As precursors, usually inexpensive materials such as nitrates, chlorides and acetates which are used. They are classified in the reactive category. Distilled water or alcohol

is often used as a solvent, So we obtain homogeneous solutions, According to previous studies , some techniques include preheating the solution. This preheating can sometimes be useful and promotes or accelerates the reaction on the substrate. This increases the deposition rate and improves the quality of the resulting films [32,33,34].

### **I.6.1 .2 Generation of droplets (transport):**

The size and homogeneity of the deposited material can be determined from the size of the spray droplets and the concentration of the solution, while its morphology can be determined by the concentration and velocity of the droplets produced by the atomizers. Concerning the atomization or in the same way as the droplet production and their dispersion in the air, several atomization methods have been employed. Thus, there are variants like the pneumatic spray method or the air, which is used as a carrier gas as well as the ultrasonic spray method [31].

### **I.6.1 .3 Chemical reaction on the substrate (deposit):**

When the aerosol droplets approach the surface of the heated substrate (200-600 ° C), under the appropriate experimental conditions, the formed vapor around the droplet prevents the direct contact between the liquid phase and the surface of the substrate. This evaporation of the droplets allows a continuous renewal of the vapor, so the droplets undergo the thermal decomposition and give rise to the formation of strongly adherent films. It is noted that the gas phase decomposition reaction occurring on the surface of the substrate is an endothermic reaction which requires relatively high substrate temperature to cause droplet decomposition, and gives a rise to the film [31].

## References

- [1] L. Holland, Vacuum deposited thin films, Chapman & Hall, London (1966).
- [2] A. Mosbah, Elaboration et caractérisation de couches minces d'oxyde de Zinc, thèse doctorat, Université de Constantine, (2009).
- [3] Technologie des couches minces  
«[http://pero.wanadoo.fr/michel.hubin/physique/couches/chap\\_cm1](http://pero.wanadoo.fr/michel.hubin/physique/couches/chap_cm1) ».
- [4] N. Bouhssira, Elaboration et Caractérisation des Couches Minces d'Oxyde de Zinc par Evaporation, mémoire de magister, Université de Constantine,( 2005).
- [5] F. Ynineb, Contribution à l'élaboration de couches minces d'Oxydes Transparents Conducteurs (TCO), mémoire de magister, Université de Constantine, (2010).
- [6] A. Richard, A.A. Durant. Les interactions ions énergétiques-solides, édition INFINE.
- [7] J.D.Torre « simulation à l'échelle atomique de la croissance de films minces », thèse de doctorat, université Paul Sabatier-Toulouse (2000).
- [8] M.Gaidi, Films minces de SnO<sub>2</sub> dopés au platine ou au palladium et utilisés pour la détection des gaz polluants : analyses in-situ des corrélations entre la réponse électrique et le comportement des agrégats métalliques, thèse doctorat, (1999).
- [9] A. F. Mayadas, J. App.Phys. 39(1968) 4241.
- [10] Z. Hadeif, « Etude de l'adhérence dans les couches minces», Mémoire de Master, Université Badji Mokhtar Annaba, 2010.
- [11] J. Garnier, élaboration de couches minces d'oxydes transparents et conducteurs par spray CVD assiste par radiation infrarouge pour applications photovoltaïques, thèse de doctorat , Ecole doctorale n° 432 : Sciences des Métiers de l'Ingénieur , (2009) .
- [12] O. Mohamed, Dépôt et caractérisation des couches minces d'oxyde de Zinc par spray pyrolyse Ultrasonique , mémoire de magister, Université de Biskra,( 2010).
- [13] H. Hosono, D.C. Paine, D. Ginley, Handbook of transparent conductors, Springer Science & Business Media, (2010).

- [14] A. Pron, P. Rannou, Processible conjugated polymers: from organic semiconductors to organic metals and superconductors, *Progress in polymer science*, 27 (2002) 135-190.
- [15] A. Hafdallah, Dépôt et Caractérisation des Electrodes en Couches Minces Transparentes et Conductrices , thèse doctorat, université de Constantine, (2016)
- [16] A. Walsh, J. L. Da Silva, S. H. Wei, C. Körber, A. Klein, L. F. J. Piper, ... & D. J. Payne, Nature of the Band Gap of  $\text{In}_2\text{O}_3$  Revealed by First-Principles Calculations and X-Ray Spectroscopy, *Physical Review Letters*. Vol.100, (2008) 167402
- [17] P. Prathap, Y.P.V. Subbaiah, Optical properties of  $\text{In}_2\text{O}_3$  films prepared by spray pyrolysis, *Materials Chemistry and Physics* 100 (2006) 375–379.
- [18] M. Girtan , H. Cachet, On the physical properties of indium oxide thin films deposited by pyrosol in comparison with films deposited by pneumatic spray pyrolysis , *Thin Solid Films* 427(2003) 406-410.
- [19] Hsin-Lun Su, Wei-Hsu Chi, Abstract, 1446, 218th ECS Meeting.
- [20] M. Girtan ,The influence of post-annealing treatment on the electrical properties of  $\text{In}_2\text{O}_3$  thin films prepared by an ultrasonic spray CVD process , *Surface and Coatings Technology* 184 (2004) 219–224.
- [21] A .Chennoufi, L'effet de la molarité et de la température du substrat sur les propriétés des couches minces d'Oxyde d'Indium déposées par spray Ultrasonique, mémoire de magister, Université de Biskra, (2012).
- [22] A. Moses Ezhil Raj, K.C. Lalithambika, V.S. Vidhya, G. Rajagopal, A. Thayumanavan, M. Jayachandran, C. Sanjeeviraja , *Physica B* 403 (2008) 544 – 554
- [23] A. Bouhdjer, Study of Thin Layers of Indium Oxide ( $\text{In}_2\text{O}_3$ ) Elaborated by Chemical Means, Thesis of Doctorate, (2016).
- [24] K. Daoudi, Elaboration et caractérisation de films minces d'oxyde d'indium dope a l'étain obtenus par voie Sol-Gel , université Claude Bernard Lyon1, (2003).
- [25] K. Makhija, Arabinda RAY, *Bull. Mater. Sci.*, Vol.28, No.1, Indian Academy of Sciences. (2005) 9–17
- [26] K. Arshak , K. Twomey, Thin films of  $\text{In}_2\text{O}_3/\text{SiO}$  for humidity sensing applications , *Sensors* 2002, 2, 205-218.

[27] B.I Kadda Benmokhtar, Adsorption du gaz par les oxydes métalliques application oxyde de zinc et oxyde d'étain, mémoire de magister, Université d'Oran Mohamed Boudiaf (2013).

[28] [www.mediaun.ch/pvd](http://www.mediaun.ch/pvd).

[29] K. Kamli, E laboration et caractérisations physico chimique des couches minces de sulfure d'étain par spray ultrasonique : Effet des sources d'étain , mémoire de magister, Université de Biskra (2013).

[30]M. Khammar, Etude d'un jet en spray d'une solution chimique sur un substrat chaud destiné à l'élaboration des couches minces, mémoire de magister, Université Constantine, (2010).

[31] B.Correa-Lozano, CH.Comninellis, A.De Battisti, Journal Of Applied Electrochemistry 26(1996)83-89.

[32] C. Mazon, J. Muci, A. Sa-Neto, A. Ortiz-Conde and F.J. Garcia, CH2953-8/91/10000- 1156. IEEE (1991).

[33]K. Okuyama, I. Wuled Lenggorro,Chemical Engineering Science 58(2003)537-547 [26]

[34] R. Schroeder, Faculty of the Virginia Polytechnic Institute and State University, Blacksburg, VA, (2001).

**CHAPTER II**

**ULTRASONIC SPRAY ELABORATION AND  
CHARACTERIZATION TECHNIQUES FOR  
INDIUM OXIDE FILMS**

## II.1 Introduction:

In this chapter .I will expose in the first part, the main stages of our work which are the ultrasonic spray elaboration of indium oxide thin films and in the second part the characterization techniques of this films such as : X-rays diffraction (XRD), Scanning Electron Microscopy (SEM), visible UV, four point . These techniques are used in order to know the crystallographic, morphological , optical and electrical properties of indium oxide films.

## II.2 Elaboration of thin layers of $\text{In}_2\text{O}_3$ by ultrasonic spray:

The Ultrasonic Spray technique is based on harnessing the energy of high frequency acoustic waves (ultrasound) to split a continuous flow of a liquid into a multitude of small droplets (cloud) of uniform size that come out of the beak. In the form of a jet. Sprayers intended to operate at relatively low frequencies (a few tens of KHz) which consist of two piezoelectric elements [1].

### II.2.1 Experimental montage used:

It is an experimental bench, made at *Physics of thin films and applications laboratory of the University of Biskra* , thin layer deposition by Ultrasonic Spray. The principle device of the deposition system is shown in Figure II.1

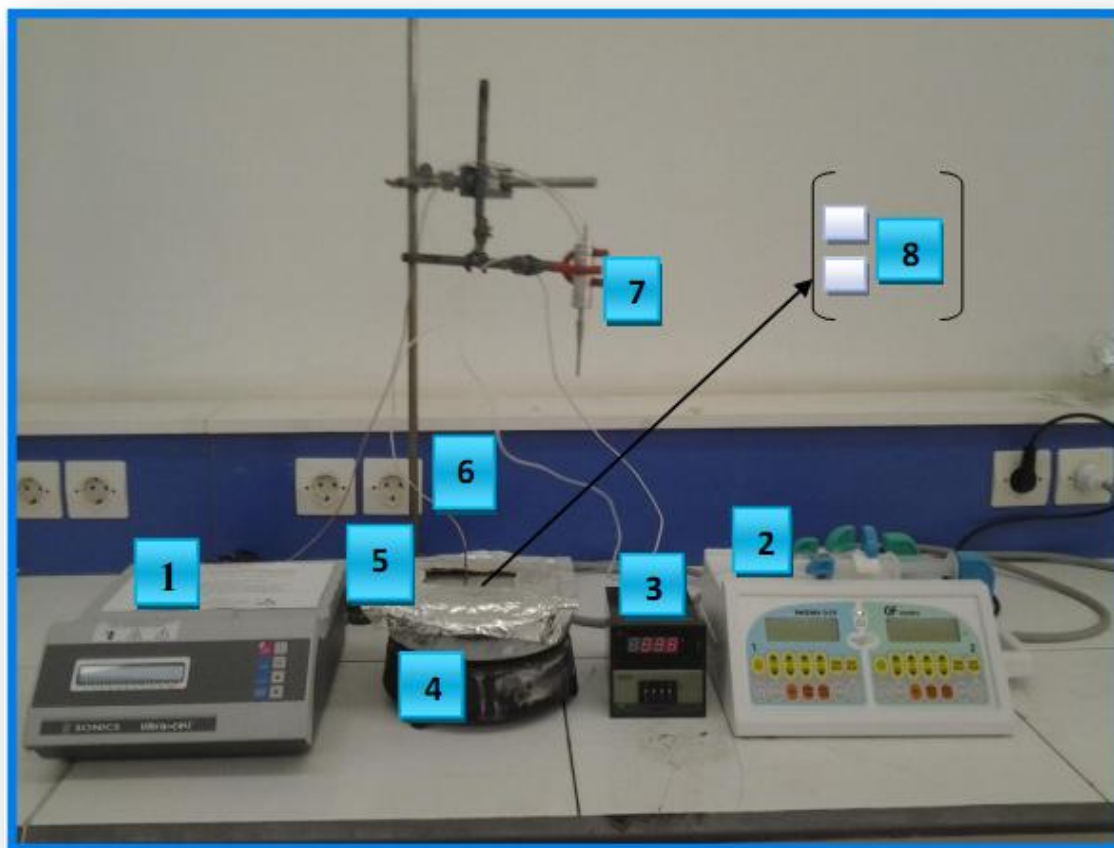


**Figure II.1:** The complete devices of the Ultrasonic Spray technique from the University of Biskra.

The design and the role of experimental montage 'elements used are shown in the following table :

**Table II.1:** Elements of the assembly

N°	Designation	The role of the elements
1	Ultrasonic generator	It creates a fog by subjecting a solution to a high frequency vibration generated by an ultrasonic transducer. This device delivers drops of very small diameter. The size of the drops depends on the physical properties of the atomized solution and the frequency of the generator.
2	Flow controller (The syringe pump )	PHOENIX D-CP Syringe Pump is designed to control spray flow. PHOENIX D-CP double-port syringe pump: The PHOENIX D-CP Syringe Pump is designed to ensure continuous infusion of flowable substances.
3	Temperature regulator	It serves the control of the temperature.
4	Resistance	It is used to heat the substrate.
5	Substrate Holder	This is a Joule-heated (iron) plate whose temperature can be regulated by a digital temperature controller that is connected to a thermocouple. This temperature set can be fixed at 400 ° C.
6	Thermocouple	It is a device for measuring the temperature.
7	Atomizer	It is the location where the transformation of the solution into droplets takes place.
8	Substrate	It is a substrate for depositing thin films

## II.2.2. Experimental procedure:

### II.2.2.1 Experimental conditions:

The ultrasonic spray is a deposit process that depends on various conditions such as: The properties of the precursor, concentration of the solution, distance between the nozzle and the substrate, nature of substrate, the deposition time and substrate temperature (these remain the main parameters influencing the quality of the films). In this work the experimental conditions coordinate with the deposition parameter studied. It is presented that as the following:

#### a) Growth rate influence (flow rate):

A 0.1 M of indium chloride  $\text{InCl}_3$  (Merk, 99.9) is dissolved in methanol and sprayed onto heated glass substrates at  $400\text{ }^\circ\text{C}$ . Firstly, In this work, we fixed the distance between spray nozzle and substrate at 5 cm. Furthermore, the deposition time was fixed during the spray process in atmospheric pressure at 2 min and we were changed only the growth rate which based on the change of the solution flow rate (20,30,40,50 and 60ml/h); that was controlled by (Syringe pump PHOENIX D-CP).

#### b) Influence of indium acetate (different molar concentrations):

$\text{In}_2\text{O}_3$  films were prepared by spray technique using indium acetate ( $\text{C}_6\text{H}_9\text{InO}_6$ ) which is dissolved in 30 ml (5 ml distilled water and 25 ml acetic acid ( $\text{C}_2\text{H}_4\text{O}_2$ )) and is sprayed onto glass substrates heated at  $400\text{ }^\circ\text{C}$ . In this work, the films are prepared with different molar concentrations that vary between 0.025 M and 0.125 M with conserving all of these following parameters constant where the distance between spray nozzle and substrate equals to 5 cm, the time fixed is 6 min during the spray process in atmospheric pressure and solution flow rate 50 ml/h.

#### c) Influence of the substrates:

The films were sprayed onto different substrates (**Glass / Corning glass / Indium tin oxide (ITO) / monocrystalline silicon (Si)**) which are heated at  $400\text{ }^\circ\text{C}$ . The solution is an indium chloride  $\text{InCl}_3$  dissolved in ethanol with 0.1 M which is deposited by spray ultrasonic with fixing the distance between

spray nozzle and substrate at 5 cm. Furthermore, the deposition time was fixed during the spray process in atmospheric pressure at 6 min.

#### d) Effect of doping:

Depending on previous studies in terms of characteristics and cost, as well as the health of the experimenter. As consequence, the un-doped and doped indium oxide films with various antimony (Sb) and molybdenum (Mo) concentrations were deposited by spray technique using 0.1 M with indium chloride  $\text{InCl}_3$  as solution and Antimony (III) chloride  $\text{SbCl}_3$  as dopant with Sb and Ammonium molybdate 4-hydrate  $(\text{NH}_4)_6 \text{Mo}_7\text{O}_{24} \cdot 4\text{H}_2\text{O}$  which are dissolved in ethanol  $\text{C}_2\text{H}_5\text{OH}$  and it is sprayed onto glass substrates heated at 400 C. All the films are prepared with parameters constant such as : distance between spray nozzle and substrate equals to 5 cm, the time fixed is 6 min during the spray process in atmospheric pressure and solution flow rate 50 ml/h with varying in the concentration of Sb dopant (2 -4-6-8 Wt.%) and Mo (1 -2-3-4 Wt.%).

#### II.2.2.2 Choice of the deposit substrate:

The indium oxide films ( $\text{In}_2\text{O}_3$ ) studied are deposited on glass substrates (solid glass) in the deposition parameters such as : flow rate, different molar concentration, effect of doping but in the other parameters the indium oxide films ( $\text{In}_2\text{O}_3$ ) are deposited on corning glass (this layer named as  $\text{In}_2\text{O}_3$  / Co. glass), ITO substrate (this layer named as  $\text{In}_2\text{O}_3$  / ITO) and monocrystalline silicon (this layer named as  $\text{In}_2\text{O}_3$  / Si).

- The choice of glass as a deposition substrate has been adopted because of a good agreement of thermal expansion which presents with the  $\text{In}_2\text{O}_3$  ( $\alpha_{\text{In}_2\text{O}_3} = -20 \cdot 10^{-7} \text{ }^\circ\text{C}^{-1}$ ,  $\alpha_{\text{verre}} = 85 \cdot 10^{-7} \text{ K}^{-1}$ ) in order to minimize the stresses at the substrate layer interface and for economic reasons, good transparency that fits well and for the optical characterization of films in the visible range.

### II.2.2.3 Cleaning of substrates:

The substrates are glass solids of square surface and thickness equal to 1 mm, cut by a diamond point pen as shown in the following figure:



**Figure II.2:** Cut glass substrates using a sharp pen

Before the deposition operation, it is necessary, as in all surface treatments, to proceed with the preparation of the substrate to ensure adequate adhesion and good uniformity (constant average thickness) of the layer deposited on the substrate to make the surface of the substrate very clean and free of impurities. The substrates undergo a cleaning decontamination of surfaces (grease, dust, etc.) according to the following steps: Firstly, the substrates were cleaned with distilled water then dipped in acetone. Secondly, they're cleaned with distilled water and were kept in methanol. Finally, the substrates were rinsed several times with distilled water then they left to dry in a hot air.

### II.2.2.4 The adhesion test:

The adhesion test for thin films is an interesting steps ; It is an essential parameter in the reliability of the deposited films, there are two methods : the test which damages the films "destructive methods", and the other which keep the films intact "Non-destructive methods" . But these type are expensive material and we don't have them . For this , we used the simple adhesion tests such as ; the stick tape test which

sees the films that adhered well the substrate. In this work, all the films was very well bonded to the substrate and this allows us to continue our study.

#### **II.2.2.5 Film thickness :**

Film thickness is determined by many methods like the optical method which used the interference fringe , and through the perpendicular section of this thin layer from the SEM micrograph(Explain later) and the gravimetric method according to the relation  $d = m / (\rho S)$  where (S) and ( $\rho$ ) are respectively the surface and the density of the thin layer studied.

### **II.3 Characterization Techniques:**

The purpose of this part is to expose the characterization techniques of thin films in order to know the properties of deposited films.

#### **II.3.1 Structural characterization methods:**

##### **II.3.1.1. X-rays diffraction:**

X-ray diffraction is an ideal analytical technique for the study of samples crystallized solids. In metallurgy of powders or single crystals, it is customary to analyze the structure of materials through X-rays diffraction. In addition, it found the measure of the lattice parameters and crystalline size . It must also make it possible to examine the state of deposits stress. X-rays, like all electromagnetic waves, cause a displacement of the electron cloud with a respect to the nucleus in the atoms; these induced oscillations cause re-emission of electromagnetic waves of the same frequency; this phenomenon is called Rayleigh scattering. The wavelength of x-rays being of the order of magnitude interatomic distances (some angstroms) and the interferences of the scattered rays are alternatively constructive or destructive. According to the direction of space, we have a large flow of X photons, or on the contrary very weak; these variations according to the directions form the phenomenon of diffraction X. This phenomenon was discovered by Max von Laue (Nobel Prize in 1914), and extensively studied by Sir William Henry Bragg and his Sir William Lawrence Bragg's son (Nobel prize in 1915). Diffraction of an X-ray radiation by a crystal using the Bragg-Brentano goniometer method gives a diffractogram representing the intensity of the lines as a function of the detection angle  $2\theta$ .

The measurement of the diffraction angles allows an easy access to inter-reticular distances and highlighting preferential crystalline orientations [2,3].

The diagram of the apparatus is presented in the figure II.3:

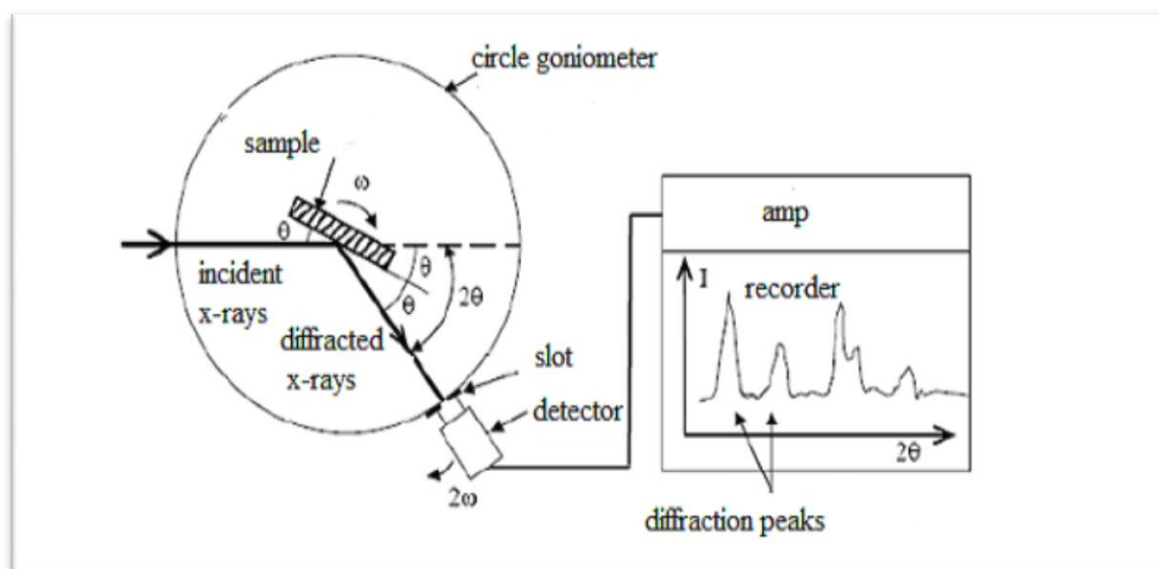


**Figure II.3:** Principle of two-circle diffraction [ 5]

The Bragg equation may be obtained geometrically, which is visualized in figure II.4

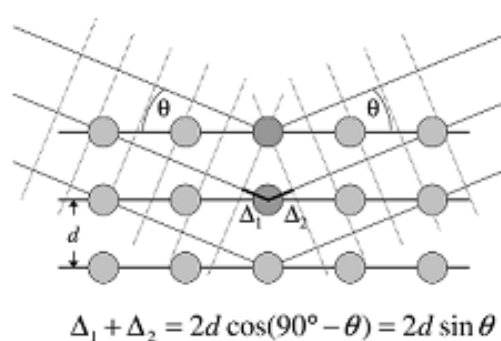


**Figure II.4:** Bragg's law giving the directions where the interferences are constructive [4]

If we calculate the directions in which we have the signal , A rewrites [4]:

$$2 d \sin (\theta) = n.\lambda \quad (\text{II} - 1)$$

Where:  $\theta$  is half of the deviation,  $n$  is an integer called "diffraction order", and  $\lambda$  is the wavelength of the X-rays.

And as long as the crystallographic planes can be identified by the Miller indices (h k l), we can index the diffraction peaks according to these indices. Thus, each material will be characterized by series of peaks which correspond to the reflections due to its various atomic planes. The analysis which is carried out using the American Society for Testing and Materials (ASTM) sheets which containing the crystalline structure of each material with all the lines (as a function of the angle  $\theta$ ) and their relative intensities. In our study, we used a type BRUKER-AXS type D8 diffractometer X-rays which produced from a copper-anode  $\text{CuK}_\alpha$  radiation source with a wavelength of  $\lambda = 1,54183 \text{ \AA}$ .

The lattice parameters ( $a = b = c$ ) have been determined by equation [6]:

$$a = d (h^2 + k^2 + l^2)^{1/2} \quad (\text{II} - 2)$$

Where  $d$  is the lattice spacing of the crystal planes (Miller indices)(h k l).

The crystallite size of the different samples was determined from the diffraction spectra. In order to ensure these grain size values of our films, we used Scherrer's relationship [7]:

$$D = \frac{0,9 \cdot \lambda}{B \cdot \cos \theta_{hkl}} \quad (\text{II} - 3)$$

Where  $D$  is the average size of the crystallites ( $[D] = \text{nm}$ ),

$B$ : Full width half maximum (FWHM)

$\theta$ : is the diffraction angle in degrees

$\lambda$ : is the wavelength of the X-rays beam ( $\text{\AA}$ ).

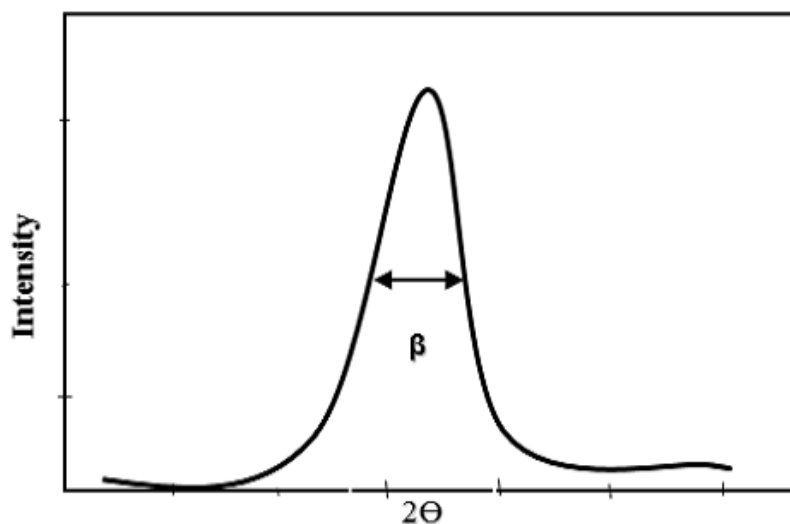


**Figure II.5:** Illustration showing the definition of grain size from the X-ray diffraction curve[8].

The mechanical strain in the films depends on two main influences which appear in metal oxide films [9]. The first one is the variation in the coefficients of thermal expansion of growing film materials and its substrate. The second is the deflection of the growing film composition from stoichiometry which lead to the formation of the strain in the lattice of films. The microstrain  $\epsilon$  in the films is also correlated with (FWHM) by [10]:

$$\epsilon = \frac{\beta}{2 \tan \theta} \quad (\text{II} - 4)$$

Where  $\theta$  is the angle of Bragg and  $\beta$  is the full width at half maximum (FWHM).

Other effects influenced in the physical and mechanical properties of nanocrystalline materials which are dislocations: linear defects propagated in the plastic microstrain in the crystal lattice during their displacement. So, the value of the dislocation density ( $\delta$ ) which gives the defect numbers in the film was calculated

from the crystallite size values  $D$  by the relationship [11]:

$$\delta = \frac{1}{D^2} \quad (\text{II} - 5)$$

### II.3.1.2 Scanning electron microscopy (SEM):

Scanning Electron Microscopy (SEM) is one of the most powerful techniques for the observation of texture and also the study of the optical quality of the thin films surface. This technique is non-destructive and allows superficial observations with a resolution of a few nanometers a very large depth of field. Its great advantage is the diversity of information provided [12]. It gives information on morphology (shape, size, particles arrangement), topography (determination of surface defects, texture), differences in composition, orientation crystalline and the defects' presence. This technique can also allow us to determine the thickness of a thin layer, using a representation of the perpendicular section of this thin layer [13].

Its principle is based on the electron-matter interaction that results from the bombardment of the sample by an electron beam. The latter is generally produced by an electron gun raised to a high voltage (a few tens of kV). The schematic presentation of the principle is illustrated in Figure (II.6). The surface of the sample is scanned line by line by an electron beam using an electronic lens system. The beam diameter varies from 30 to 200 Å depending on the acceleration voltage applied to the electrons [14].

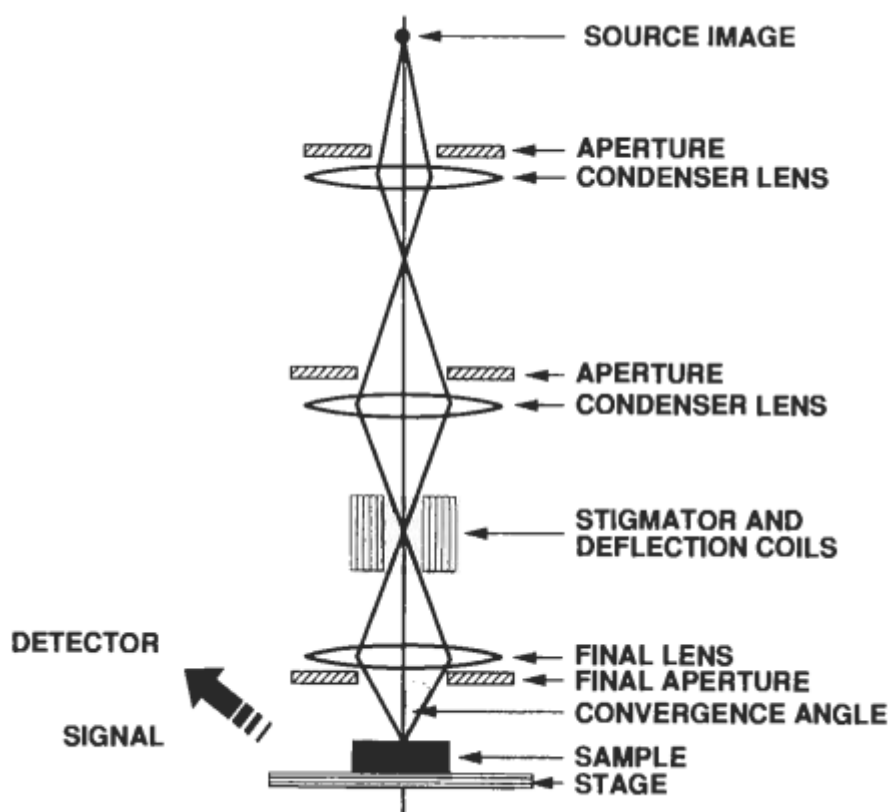


**Figure II.6:** Schematic of the electron optics constituting the SEM [20].

SEM is a technique based on electron interactions - matter. These electrons that irradiate the surface of a sample penetrate into the material and affect a volume called "Scattering pear" (Figure II.7). The reemitted photons are replaced by everything a spectrum of particles or radiations such as secondary electrons, backscattered electrons, Auger electrons or X-rays. These different particles or radiations bring different types of information about the sample.

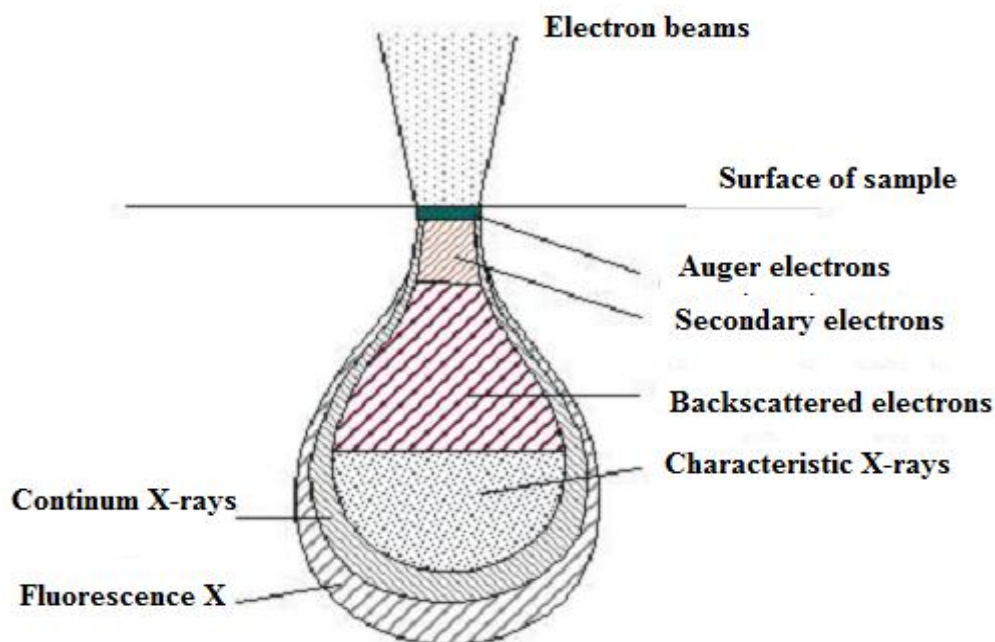


**Figure II.7** Scattering pear [15]

Through the perpendicular section of this thin layer , The thickness of the thin layers can be measured directly from the SEM micrograph, using software called a Visiometer (Figure II.8).

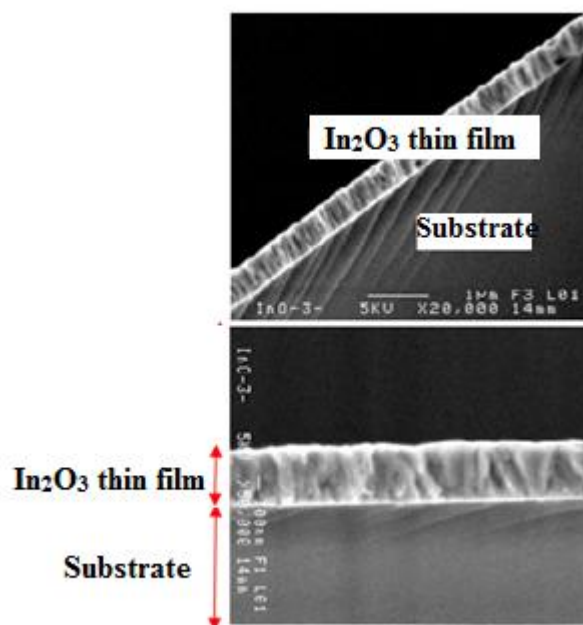


**Figure II.8:** Direct measurement of the thickness of the  $\text{In}_2\text{O}_3$  layer from the obtained image by SEM.

The chemical composition of a sample can also be determined by a Energy Dispersive X-Ray Spectroscopy (EDS), a device connected to the SEM , The X-radiation emitted in the vicinity of the surface during the rearrangement of the electronic train which is characterized by the energy dispersion analysis method. When an electron of the inner layers is torn off by the electron beam, it leaves a vacant place. An electron of the upper layers can then move on it, in this case, there is emission of a characteristic radiation to the excited atom.

$$E = h \nu = E_K - E_L \quad (\text{II-6})$$

The analysis of this radiation makes it possible to know the nature of the elements constituting the material. In addition, the detected emission being proportional to the quantity of the element presented in the sample it is, therefore , possible to carry out a quantitative analysis in parallel. The analysis must be carried out under rigorous conditions, it is necessary to carry out a correction which takes into account an atomic number, matrix effects, fluorescence effects. All these corrections are directly taken into account by the operating system [12].

### **II.3.2 Optical characterization method:**

#### **II.3.2.1 UV-Visible spectroscopy:**

The fields of spectroscopy are generally distinguished according to the wavelength range in which the measurements are made. The areas that can be distinguished like ultraviolet-visible, infrared and microwave. In our case, we have used a dual-beam recording spectrophotometer, whose operating principle is shown in (Figure II.9), by which we could plot curves representing the variation of the transmittance, depending on the length In the field of UV-Visible and near infrared (200-800nm). By exploiting these curves, it is possible to estimate the thickness of the film and determine its optical characteristics such as optical absorption, absorption coefficient, bandgap width, Urbach energy and refractive index [16].

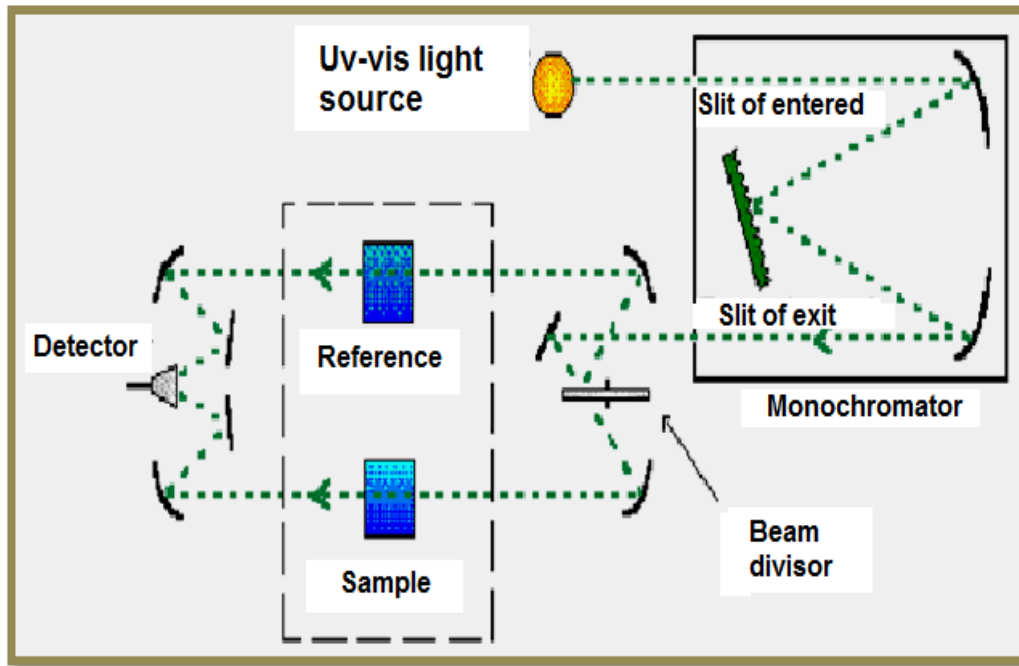


**Figure II.9:** Schematic representation of the UV-Visible spectrophotometer [16].

The spectra obtained gives the relative variation of the transmittance  $T$  (%) of the film as a function of the wavelength  $\lambda$  (nm). And from this spectra we can determine : Bandgap , Disorder, Refractive index. Which uses the following methods:

The determination of the optical gap is based on the model proposed by Tauc where  $E_g$  is related to the absorption coefficient  $\alpha$  by[17]:

$$(\alpha h\nu)^2 = A(h\nu - E_g) \quad (\text{II-7})$$

Where,  $\alpha$  is an absorption coefficient,  $A$  is a constant,  $h$  is the Planck constant and  $E_g$  is the energy band gap of the semiconductor which was evaluated by proposing a direct transition between the valence and the conduction bands; by the extrapolation of the linear region to  $(\alpha h\nu)^2 = 0$ .

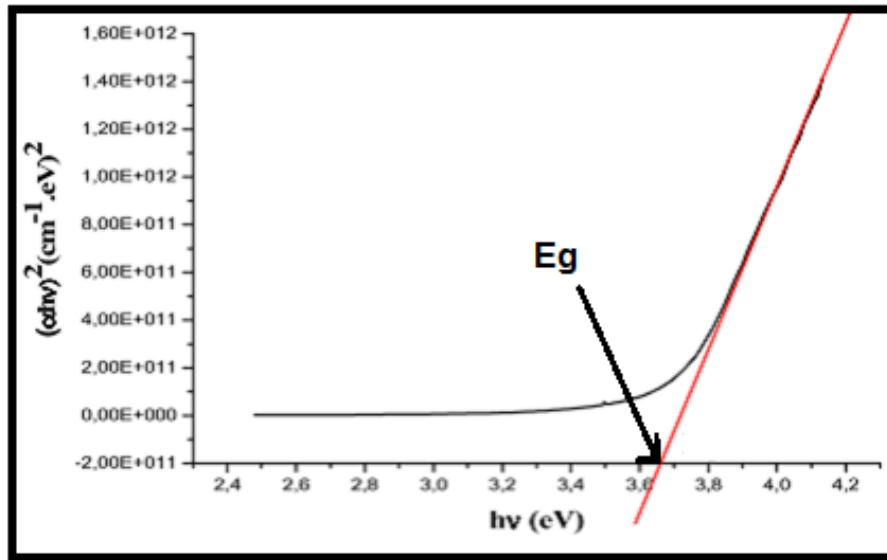


**Figure II. 10 :** Determination of the optical gap according to the Tauc method for a thin layer of  $\text{In}_2\text{O}_3$ .

The formation of band tails due to the localized states which appear near the bands edges, and this leads to the disorder in film lattice because Ultrasonic pyrolysis Spray is a deposition method in which the film growth by condensation. In this situation the atoms arriving on the substrate can stick to the point of their landing. Consequently, the atoms in the film network are not generally in an ideal position, hence, the appearance of the gaps in the width of the In-O bond. In this case, the band edges described in the case of crystalline networks and delimited by a valence band ( $E_v$ ) and a conduction band ( $E_c$ ) which can disappeared (figure II.11).

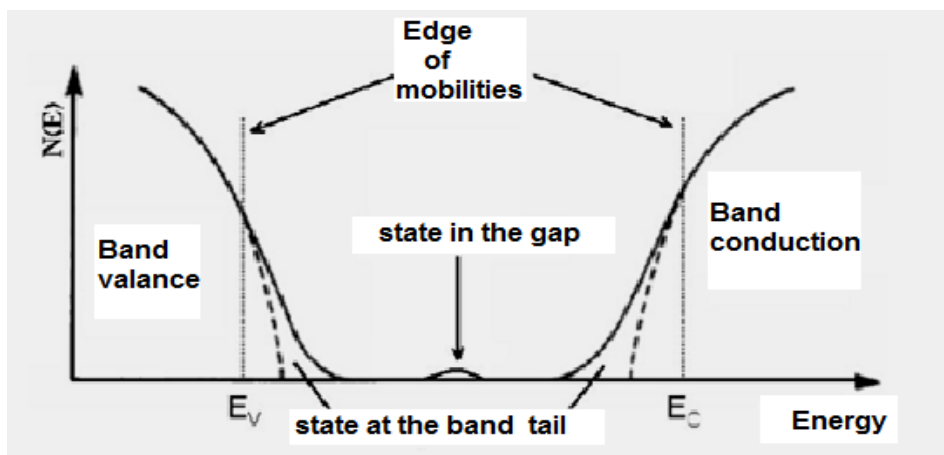


**Figure II.11:** Function of distribution of the energy states in the bands.

It is ,therefore, possible to deduce the disorder from the variation of the absorption coefficients. The absorption coefficient is linked to the disorder by law[17]:

$$\alpha = \alpha_0 \cdot \exp\left(\frac{h\nu}{E_{00}}\right) \quad (\text{II-8})$$

Where,  $\alpha_0$  is a constant and  $E_{00}$  is the band tail commonly urbach tail or disorder energy, it is calculated from the slope of  $\ln(\alpha)$  versus photon energy ( $h\nu$ ).

$$\ln \alpha = \ln \alpha_0 + \frac{h\nu}{E_{00}} \quad (\text{II-9})$$

As it is indicated in the following figure:

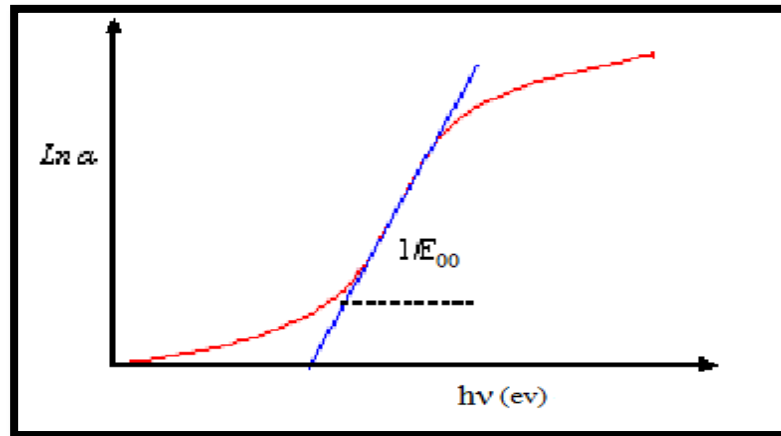


Figure II.12: Determination of Urbach energy .

For another parameter .The refractive index can also be evaluated. Numerous studies suggest that there is a direct correlation between the refractive index and the optical reflectance. The refractive index ( $n$ ) is calculated using relationship is as follows [18]:

$$n = 1 + R^{1/2} / 1 - R^{1/2} \quad (\text{II-10})$$

R is the optical reflectance.

The extinction coefficient ( $k$ ) can be calculated from the relation [19]:

$$K = \alpha \lambda / 4\pi \quad (\text{II-11})$$

Where,  $\alpha$  is the absorption coefficient.

### II.3.2.2 Photoluminescence spectroscopy

Luminescence refers to the emission of light by a material through any process other than blackbody radiation. The term Photoluminescence (PL) narrows this down to any emission of light that results from optical stimulation.

In PL, the energy earned by a material through absorbing light at some wavelength by transmission an electron from a low to a high energy level. It is made by the transition of the atom or the molecule from the founded state to an excited state , or from the valence band to the conduction band of a semiconductor crystal with electron-hole pair creation. The system then submits a nonradiative internal relaxation relating interaction with crystalline or molecular vibrational and rotational modes, and the excited electron moves to a more stable excited level, such as the bottom of the conduction band or the lowest vibrational molecular state. (See Figure II.13.)

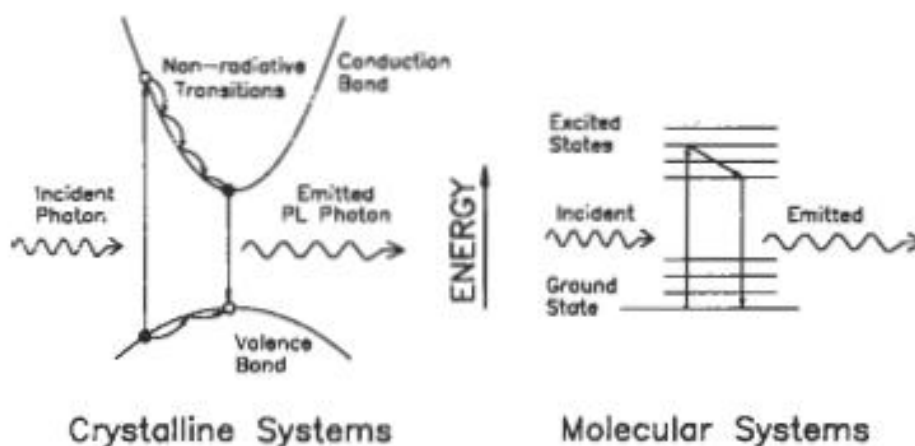


**Figure II. 13:** Schematic of PL from the standpoint of semiconductor or crystalline systems and molecular systems[20].

If the cross-coupling is strong enough this may include a transition to a lower electronic level, a lower energy indirect conduction band, or a localized impurity level. A common occurrence in insulators and semiconductors are the formation of a bound state between an electron and a hole (called an exciton) or involving a defect or impurity (electron bound to an acceptor, exciton bound to a vacancy, etc.).

In the excited state, After the characteristic lifetime depended by the system which may last from picoseconds to many seconds, the electronic system will return to the

ground state. The incident light is shorter than that of The wavelength of this emission .This emitted light is detected as photoluminescence, and the spectral dependence of its intensity which is analyzed to provide information about the properties of the material. The time dependence of the emission can also be measured to provide information about energy level coupling and lifetime. In the range 0.6- 6 eV (roughly 200-2000 nm) the light involved in PL excitation and the emission usually falls. A lot of electronic transitions of interest lie in this range, and the efficient sources and detectors for these wavelengths are available. The emission spectrum that is characterized by the intensity, line shape, line width, number, and energy of the spectral peaks is given by scanning a range of wave lengths .Several spectra may be taken as a function of some external perturbation on the sample, such as temperature, pressure, or doping variation, magnetic or electric field, or polarization and direction of the incident or emitted light relative to the crystal axes and that depending on the desired information, The PL spectrum provides information about the nature of defects as vacancies, interstitial atoms or impurities in the network.

### **II.3.3 Infrared Spectroscopy:**

Fourier Transform Infrared Spectroscopy, FTIR, is one of the methods for measuring the frequencies of the vibrations of chemical bonds between atoms in solids. It is the most commonly used and inexpensive. As one of the few techniques that can provide information about the chemical bonding in a material, it is particularly useful for the non destructive analysis of solids and thin films. The wavelength region of 1 to 100  $\mu\text{m}$  in that extends the region of the visible light to a longer wavelengths and a smaller frequencies/energies. The principles of IR spectroscopy are like the principles spectroscopic techniques as VIS/UV spectroscopy. The transitions of valence electrons are not induced by the energy of infrared light because it is insufficient but these radiations can be excited to vibrational and rotational motions in molecules.

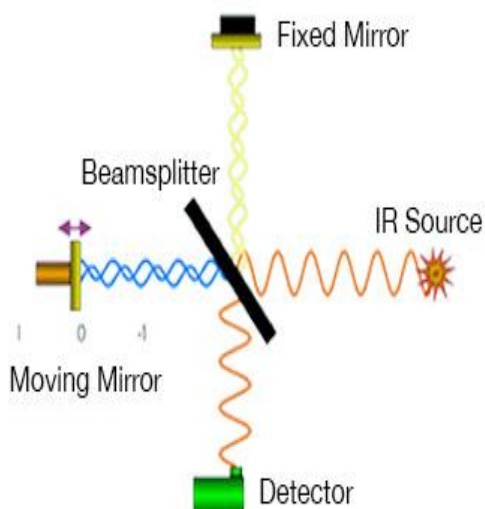


**Figure II. 14:** Diagram of a Fourier Transform Spectrometer.

The molecules of matter have bonds which is moving around and vibrating with stretch motions or bend motions where that the change in inter-atomic distance along bond axis is called *Stretching* and the change in the angle between two bonds which is called *Bending*. These latter Vibrations have four types of bend: rocking, scissoring, wagging and twisting.

The detector signal appears as an interferogram, i.e: a signature of the intensity as a function of the position of the mirror. The interferogram is the sum of all the frequencies of the beam. The analyst requires a frequency spectrum (a plot of the intensity at each individual frequency) in order to make an identification, the measured interferogram signal can not be interpreted directly. A means of “decoding” the individual frequencies is required. This can be accomplished via a well-known mathematical technique called the Fourier transformation. This transformation is performed by the computer which then presents the user with the desired spectral information for analysis.

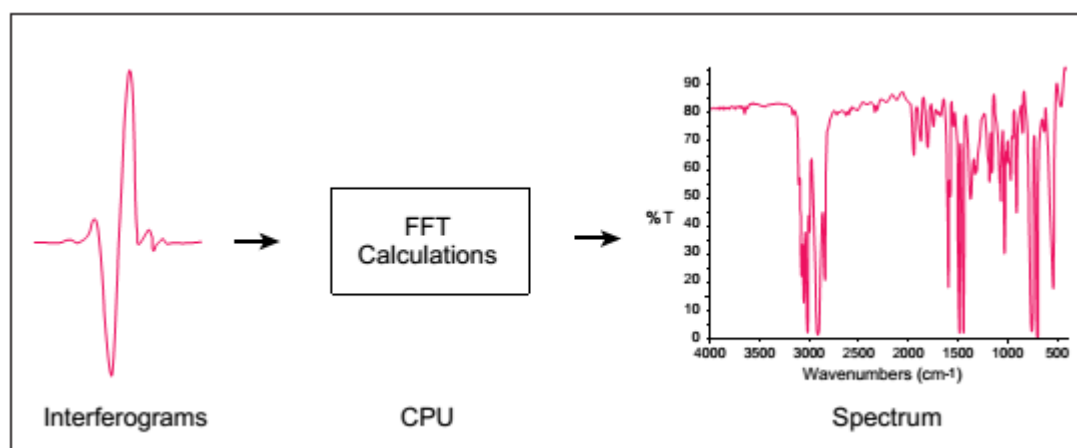


**Figure II. 15:** Interferogram at the output of the detector and example of infrared spectrum of one of the films .

The information drawn from the spectra is of two types:

**Qualitative information type:** The wavelengths in which the sample absorbs are characteristics of the chemical groups presented in the analyzed material where all the characteristic vibration bands are according frequency vibration

**Quantitative information type:** The intensity of absorption at the characteristic wavelength is related to the concentration of the chemical group responsible for absorption by measuring the area of the characteristic signal is possible.

### II.3.3 Electrical characterization:

The electrical resistivity can be measured by several methods have been developed. We have focused on the so-called four-point method in this work which can be used for either thick material or thin layer deposited on an insulating substrate or isolated by junction. We apply the four points aligned with the film deposited on an insulating Pyrex substrate, the gap between the points being 1 mm (Fig II.16). The two external points (1,4) are used to inject a current  $i$ , the other two points (3,2) are used to take drop of the potential  $\Delta V$ .

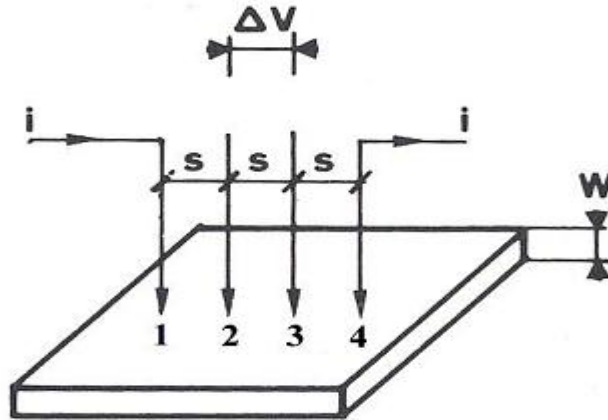


**Figure II.16:** Four-point method [21].

The samples used are two-dimensional with the thickness  $w$ , it is small compared to  $s$ . ( the distance between the boards is much greater than the thickness ). The current density at a distance  $r$  from the tip is:

$$\mathbf{J} = \frac{i}{2\pi r w} \quad (\text{II-12})$$

The potential drop between  $r$  and  $r + dr$  is :

$$\mathbf{dV} = \frac{-\rho i}{2\pi r w} \mathbf{dr} \quad (\text{II-13})$$

$\rho$  : the resistivity

And finally, according to the superposition theorem:

$$\mathbf{\rho} = \left( \frac{\pi}{\ln 2} \right) w \frac{|\Delta V|}{i} = \mathbf{4.53} w \frac{|\Delta V|}{i} \quad (\text{II-14})$$

The resistance by square  $R$  is therefore:

$$\mathbf{R_s} = \mathbf{4.53} w \frac{|\Delta V|}{i} = \frac{\rho}{w} \quad (\text{II-15})$$

From this equations can then deduce the conductivity of the films as follows:

$$\mathbf{\sigma} = \frac{1}{\rho} \quad (\Omega^{-1} \text{cm}^{-1}) \quad (\text{II-16})$$

## Reference

- [1] F. Ynineb, Contribution à l'élaboration de couches minces d'Oxydes Transparents Conducteurs (TCO), mémoire de magister, Université de Constantine, (2010).
- [2] A. Mosbah, Elaboration et caractérisation de couches minces d'oxyde de Zinc, thèse doctorat, Université de Constantine, (2009).
- [3] K. Kamli, Elaboration et caractérisations physico chimique des couches minces de sulfure d'étain par spray ultrasonique : Effet des sources d'étain , mémoire de magister, Université de Biskra (2013).
- [4] S. Guitouni, Corrélation entre les propriétés thermophysiques des gouttelettes et les propriétés des couches minces déposées par le procédé spray, mémoire de magister, université de Constantine, (2010).
- [5] S. Hariech, Elaboration et caractérisation des couches minces de sulfure de cadmium (CdS) préparées par bain chimique (CBD), mémoire de magister, université de Constantine, (2009).
- [6] M. J. Buerger, John Wiley & Sons, X-ray crystallography, INC. P 23.
- [7] B. Ghosh, M. Das, P. Banerjee, S. Das, Fabrication and optical properties of SnS thin films by SILAR method ,Appl. Surf. Sci. 254 (2008) 6436–6440.
- [8] A. Djadai, L'effet de l'amplitude d'onde ultrasonique sur les propriétés optiques et électriques des couches minces de ZnO, mémoire de magister, Université de Biskra, (2012).
- [9] L.S. Palatnik, M.Y. Fuks , V.M. Kosevich, Mechanism of Formation and Substructure of Condensed Films, Moscow. Nauka, (1972) 320
- [10] L.I. Maissel, R. Glang (Eds.), Handbook of Thin Film Technology, McGraw-Hill Book Company, New York, USA, (1970).
- [11] I. B. Kherchachi, A. Attaf, H. Saidi, A. bouhdjar, H. bendjidi, B. Youcef and R. Azizi, Main Group Chemistry, Vol.15 (2016) 231–242
- [12] F. Bouaichi, Dopage et caractérisation des couches minces d'oxyde de Zinc déposée par Spray Pyrolyse Ultrasonique, mémoire de magister, Université de Biskra, (2010).

- [13] Ca. Matei Ghimbeu « Préparation et Caractérisation de couches minces d'oxydes métalliques semiconducteurs pour la détection de gaz polluants atmosphériques », thèse doctorat, l'Université Paul Verlaine de Metz ,( 2007).
- [14] O. Mohamed, Dépôt et caractérisation des couches minces d'oxyde de Zinc par spray pyrolyse Ultrasonique , mémoire de magister, Université de Biskra,( 2010).
- [15] S.benkara, Etude des propriétés électroniques et photoniques des couches minces à base d'oxydes nanostructurés, Université du 20 Août 1955 Skikda, (2014)
- [16] M. Maâche «Dépôt et Caractérisation de Couches Minces de ZnO par Spray Pyrolyse»,Université de Biskra,(2005).
- [17] A. Hafdallah, Étude du Dopage des Couches Minces de ZnO Élaborées par Spray Ultrasonique, mémoire de magister, université de Constantine, (2007).
- [18] M. Di Giulio, G. Micocci, R. Rella, P. Siciliano, A. Tepore, optical absorption and photoconductivity in amorphous indium selenide thin films ,Thin Solid Films. 148 (1987) 273.
- [19] A.M. Elkorashy, Optical constants of tin monosulphide single crystals in the transparency region, Semicond. Sci. Technol. 4 (1989) 382.
- [20] C. Richard Brundle,Charles A. Evans, Jr.Shaun Wilson, encyclopedia of materials characterization, materials characterization series surfaces, interfaces,thin films, Butxetworch-Heinemann,(USA) ,(1992 )
- [21] K.Daoudi, élaboration et caractérisation de films minces d'oxyde d'indium dope a l'étain obtenus par voie sol-gel, these, universite claudes bernard – lyon 1,(2002).

# **The second part:**

The results and discussion

## **CHAPTER III:**

### **GROWTH RATE INFLUENCE ON INDIUM**

### **OXIDE THIN FILMS**

### III.1 Introduction:

The electrical conductivity of  $\text{In}_2\text{O}_3$  films is due to transport of electrons. The high n-type conductivity detected in  $\text{In}_2\text{O}_3$  films results from their anion paucity which is usually shown in the form of oxygen vacancies in the crystal network. However, when  $\text{In}_2\text{O}_3$  film is perfectly stoichiometric, it can only be an ionic conductor. Such materials are not important as transparent conductors because of the high activation energy desired for ionic conductivity. In fact, the  $\text{In}_2\text{O}_3$  films used for transparent conductors are barely perfectly stoichiometric. The previous explanation reveals a way to better the electrical properties of the  $\text{In}_2\text{O}_3$  films, i.e. to prevent more oxygen incorporating into the films at the film growth process, but this is very complexed for the films deposited by ultrasonic spray process because the presence of  $\text{O}_2$  molecular can not be avoided.

In order to prevent the incorporation of the oxygen molecular in the film network, we have increased in the value of the growth rate of these films [1] by increasing the quantities of the solution sprayed on the heated substrate. Furthermore, we have studied the influence of the growth rate on the films' textural, morphological, optical and electrical properties.

### III.2. Growth rate:

Fig.1 shows the growth rate variation as a function of solution flow rate and the films thickness change is given in the inset figure. The growth rate is estimated from the ratio of film thickness on the deposition time. As can be seen, the growth rate increases with the increase of solution's flow rate due to the increase of the volume solution sprayed on the substrate from 20 to 60 ml/h; however, it is interesting to note that the growth rate increases slightly at the beginning which indicate that the rate of horizontal growth in this case is faster than the perpendicular growth of the  $\text{In}_2\text{O}_3$  film.

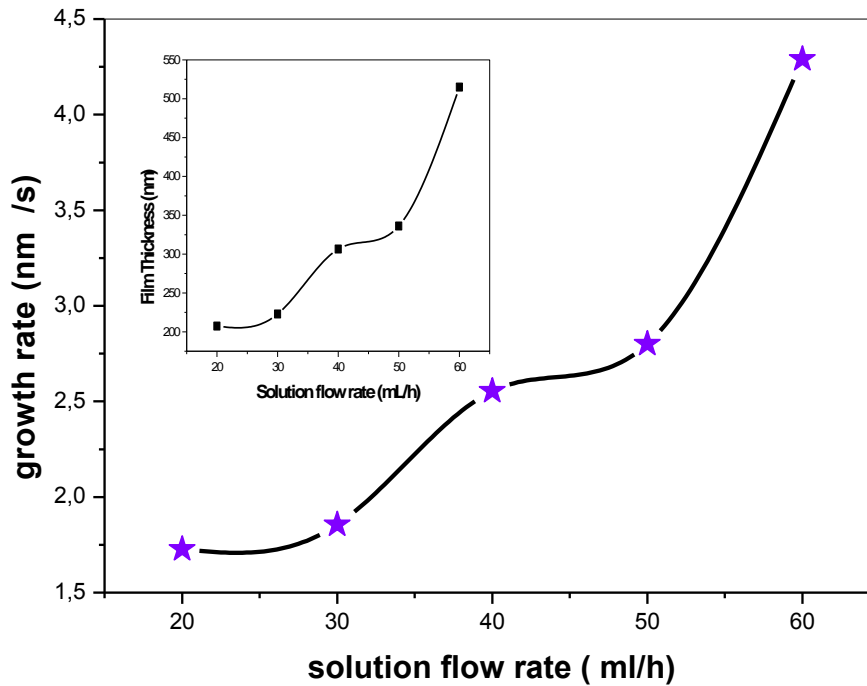
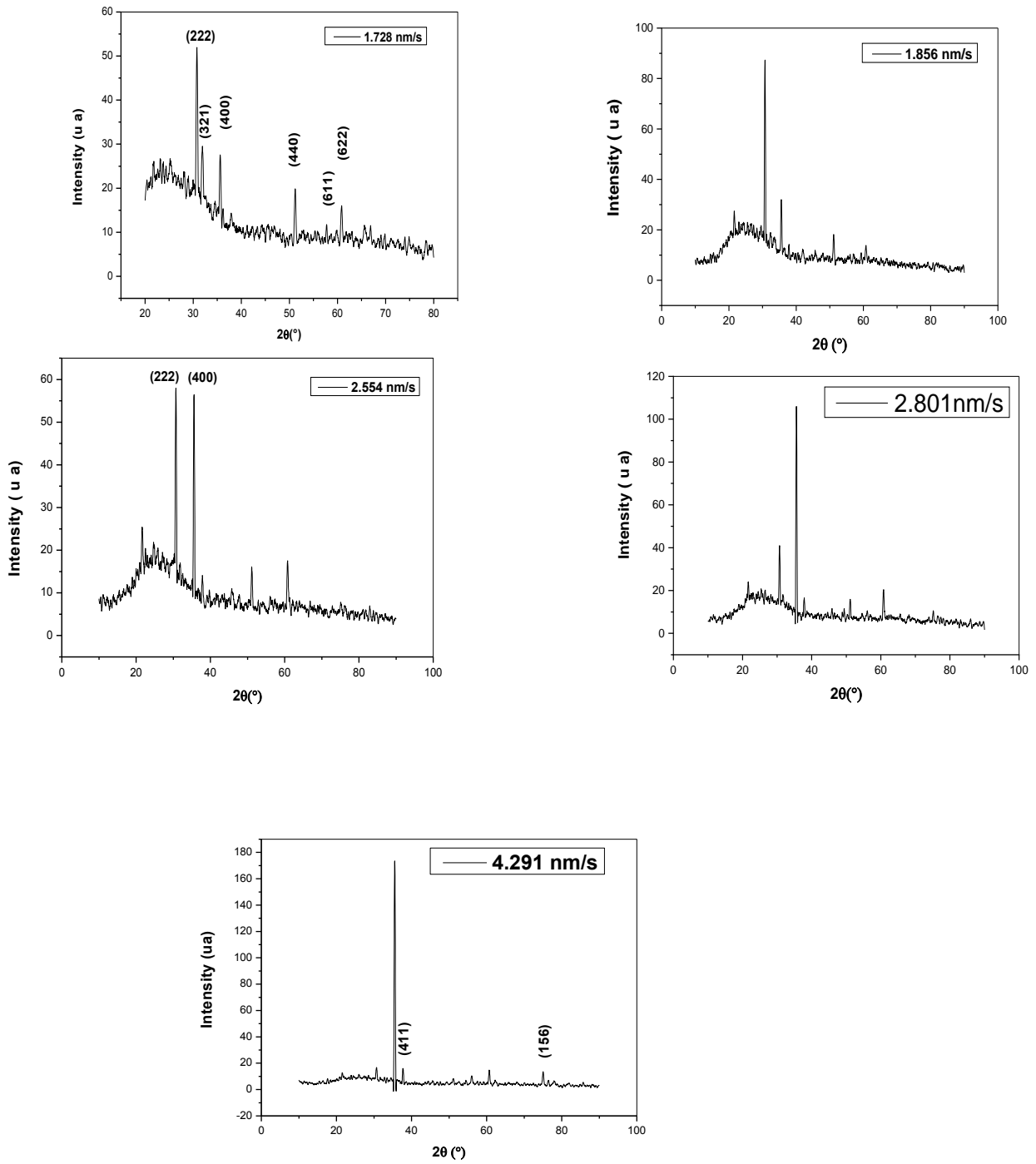


**Figure III. 1.** Growth rate as a function of solution flow rate and inset shows the film thickness dependence on solution flow rate

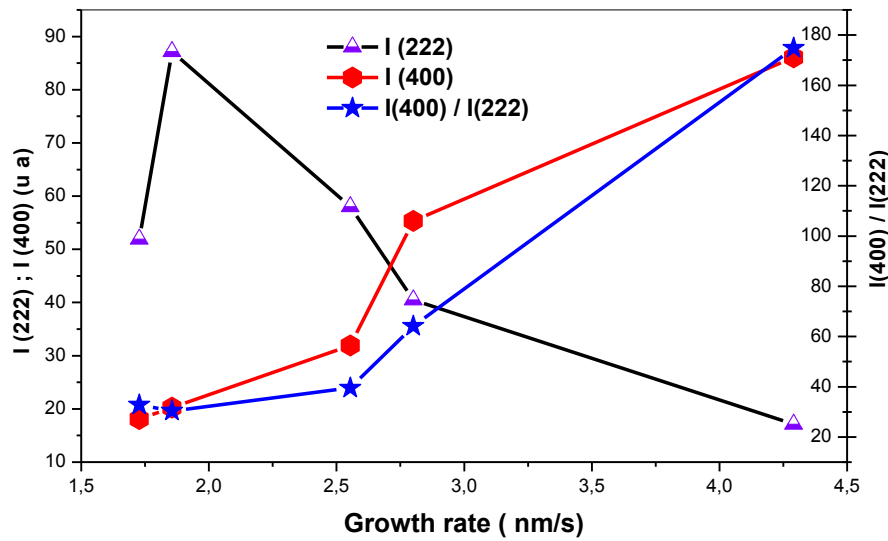
### III .3 Structural properties:

Fig.2 shows the XRD patterns for  $\text{In}_2\text{O}_3$  thin films grown at various growth rate. It is clear that the  $\text{In}_2\text{O}_3$  thin films reveal polycrystalline structure with various orientated crystalline planes such as (222), (321), (400), (411), (156), (611), (440) and (622) which is agreed with the JCPDS card (n° 06-0416). However, there is a preferential growing competition between (222) and (400) planes, this indicates that the growth rate has important effect on the growth mechanism of the  $\text{In}_2\text{O}_3$  films deposited by spray ultrasonic process. The influence of growth rate on the predominant growth orientation of the films evaluated by the peak intensity ratio  $I(400)/I(222)$  (see figure 3). Fig.3 shows that the  $I(400)/I(222)$  increases with rising in the growth rate. Thilakan and all [14] found that the preferred orientation changed from (222) to (400) with the augment of the growth rate. Also, they have proved that  $I(400)/I(222)$  increases with the increasing of deposition time [2] or with the film thickness increase [3]. The values of the peak intensity ratio obtained in this study indicate that the films grown to a high growth rate possess a high degree of texturing

along the [100] direction. Although, the high surface free energy in the bixbyite structure is found in (100) texture[4]. This is owing to the quantity of oxygen in the film network, whereas increasing the growth rate reduces the accumulation of the oxygen in the films; this means that it represses more oxygen into the films during the film growth process[4], which will permit the presence of the preferred growth of (400) grains. In general, the change of the oxygen concentration in the films influences in the intensity of the films orientations. Sundry studies revealed that the decrease of the oxygen concentration in the  $\text{In}_2\text{O}_3$  films represses the intensity of the (222) orientation and motivates the (400) orientation of the  $\text{In}_2\text{O}_3$  films [ 5,6,7]. According to the characteristic peaks that appeared in XRD patterns, we can confirm that the cubic bixbyite structure of the prepared films have a lattice parameter smaller than the reported value  $10.118 \text{ \AA}$  for pure indium oxide [8]. This indicates the compression of unit cell volume which in turn reveals the presence of stress in all the films. When growth rate increases, the lattice parameter was found to increase impending near the value of pure indium at high growth rate. The expected reason for this is the increasing of the oxygen vacancy in the films.



**Figure III. 2** XRD pattern of  $\text{In}_2\text{O}_3$  thin films deposited with different growth rates



**Figure III. 3** The Influence of the preferred orientation intensity with the film growth rate.

The full width at half maximum (FWHM) of XRD line may be because of the crystallite size or the microstrain, whereas the crystallite size ( $D$ ) of the  $\text{In}_2\text{O}_3$  films is associated with (FWHM) by the classical formula of Scherrer [9]. Table.1. reports the variations of the crystallite size. The crystallite size of the films was found in the range of 26– 32 nm. We have observed that the crystallite size is increased with the increasing of the growth rate which can be attributed to the amelioration of crystallinity. Also, when we increasing in the growth rate, the film formation process is fast yielding and the autographed amalgamation of droplets of solution above the substrate is due to the increased capacity of adatoms to move towards stable sites in the network. This means that best nucleation, larger crystallite size are formed from it [10]. However, it is clear that the increasing of crystallite size is very slight; the growth of  $\text{In}_2\text{O}_3$  crystallite almost stops. This can be imputed to the fixed-increase of crystallite size with the rise of the film thickness up to 221 nm. G. Korotcenkov and all found the similar observation; when ( $D$ ) is up to more than 30–35 nm, the growth of grains breaks off [3].

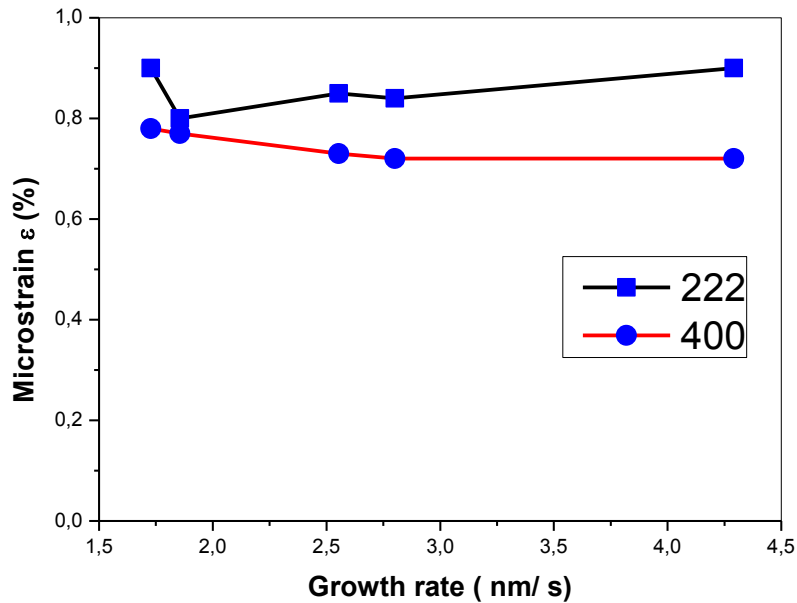


**Figure III. 4.**Microstrain  $\epsilon$  as a function of growth rate.

The mechanical strain in the films depends on two main influences which appear in metal oxide films [11]. The first one is the variation in the coefficients of thermal expansion of the materials of growing film and substrate. The second is the deflection of the growing film composition from stoichiometry which lead to the formation of the strain in the lattice of films. The microstrain  $\epsilon$  in the films is also correlated with (FWHM) [12].

Fig.4 shows the microstrain of two delegate orientations as a function of growth rate. We have observed that the microstrain generally decreases with the increase of growth rate (film thickness), and we have noted that the microstrain of (400) orientation is always smaller than that of (222) orientation. Similar results shown that generally the microstrain rises with increasing in the distortion of lattice. This is physically reasonable because of the great oxygen interstitials which are incorporated in to the crystal lattice and the microstrain leading to larger of lattice distortion . In addition, it is observed that the big lattice distortion for the (222) orientation is compared with the other orientations[13].

**Table III. 1.** Grain size, lattice parameter, optical band gap and disorder energy of In<sub>2</sub>O<sub>3</sub> thin films as a function of the growth rate.

Growth rate (nm/s)	Solution flow rate (ml/h)	Lattice parameter r a=b=c (Å°)	Crystallite size (nm)		Band gap E <sub>g</sub> (ev)	disorder energy E <sub>00</sub> (ev)	δ . 10 <sup>15</sup> (lines /m <sup>2</sup> )	
			(222)	(400)			(222)	(400)
1.728	20	10.04	24.71	28.27	3.93	0.268	1.637	1.251
1.856	30	10.08	30.46	30.1	3.888	0.314	1.077	1.103
2.554	40	10.09	30.59	30.97	3.773	0.325	1.068	1.042
2.801	50	10.09	31.17	32.06	3.666	0.332	1.029	0.972
4.291	60	10.11	29,15	31.52	3.624	0.340	1.176	1.006

Other effects influenced in the physical and mechanical properties of nanocrystalline materials which are dislocations: linear defects propagated in the plastic microstrain in the crystal lattice during their displacement. So, the value of the dislocation density (δ) which gives the defect numbers in the film was calculated from the crystallite size values D [14]. The dislocation density values were reported in **Table .1**. As we can see, the dislocation density decreases generally with the growth rate increasing in the two orientations. This may be due to the improvement of the films structure.

### III.4 Surface morphology:

The surface morphology of In<sub>2</sub>O<sub>3</sub> films are shown in Fig.5. We have observed that all the films have a homogeneous surface and relative roughness. Generally, the morphology does not change significantly except for the last film which is deposited at high growth rate (4.29 nm/s ). It exhibit a dense inner structure with a lot of agglomerates up to the surface of the film. As we can see, the growth rate is lower than (4.29 nm/s ), the shape of the grains in the thinner films is similar approximately to that reported for the thicker films with increasing in the growth rate, i.e., the grain size on top of the film does not change approximately. This result supports the XRD observations, but in the film deposited at 60 ml/h, we have observed that the

agglomerates of very fine particles due to the high amount of solution. The cross-sectional microstructure of the  $\text{In}_2\text{O}_3$  has been detected by scanning electron microscopy (SEM) are shown in Fig.6. the grains grew in the through –thickness direction Fig.6.a but in an increases growth rate which can be seen in Fig.6.b that there is very clear columnar structure that corresponding with structural study where in the low growth rate, it is observed randomly orientation in the film growth but after that it is noticed the determination of preferential orientation in the film growth. EDS analysis of the  $\text{In}_2\text{O}_3$  thin film deposited at growth rate (2.55 nm /s )show that the film is composited from O and In atoms in addition to Si which comes from the substrate(see figure 7).

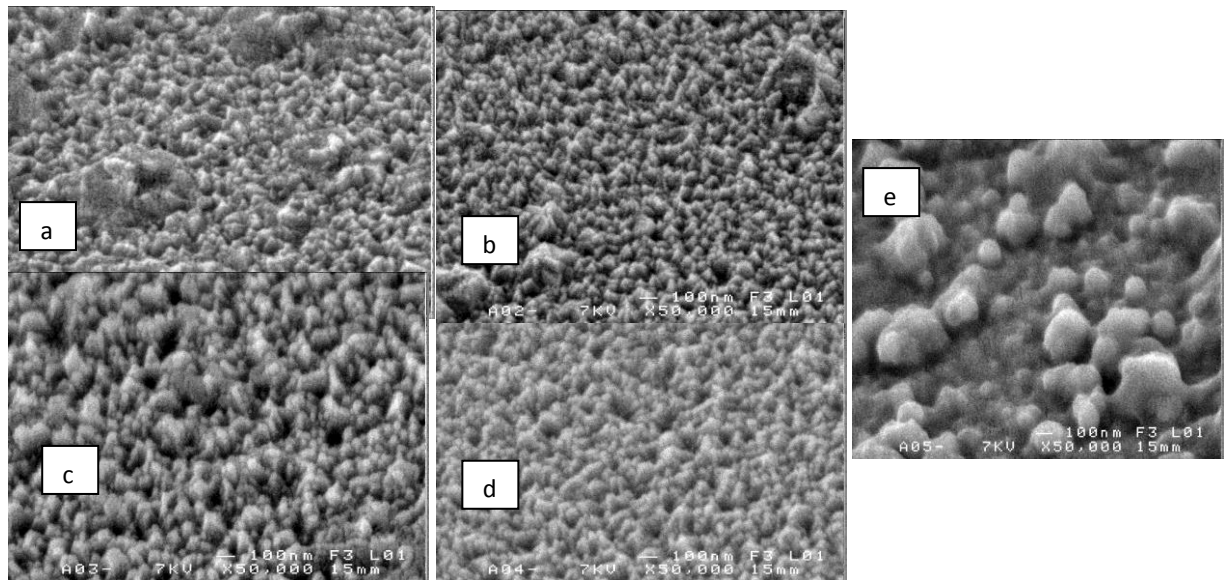


**Figure III. 5.** SEM surface images of the  $\text{In}_2\text{O}_3$  thin films deposited at various growth rate.(a :1.728 nm/s , b:1.856 nm/s , c: 2.554 nm/s , d:2.801nm/s, e:4.291nm/s )

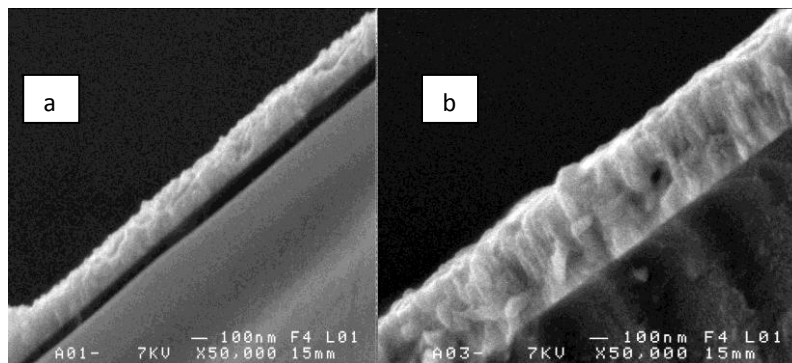


**Figure III. 6** SEM micrographs of the cross section of  $\text{In}_2\text{O}_3$  as a function of growth rate (a) 1.728 nm/s ,(b) 2.801 nm/s .

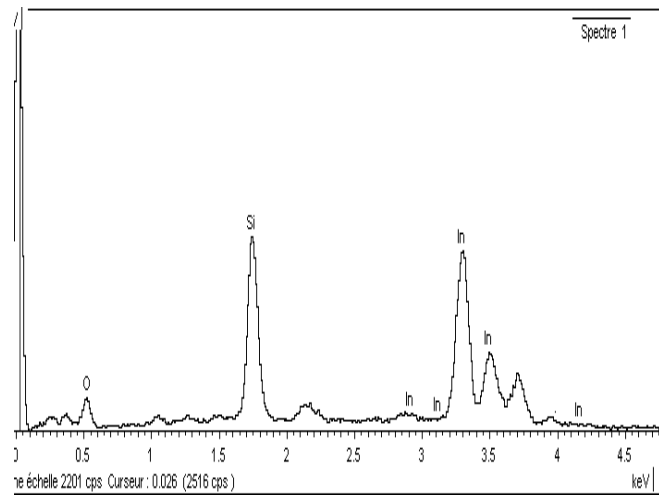


**Figure III. 7.** EDS analysis of the  $\text{In}_2\text{O}_3$  thin film deposited at 2.554 nm/s.

### III.5. Optical properties.

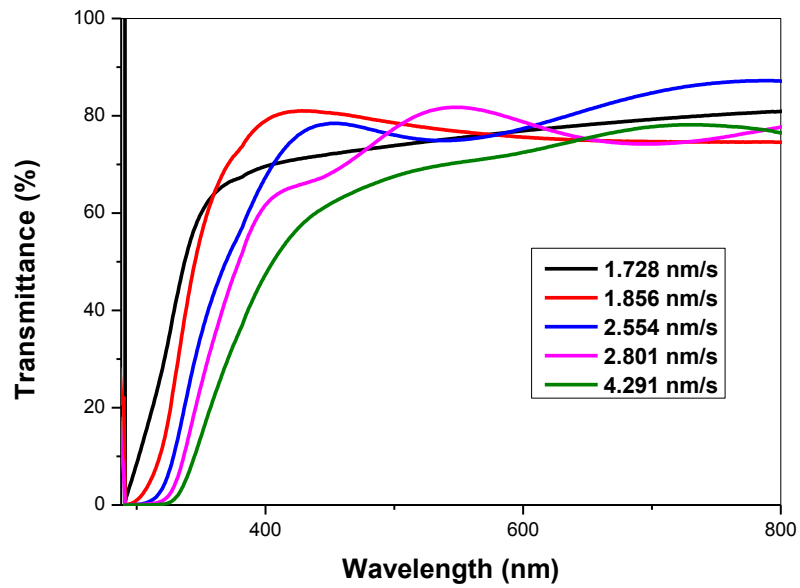


**Figure.III .8.** Optical transmittance spectra of  $\text{In}_2\text{O}_3$  thin films as a function of growth rate.

The transmittance spectra in UV–visible region of the prepared  $\text{In}_2\text{O}_3$  films are shown in Fig.8. We note that the growth rate affects the optical transmittance, whereas in the film deposited at low growth rate (1.728 nm/s), the transmittance is lower than the others except 4.291 nm/s although it has the smallest thickness. This result opposes with the previous different studies where they found that the lower thickness has higher transmittance[15]. We can explain our result depending on the structure and the morphology of the films, whereas this sample has poor crystallinity and random orientation thickness as presented in Fig.5. This leads to more light scattering [16,17,18] .

The energy loss due to light scattering and the microstrain is higher than other films; thus, it renders low optical transmittance. Furthermore, the optical transmittance in the rest of the films is higher than the last. Enhanced light transmitting due to continuous grain growth which is the best crystallinity films and of a reduced microstrain's effects, but in the high growth rate 4.291 nm/s, we have seen that the transmittance is smaller than all the films; it can be explained by the thickness of the film. It was found that there is an inversely relation between the transmittance and the thickness of the films. We have concluded that the films have structural homogeneity and the best crystallinity leading to less light scattering effects and higher transmittance. Moreover, with the increasing of the growth rate the absorption edge was moved to greater wavelengths suggesting the decrease of the energy band gap in the films.

The energy band gap  $E_g$  was calculated by relationship [19]. It is the energy band gap of the semiconductor which was evaluated by proposing a direct transition between valence and conduction bands.

Fig.9 shows the typical variation of the quantity  $(\alpha h\nu)^2$  as a function of photon energy, inset shows the optical band gap energy as a function of growth rate. As we can see there is a decrease in the values of the optical band gap from 3.93 to 3.62 eV with an increase in the growth rate. It may be due to the increase of the lattice parameter. It is well-known that the various factors such as grain size, carrier concentration, presence of impurities, deviation from stoichiometry of the film and lattice constants change the  $E_g$  value[20]. Additionally, the film

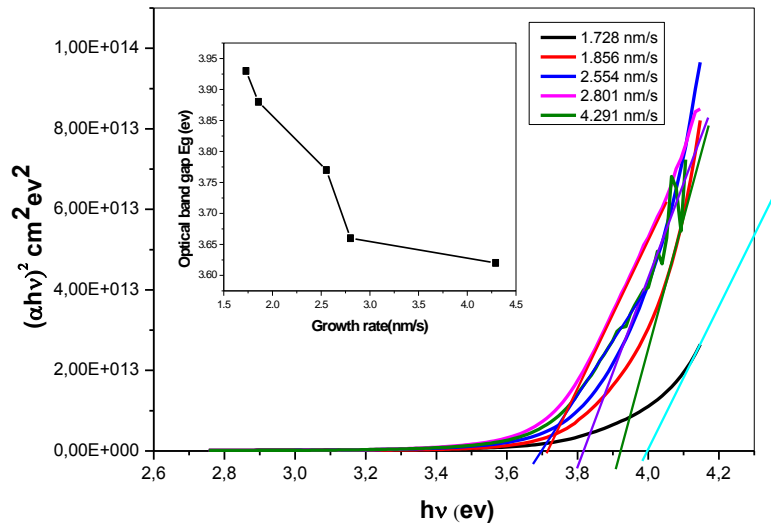


**Figure III. 9.** Typical variation of the quantity  $(\alpha hv)^2$  as a function of photon energy, inset shows optical band gap energy with various growth rates.

thickness increases resulting in a reduction of the band gap due to the localized states in the band structure which may amalgamate with the band edges given in the literature [21,22,23]. Furthermore, it is interesting to note that a high value of band gap can be correlated with the preferential orientation of the (222) plane. Similar behaviour in spray deposited  $\text{In}_2\text{O}_3$  thin films where there is a high value of optical band gap which is obtained in the films deposited at low growth rate, whereas the peak (222) is the preferential orientation .

The band gap is related to the oxidation of the components due to the oxygen concentration of the films in oxide semiconductors[22].

The formation of band tails due to the localized states which appear near the bands edges, and this leads to the disorder in film lattice showing in inset Fig. 9. In the low energies range, the photons are absorbed by these band tail states .

Fig .10 shows the disorder energy values variations with the growth rate. The enhancement in the disorder energy values with the variation of growth rate which is changed due to the film growth mechanism, whereas at low growth rate the droplets is arrived slowly on surface substrate then they occupy a favorable site and organize themselves formally. However in high growth rate, the formation of the films are quickly leading to more disordered lattice. We also observe an inverse relation between the band gap and band tail as it shown in Fig .10. This is clear physically at the enhancement in the band tail that leads to the reduction of band gap presented in inset Fig .9.

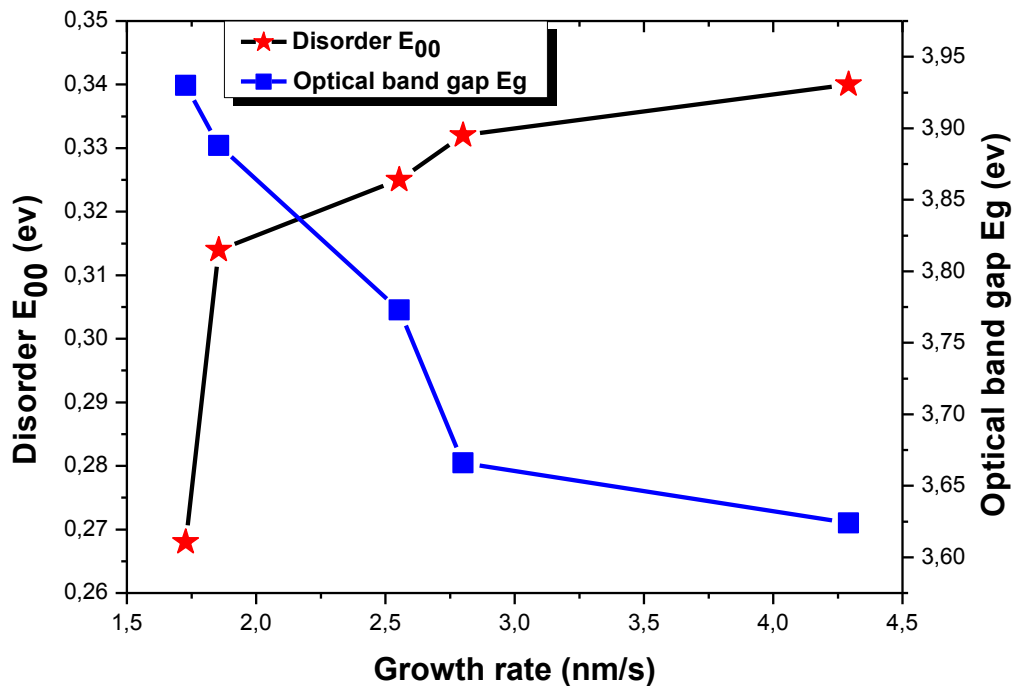


**Figure III .10.** Variations of the optical band gap and disorder in thin films as a function of the growth rate.

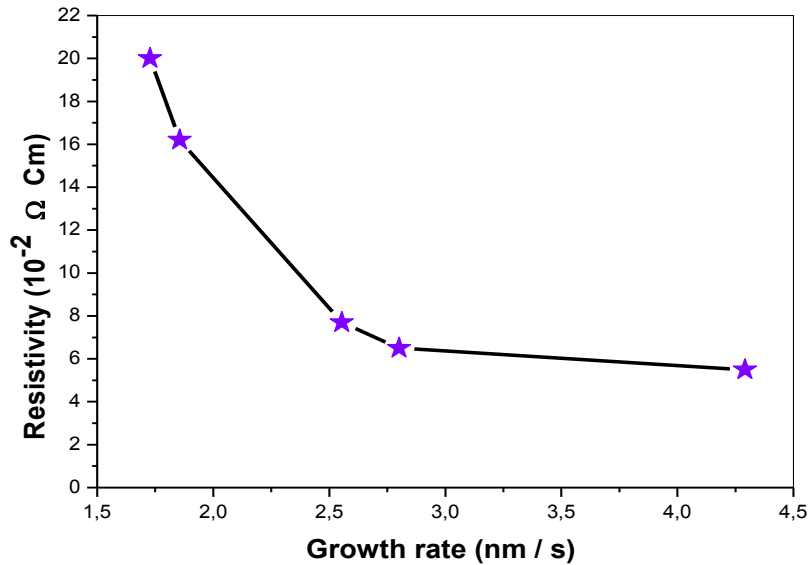


**Figure III. 11.** Electrical resistivity of  $\text{In}_2\text{O}_3$  thin film with various growth rates.

### III.6. Electrical properties:

Fig.11 shows the electrical resistivity ( $\rho$ ) as a function of the growth rate. The resistivity decreases with the increase in the growth rate. This is due to the quantity of oxygen in the films because as was noted already that the lower oxidation due to the deficiency of oxygen quantity in the films causes an increasing growth rate. It is common and physically reasonable that in oxygen deficient films, the carriers are resulted by the oxygen vacancies and the edge of conductivity band are formed by the defect of oxygen vacancies and/or in interstitials levels. Consequently, these impurity levels are responsible for low resistivity. Another reason leads to the decrease of resistivity values that can be attributed to the improvement of the crystallization; however in our case, we believe that the improvements in the crystalline state don't affect the electrical properties because the growth of  $\text{In}_2\text{O}_3$  crystallite almost stops as we said in The XRD results. On the other hand, it was observed that the resistivity of the films with (400) preferred plane is lower than the (222) preferred plane [11,23].

### III.7 . Conclusions:

Indium oxide thin films are prepared by ultrasonic Spray technique onto glass substrates. An investigation of the influence of the growth rate on films properties is carried out. X-ray diffraction studies indicated that the nature of films is Polycrystalline, while the predominant plane in the film changes from normally occurring (222) plane to (400) plane. It is very sensitive to growth rate and the microstrain generally decreases with an increasing growth rate. As we have noted that the microstrain of (400) orientation is always smaller than that of (222) orientation and the dislocation density decreases with the growth rate increasing. These results indicate an improvement in the structural films. SEM images show that the films have homogeneous surface that is relatively rough. The morphology does not change significantly except for the last film with a change in the preferential growth orientation. As we found that the variation of the growth rate affected the optical properties of the films, whereas the films homogenous in structure and of the best crystallinity lead to less light scattering effects and a higher transmittance (about 80% in the visible region). The increase in growth rate leads to a decrease in the optical gap (from 3.93 to 3.62 eV), and the electrical resistivity ranges from 20 to 5.5 ( $10^{-2} \Omega \text{ Cm}$ ).

## References

- [1] Z. Qiao, R. Latz, D. Mergela, Thickness dependence of  $\text{In}_2\text{O}_3:\text{Sn}$  film growth, *Thin Solid Films*. Vol. 466, (2004) 250
- [2] A. Bouhdjer, A. Attaf, H. Saidi, H. Bendjedidi, Y. Benkhetta, and I. Bouhaf, Correlation between the structural, morphological, optical, and electrical properties of  $\text{In}_2\text{O}_3$  thin films obtained by an ultrasonic spray CVD process, *Journal of Semiconductors*. Vol. 36, (2015) 8
- [3] G. Korotcenkov, V. Brinzari, A. Cerneavski, A. Cornet, J. Morante, A. Cabot, J. Arbiol, Crystallographic characterization of  $\text{In}_2\text{O}_3$  films deposited by spray pyrolysis. *Sensors and Actuators B: Chemical*, *Sens. Actuators B*. Vol. 84 (2002) 37–42
- [4] K.H.L. Zhang, A. Walsh, C.R.A. Catlow, V.K. Lazarov, R.G. Egdell, Surface Energies Control the Self-Organization of Oriented  $\text{In}_2\text{O}_3$  Nanostructures on Cubic Zirconia. *Nano Letters*. Vol. 10, (2010) 3740–3746
- [5] E. Terzini, Mater, Properties of ITO thin films deposited by RF magnetron sputtering at elevated substrate temperature. *Sci. Eng. B*. Vol. 77, (2000) 110
- [6] D.P. Pham, B. T. Phan, V. D. Hoang, H. T. Nguyen, T. K. H. Ta, S. Maenosono, C. V. Tran, Control of preferred (222) crystalline orientation of sputtered indium tin oxide thin films, *Thin Solid Films*. Vol. 570, (2014) 16–19
- [7] S.W. Sun, L.D. Wang, H.S. Kwok, Improved ITO thin films with a thin ZnO buffer layer by sputtering, *Thin Solid Films*. Vol. 360, (2000) 75
- [8] D. Raoufi, L. Eftekhari, Crystallography and morphology dependence of  $\text{In}_2\text{O}_3:\text{Sn}$  thin films on deposition rate. *Surface & Coatings Technology*, 274 (2015) 44–50.
- [9] Y. Benkhetta, A. Attaf, H. Saidi, A. Bouhdjar, H. Benjdidi, I. B. Kherchachi, Influence of the solution flow rate on the properties of zinc oxide (ZnO) nanocrystalline films synthesized by ultrasonic spray process, M. Nouadji, N. Lehraki, *Optik*. Vol. 127, (2016) 3005–3008
- [10] G. Korotcenkov, V. Brinzari, M. Ivanova, A. Cerneavski, J. Rodriguez, A. Cirera, A. Cornet, J. Morante, Structural stability of indium oxide films deposited by spray pyrolysis during thermal annealing, *Thin Solid Films*. Vol. 479, (2005) 38–51 (2005).

- [11] L.S.Palatnik, M.Y.Fuks, V.M.Kosevich, Mechanism of Formation and Substructure of Condensation Films, Moscow, Science, (1972) 320
- [12] L.I.Maissel, R.Glang (Eds.), Handbook of Thin Film Technology, McGraw-Hill Book Company, New York, USA, (1970).
- [13] Z. Qiao, D. Mergel, Comparison of radio-frequency and direct-current Magnetron sputtered thin  $\text{In}_2\text{O}_3:\text{Sn}$  films, Thin Solid Films. Vol. 484, (2005) 146-153
- [14] I. B. Kherchachi, A. Attaf, H. Saidi, A. bouhdjar, H. bendjidi, B. Youcef and R. Azizi, The synthesis, characterization and phase stability of tin sulfides ( $\text{SnS}_2$ ,  $\text{SnS}$  and  $\text{Sn}_2\text{S}_3$ ) films deposited by ultrasonic spray. Main Group Chemistry, Vol.15 (2016) 231–242
- [15] P.Prathap, N.Revathi, K.T.Ramakrishna Reddy, R.W.Milesb, Mg-composition induced effects on the physical behavior of sprayed  $\text{Zn}_{1-x}\text{Mg}_x\text{O}$  films, Thin Solid Films. Vol. 518, (2009) 1271–1278.
- [16] P.Prathap, Y.P.V.Subbaiah, M.Devika, K.T.Ramakrishna Reddy, Optical properties of  $\text{In}_2\text{O}_3$  films prepared by spray pyrolysis. Materials Chemistry and Physics, Mater.Chem.Phys. Vol.100, (2006) 375-379.
- [17] P.Prathap, G.Gowri Devi, Y.P.V.Subbaiah, K.T.Ramakrishna Reddy, V.Ganesan, Cur. Appl.Phys. Vol.8, (2008) 120
- [18] N.G.Pramod, S.N.Pandey, Ceramics International, Influence of Sb doping on the structural, optical, electrical and acetone sensing properties of  $\text{In}_2\text{O}_3$  thin films. Ceramics International, Vol. 40, (2014) 3461–3468
- [19] A. Bouhdjer, A. Attaf, H. Saidi, Y. Benkhetta, M.S. Aida, I. Bouhaf, A. Rahil, Influence of annealing temperature on  $\text{In}_2\text{O}_3$  properties grown by an ultrasonic spray CVD process, Optik. Vol. 127, (2016) 6329–6333
- [20] N.G.Pramod, S.N.Pandey, Effect of Li doping on the structural, optical and formaldehyde sensing properties of  $\text{In}_2\text{O}_3$  thin films. Ceramics International, Ceramics International. Vol.41, (2015) 527–532

[21] M.Higuchi, S.Uekusa, R.Nakano, K.Yokogawa, Micrograin structure influence on electrical characteristics of sputtered indium tin oxide films. *Journal of Applied Physics*, Vol. 74, (1993) 6710

[22] P.Thilakan, J.Kumar, Oxidation dependent crystallization behaviour of IO and ITO thin films deposited by reactive thermal deposition technique, *Materials Science and Engineering B*. Vol.55, (1998) 195–200

[23] P.Thilakan, J. Kumar, Studies on the preferred orientation changes and its influenced properties on ITO thin films, *Vacuum*. Vol.48, (1997) 463-466

## **CHAPTER IV:**

# **INFLUENCE OF INDIUM ACETATE ON PROPERTIES OF INDIUM OXIDE THIN FILMS**

## IV .1 Introduction:

Indium oxide is one of transparent conductive oxides (TCOs) , the properties of indium oxide films are related to preparation conditions and processes parameters like substrate temperature [1], flow rate [2], annealing [3], solution concentration [4], temps of deposition [5], and doping [6]. Moreover, the variety of the precursor solutions to prepare the  $\text{In}_2\text{O}_3$  thin films; the initial materials used are usually  $\text{InCl}_3$  [7,8], sometimes  $\text{InNO}_3$  [9,10] and rarely indium acetylacetonate (In-acac) [11]. In this work, indium acetate is used as precursor by ultrasonic spray method.

The main aim of this work is to obtain  $\text{In}_2\text{O}_3$  films with suitable properties for optoelectronic application can be used as transparent conductive oxide (TCO) thin films in order to reduce the losses during photovoltaic conversion, through studying the effect of molar concentration with very small values varying from 0.025M to 0.125M to reduce the fabrication cost and make it economically more viable. The effect of these parameters on structural, optical and electrical properties of  $\text{In}_2\text{O}_3$  films has been investigated.

## IV.2. Growth rate:

Fig.1 shows the growth rate's variation as a function of molar concentrations; in addition to another smaller figure found within Fig.1 which is about the films thickness. As it can be seen, the growth rate is almost linear with the increase of molar concentration from 0.025 to 0.1 M; after that, the diminution in growth rate is observed when molarities are greater than 0.1 M. This diminution in growth rate is due to the saturation of  $\text{In}_2\text{O}_3$  layer growth because of higher molar concentration; the quantum oxygen molecules of the solvent may not be sufficient to increase the growth rate which leads to the saturation of the reactants on the surface substrate; however, at the lower molar concentration, the continuous adsorption of the solution leads to the linear growth. The same results are observed at CuS thin films [12]; they found that the films deposited with concentrations above 0.1M contain the reduction in the thickness which may be because of the outer porous films formation which lead to developing stress , so it happens delamination leading to peeling off the films [13].

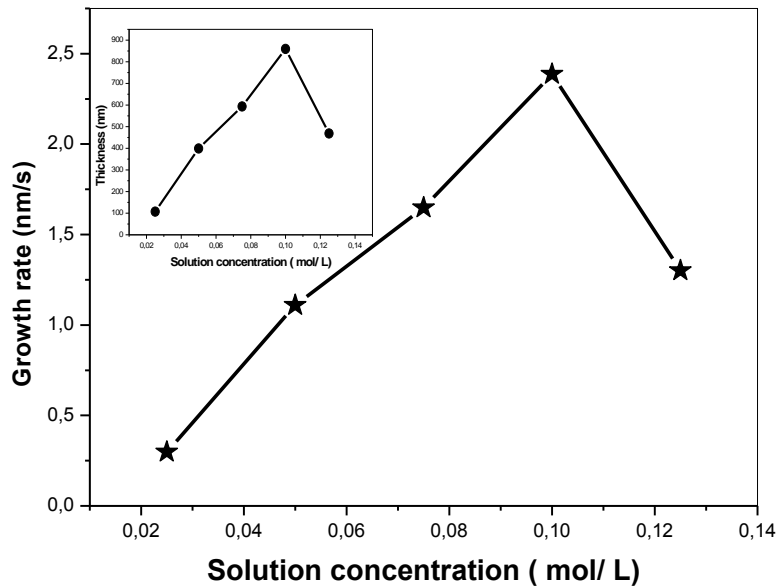
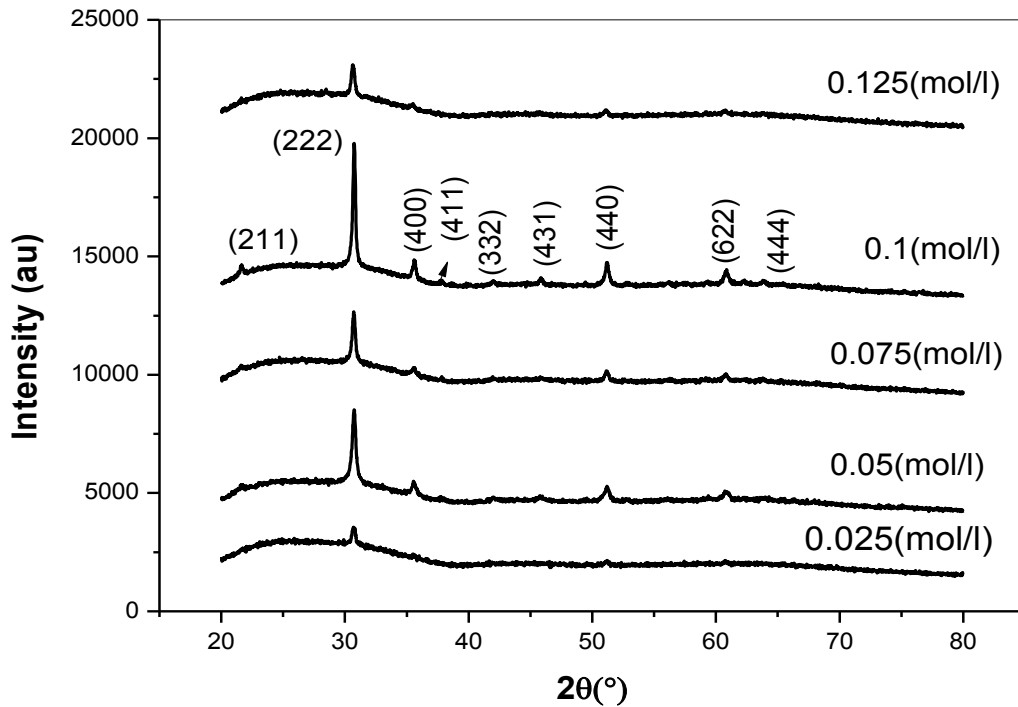


**Figure IV. 1.** Variation of growth rate as a function of solution concentration and inset shows film thickness dependence on solution concentration.

### IV .3 XRD Analysis :

The XRD patterns of  $\text{In}_2\text{O}_3$  films deposited at different molar concentration showed in Fig.2 The pattern indicates that the films are polycrystalline and shows clearly the rise in the peak intensity of the (222) with the increase of molar concentrations. This confirms the increase in crystallinity due to higher molar concentration until 0.1 M . Furthermore, the rise of metal ions number which grew in the predominant orientation (222) with the best crystallinity, except for the last film deposited at 0.125 M. the peak intensity of the (222) decreases and can be attributed at the higher molar concentration due to the quantum of oxygen that may not be suitable to increase the growth rate which leads to the saturation of the reactants on the surface substrate resulting the saturation of  $\text{In}_2\text{O}_3$  film growth [14]. As it can be seen, other peaks lower intensities like (400), (411) ...(see Fig .2). This result submits that the molar concentration affects the crystallinity of films as well as crystallites orientation in them. On another hand, the glass substrate is an amorphous material; the growth of the films usually occupies place by nucleation with the random orientations. Then, the growth of nuclei is followed by coalescence [7]. This growth of nuclei on substrate may be with different orientations as we noticed that the crystals grew along the

preferred orientation (222) and small amount of crystals grew along other orientations because the surface energy of the (222) orientation of  $\text{In}_2\text{O}_3$  is lower than other crystallographic orientations [15].



**FigureIV. 2.** XRD pattern of  $\text{In}_2\text{O}_3$  thin films deposited with different molar concentration .

The full width of the half maximum (FWHM) of XRD line may be because of the crystallite size or the microstrain, whereas the crystallite size ( $D$ ) of the  $\text{In}_2\text{O}_3$  films is associated with (FWHM) by the classical formula of Scherrer given by [16].The number of film defects was calculated from the crystallite size values  $D$  by the relationship of the dislocation density ( $\delta$ ) [17]

The mechanical strain in the films depends on two main influences which appear in metal oxide films [18].The first one is a variation in the coefficients of thermal expansion of the materials of growing film and substrate. The second one is a deflection of growing film composition from stoichiometry which lead probably to

strain in the lattice of growing film. The microstrain  $\epsilon$  in the films is also correlated with (FWHM) by [16].

Fig.3. shows the variations of the crystallite size, the microstrain and dislocation density in the films as a function of molar concentration. It was found that the crystallite size is almost constant when the molar concentration is less than 0.075 M, but up to last value, an increase in crystallite size to 32.7 nm at 0.1 M is noticed. The increase in crystallite size may be due to the rise of the metal ions number which reaches the substrate, and the gathering increases in the centers of nucleation and their growth leading to the larger crystallites [19,20].

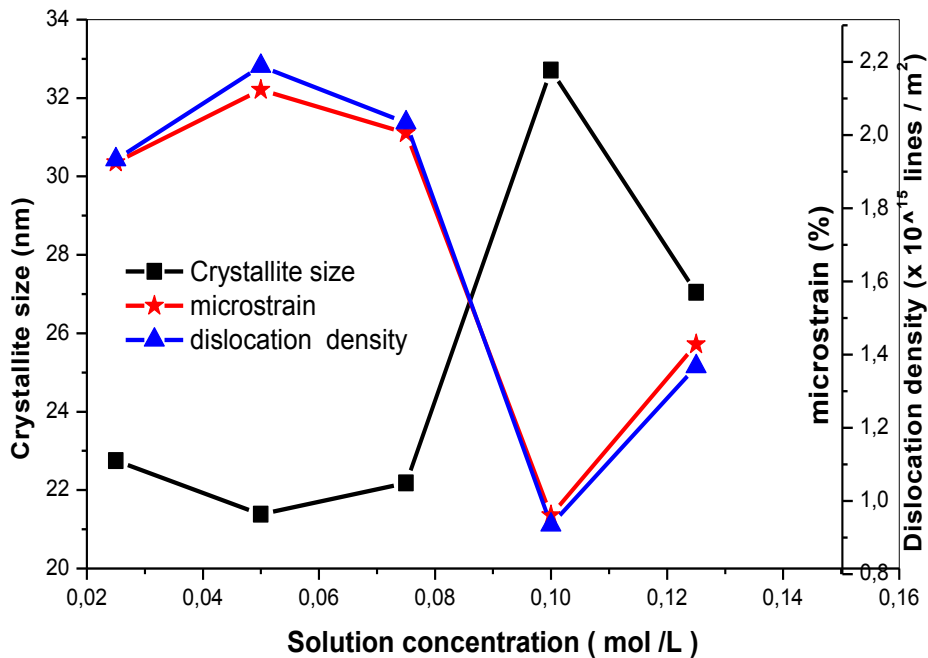


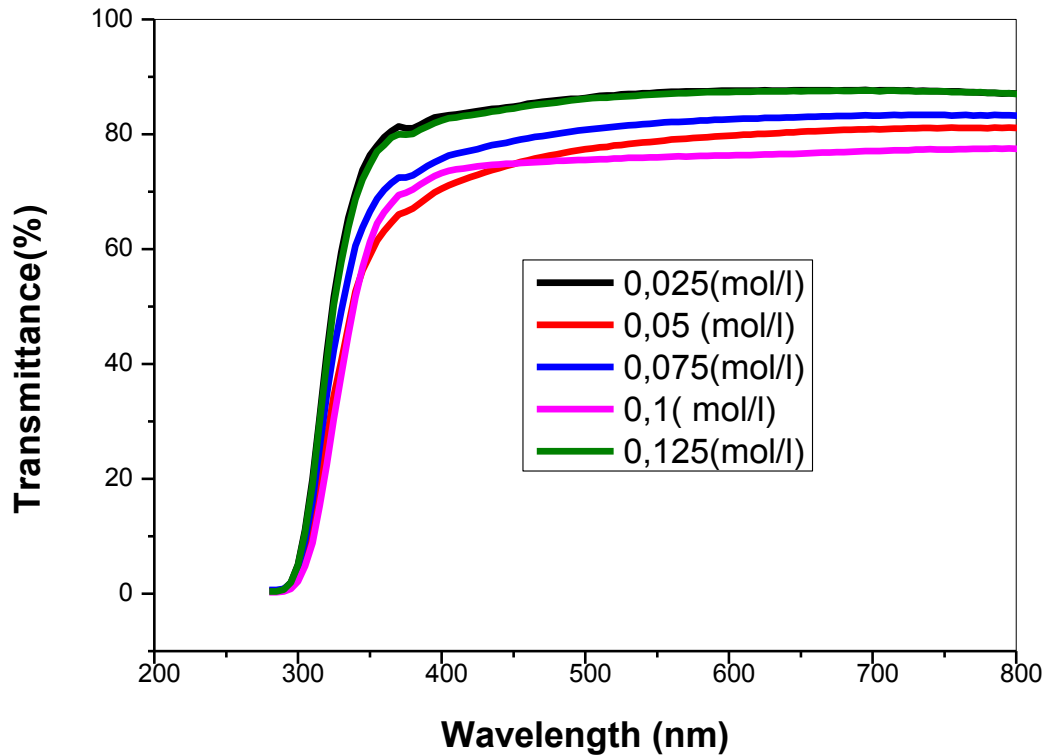
**Figure IV. 3.** The variations of the crystallite size, the microstrain and dislocation density in the films as a function of molar concentration.

It may be due to the electrostatic interaction between solute particles when increasing the amount of solution: it becomes larger resulting in the formation of a collection [21]. Then, it decrease to 27 nm for the molar concentration of 0.125 M. The decrease of the crystallite size by increasing molarity beyond 0.1 M may be because of the process of nucleation is affected by the rise of the particle solute which becomes quicker than other films because the increase of nucleation centers densities which

lead to the small crystallites [22]. In addition, the decrease of crystallite size due to the degradation in crystallinity causes the structural defects in the films [23,24]. It was also noted that there is an inverse relationship between crystallite size and microstrain . Due to the decrease of microstrain with the increase in molar concentration, the crystallinity becomes better up to 0.1 M and it is also observed that there is a harmony between dislocation density and the microstrain. It means the crush of grain is helped by the dislocation density [25,26]. Larger  $D$  and smaller  $\delta$  values mean better crystallization of the films deposited at 0.1 M .

#### **IV.4 UV-VIS transmittance Analysis:**

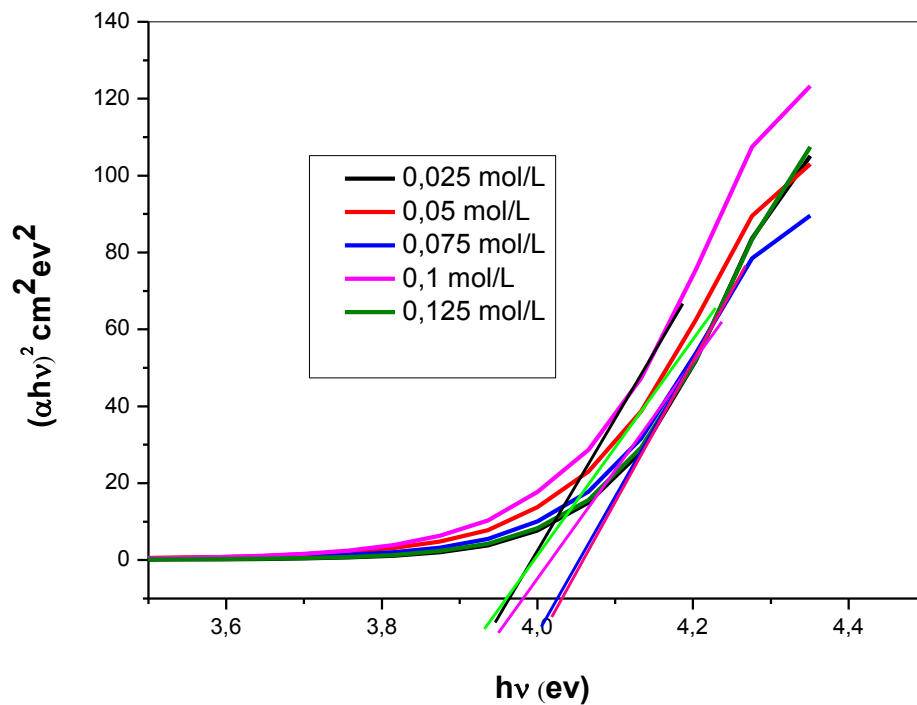
The optical transmittance spectrum of the  $\text{In}_2\text{O}_3$  films as a function of the wavelength is presented in Fig.4 for different molar concentration . In the visible range, the average optical transmittance of the films varies between 73 and 87 % . Generally, the transmittance decreases with the increase of the films thickness except for the film deposited at 0.05 M which has both lower thickness and low transmittance and that can be explained by the scattering light and morphology surface; similar result found that [27,1] .



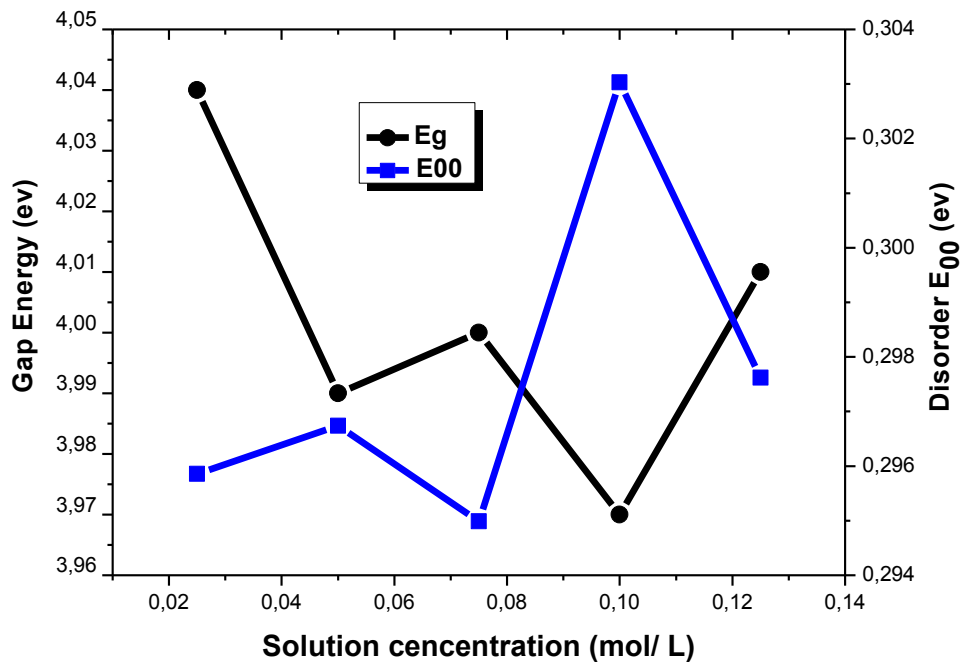
**Figure IV.4.** Optical transmittance spectra of  $\text{In}_2\text{O}_3$  thin films at different of molar concentration.

The disorder in the materials changed the Urbach tail which results in the extension of the parabolic density states in the band edge. Among these disorders, the structural disorder resulting from the defects and impurities in the films or the thermal disorder is caused by thermal occupation of the states of phonon [28]. Fig.6 shows the values of optical band gap and disorder energy together with the variation in the molar concentration. In general, it is observed that the optical band gap values decreases with the increasing in the molar concentration and that may be due to many factors like the increasing in films thickness, deviation from stoichiometry of the film, lattice constants, carrier concentration and presence of impurities [6] And similar behavior is observed in ZnO films [29], they are explained by various mechanisms which cause the shifts of gap such as: (i) crystallinity degradation, (ii) the change of the crystallite dimension which leads to modifications in the height of the barrier, (iii) the effects of quantum size, (iv) the impurities density and (v) compressive or tensile strains. Furthermore, it is interesting to find that inverse relation between the band gap

and band tail because when the molar concentration increases, the films thickness increase leading to the localization of the states in the band structure that is merged with the band edges resulting in the reduction of the band gap [30,31]. Said Benramache and all have found that the correlation between the structural and optical properties of Co doped ZnO is investigated. They have estimated the relationships between the band gap and the structural parameters as a function of the average crystallite size and the intermediate strain [32].



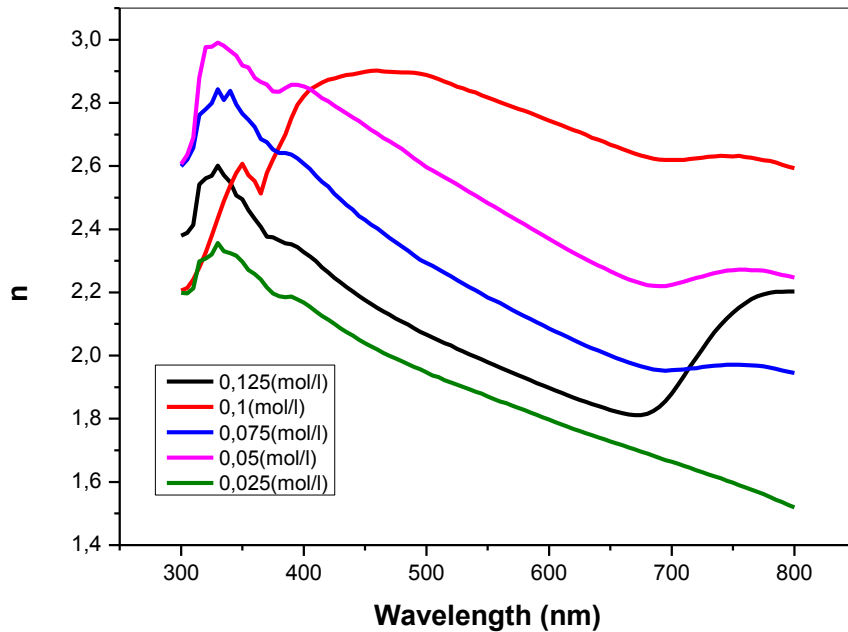
**Figure IV.5.** Typical variation of the quantity  $(\alpha h\nu)^2$  as a function of photon energy with various solution concentration .



**Figure IV. 6.** Variation of the optical band gap and disorder in thin film as a function of solution concentration .

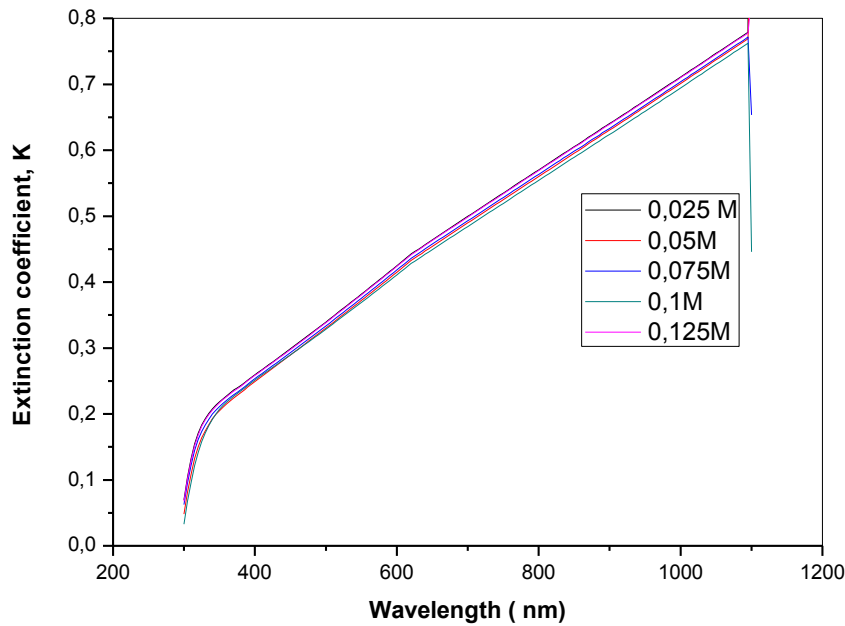
#### IV.5. Reflectance Analysis :

Fig.7 shows the variation of refractive index ( $n$ ) as a function of the wavelength. The value of  $n$  is found to vary in the range 1.52-2.99 for different molar concentrations when the wavelength increases, it is observed that the decrease is continuous in the refractive index of  $\text{In}_2\text{O}_3$  films. As noted at the absorption edge, the values of this refractive index have maximum values. Similar observation reported by other authors [11]. On another hand, it is noticed that the values of refractive index increase with the increase in thickness of films, and this may be causing the density of grains in the films because the refractive index is significant to reveal the packing density. Bragg and Pippard model determined this [33]. Also, Harris and all have modified it [34].



**Figure IV.7** variation of refractive index ( $n$ ) as a function of the wavelength with various solution concentration

The variation of extinction coefficient ( $k$ ) values for  $\text{In}_2\text{O}_3$  films are shown in Fig.8 It varies in the range 0.05 -0.77 for different molar concentrations. At the low wavelengths ( $\leq 333 \text{ nm}$ ), we observed low extinction coefficient value of our films. Above these wavelengths, the extinction coefficient increases with the rise in the wavelengths which may be due to the existing of vacuum in the films and the limits of their grains and appears to have a slight change of the extinction coefficient with a different molar concentration. This change corresponds with the thickness of the films (molar concentration), whereas the increase in this latter leads to a decrease in the extinction coefficient values. As we noted, the lower extinction coefficient values in the films deposited at 0.1 M may cause an improvement in the crystallinity and minimum impurity. However, the low extinction coefficient value is related to the stellar surface smoothness of the films [35].



**Figure IV.8.** Variation of extinction coefficient (K) as a function of the wavelength with various solution concentration .

#### IV.6. FTIR Analysis:

Fig.9 shows the Fourier transform infrared (FTIR) spectrum of  $\text{In}_2\text{O}_3$  films deposited on glass substrate. The In-O and In-In stretching vibrations are found in the region  $800\text{--}300\text{ cm}^{-1}$  [36,37]. The In-O stretching is usually observed in the region  $700\text{--}300\text{ cm}^{-1}$  [56]. In this spectrum, it is observed that the bands absorptions around ( $500, 600\text{ cm}^{-1}$ ) are due to the In-O vibrations , but the band absorptions at ( $1050\text{ cm}^{-1}$ ) is attributed to the absorption of C-O vibrations [38]; moreover, a low absorption at  $1568\text{ cm}^{-1}$  is shown on the IR spectrum of the layers that may indicate the C=O vibrations [39,40] and those at  $2916\text{ cm}^{-1}$  and  $2837\text{ cm}^{-1}$  can be attributed to the C-H vibrations of the organics [38]. Generally, we also watched that the intensity of this band increases with the increasing of concentration of the solution which because of the improvement crystallinity of the films. These results confirm the results obtained from X-ray diffraction (XRD).

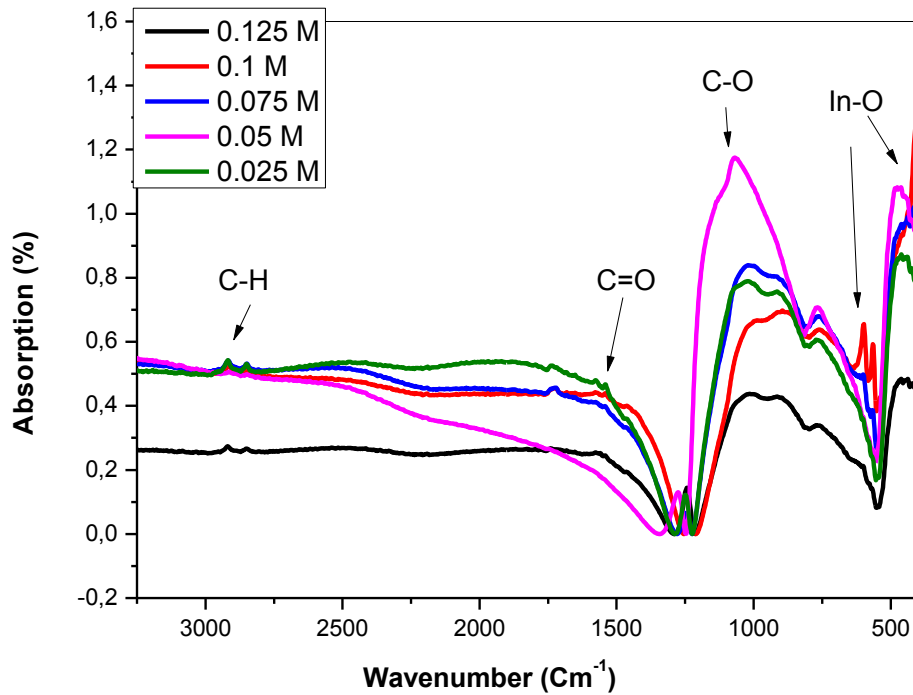


**Figure IV.9.** Fourier transform infrared (FTIR) spectrum of  $\text{In}_2\text{O}_3$  films with various solution concentration .

### IV.7 Electrical study:

Fig.10 shows that the electrical resistivity and the conductivity as a function of the concentration of solution. It is noticed that the electrical resistivity almost constant in the small solution concentrations (less than 0.1 M). At this values, the resistivity decreases to low value may be due to the rise of the free carriers by increasing atoms of Indium in the interstitial location .As we can see, this reduction of resistivity might be because the improvement of crystallinity. This is consistent with the results of DRX, whereas when the grain size increases, the density of grain boundaries decreases and the mobility increases resulting in the decrease of the electrical resistivity. After that value ( $> 0.1 M$ ), the electrical resistivity increases and that can be explained by the degradation of crystallinity, the reduction in the film thickness, the rise of structural defect and the grain boundaries which are considered as traps for the electrons. On another hand, the variation of the electrical resistivity can be also explained by the effect of oxygen quantum which have proportionate relationship between them. Several studies reported that [30,31], they found that the decreasing in

resistivity is due to the reduction in oxygen content of the films and the rise of carrier concentration. This might be because of the free electrons generated by the oxygen vacancies. As observed, there is an inversely relation between the electrical resistivity and the conductivity.

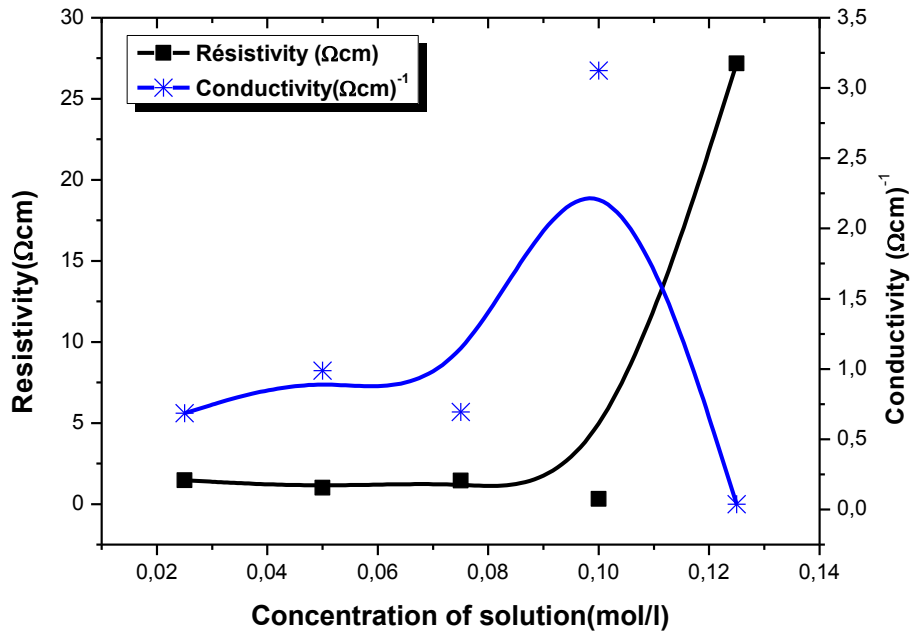


**Figure IV. 10** The electrical resistivity and the conductivity as a function of the concentration of solution.

#### IV.8.Conclusion:

$\text{In}_2\text{O}_3$  thin films deposited by ultrasonic spray using indium acetate as precursor solution with various molar concentration. The XRD, UV-VIS transmittance, Reflectance, FTIR and Electrical studies are presented. These films are of polycrystalline nature and show clearly the rise in the peak intensity of the (222) with an increase of molar concentrations, the grain size is almost constant when the lower molar concentration, but if there is an increase in this latter, the grain size increases due to the rise of the metal ions. As found, the larger  $D$  and smaller  $\delta$  values mean better crystallization of the films deposited at 0.1 M. The average optical transmittance of the films varies between 73 and 87 %. Usually, the transmittance decreases with an increase in the thickness of these films, while the optical band gap values decreases with an increasing in the molar concentration, and an inverse relation is found between the band gap and the thickness of these films because the localized states are formed in the band structure. The values of refractive index ( $n$ ) vary in the range 1.52-2.99. The extinction coefficient ( $k$ ) varies also in the range 0.05 -0.77. The FTIR spectrum indicates that these films are  $\text{In}_2\text{O}_3$  layers. The film prepared at 0.1 M presents a low resistivity. Through the analyses above, the optimal indium acetate concentration is 0.1 M.

## References

- [1] P. Prathap, Y.P.V. Subbaiah, M. Devika, K.T. Ramakrishna Reddy , Optical properties of  $\text{In}_2\text{O}_3$  films prepared by spray pyrolysis, *Materials Chemistry and Physics* .100 (2006) 375–379
- [2] A. Bouhdjer , H. Saidi , A. Attaf,\* , M.S. Aida , Mohamed JlassI , I. Bouhaf, Y.Benkhetta , H. Bendjedidi, Structural, morphological, optical, and electrical properties of  $\text{In}_2\text{O}_3$  nanostructured thin films, *Optik* .127 (2016) 7319–7325.
- [3] Nasreddine Beji, Meriem Reghima, Mehdi Souli, Najoua Kamoun Turki , Effect of nitrogen annealing on the structural, optical and photoluminescence properties of  $\text{In}_2\text{O}_3$  thin films, *Journal of Alloys and Compounds*. 675 (2016) 231- 235.
- [4] L.N. Lau, N.B. Ibrahim \*, H. Baqiah, Influence of precursor concentration on the structural, optical and electrical properties of indium oxide thin film prepared by a sol–gel method, *Applied Surface Science* . 345 (2015) 355–359.
- [5] Boen Houng , Su Lu Lin , Sih Wei Chen , Adam Wang , Influence of an  $\text{In}_2\text{O}_3$  buffer layer on the properties of ITO thin films, *Ceramics International* . 37 (2011) 3397–3403.
- [6] N.G. Pramod, S.N. Pandey, Effect of Li doping on the structural, optical and formaldehyde sensing properties of  $\text{In}_2\text{O}_3$  thin films, *Ceramics International* 41 (2015) 527– 532.
- [7] P.K. Manoj, K.G. Gopchandran, P. Koshy, V.K. Vaidyan, B. Joseph, Growth and characterization of indium oxide thin films prepared by spray pyrolysis, *Optical Materials*. 28 (2006) 1405–1411
- [8] G. Korotcenkov, A. Cerneavschi , V. Brinzari , A. Vasiliev , M. Ivanov , A. Cornet , J. Morante , A. Cabot , J. Arbiol ,  $\text{In}_2\text{O}_3$  films deposited by spray pyrolysis as a material for ozone gas sensors, *Sensors and Actuators B*. 99 (2004) 297–303
- [9] B.-C. Kim, J.-Y. Kim, D.-D. Lee, J.-O. Lim, J.-S. Huh, Effect of crystal structures on gas sensing properties of nanocrystalline ITO thick films, *Sens. Actuators B* . 89 (2003) 180–186.

- [10] J.-H. Lee, B.-O. Park, Transparent conducting  $\text{In}_2\text{O}_3$  thin films prepared by ultrasonic spray pyrolysis, *Surf. Coat. Technol.* 184 (2004) 102–107
- [11] M. Jothibas , C. Manoharan , S. Ramalingam , S. Dhanapandian , S. Johnson Jeyakumar , M. Bououdina , Preparation, characterization, spectroscopic (FT-IR, FT-Raman, UV and visible) studies, optical properties and Kubo gap analysis of  $\text{In}_2\text{O}_3$  thin films, *Journal of Molecular Structure* .1049 (2013) 239–249.
- [12] M.A. Sangamesha, K. Pushapalatha , G.L. Shekar, effect of concentration on structural and optical properties of CuS thin films, *International Journal of Research in Engineering and Technology* . 02 (2013) 11.
- [13] J. A. Thornton, The microstructure of sputter-deposited coatings, *J. Vac. Sci. Technol. A* 4 (1986) 3059.
- [14] A. Moses Ezhil Raj, K.C. Lalithambika et al , Growth mechanism and optoelectronic properties of nanocrystalline  $\text{In}_2\text{O}_3$  films prepared by chemical spray pyrolysis of metal-organic precursor, *Physica B*. 403 (2008) 544–554
- [15] F.O. Adurodija, L. Semple, R Brüning, Real-time in situ crystallization and electrical properties of pulsed laser deposited indium oxide thin films , *Thin Solid Films*. 492 (2005) 153.
- [16] H.P. Klug, L.E. Alexander, *X-ray Diffraction Procedures for Polycrystalline and Amorphous Materials*, Wiley, New York, 1974.
- [17] A. Akkari, M. Reghima, C. Guasch, N. Kamoun-Turki, Effect of copper doping on physical properties of nanocrystallized SnS zinc blend thin films grown by chemical bath deposition , *J. Mater. Sci.* 47 (2012) 1365–1371 .
- [18] L.S.Palatnik, M.Y.Fuks, V.M.Kosevich, Mechanism of formation and substructure of condensed films, *Moscow, Science* . (1972) 320 (in Russian)
- [19] Vignesh Saravanan, Prabakaran Shankar, Ganesh Kumar Mani , John Bosco Balaguru Rayappan, Growth and characterization of spray pyrolysis deposited copper oxide thin films: Influence of substrate and annealing temperatures, *Journal of Analytical and Applied Pyrolysis* . 111 (2015) 272–277

- [20] Chetoui Abdelmounaïm, Zouaoui Amara, Ayat Maha, Djebbouri Mustapha, Effects of molarity on structural, optical, morphological and CO<sub>2</sub> gas sensing properties of nanostructured copper oxide films deposited by spray pyrolysis, *Materials Science in Semiconductor Processing* 43 (2016) 214–221
- [21] T.P. Rao, M.C. Santhosh Kumar, Effect of thickness on structural, optical and electrical properties of nanostructured ZnO thin films by spray pyrolysis, *Applied Surface Science* 255 (2009) 4579–4584
- [22] Allag Abdelkrim, Saâd Rahmane, Ouahab Abdelouahab, Nadjate Abdelmalek, Gasmi Brahim, Effect of solution concentration on the structural, optical and electrical properties of SnO<sub>2</sub> thin films prepared by spray pyrolysis, *Optik* 127 (2016) 2653–2658
- [23] X.Y. Li, H.J. Li, Z.J. Wang, H. Xia, Z.Y. Xiong, J.X. Wang, B.C. Yang, Effect of substrate temperature on the structural and optical properties of ZnO and Al-doped ZnO thin films prepared by dc magnetron sputtering, *Optics Communication* 282 (2009) 247–252.
- [24] Said Benramache, Foued Chabane, Boubaker Benhaoua, and Fatima Z. Lemmadi, Influence of growth time on crystalline structure, conductivity and optical properties of ZnO thin films, *Journal of Semiconductors* Vol. 34, No. 2 (2013).
- [25] B.A. Taleatu, W.O. Makinde, M.A. Eleruja, A.Y. Fasasi, Band alignment and charge transport characteristics of TPP/ZnO hybrid for photovoltaic cell potential, *Curr. Appl. Phys.* 13 (2013) 97–102.
- [26] Mazabalo Baneto, Alexandru Enesca, Yendoubé Lare, Koffi Jondo, Kossi Napo, Anca Duta, Effect of precursor concentration on structural, morphological and optoelectric properties of ZnO thin films prepared by spray pyrolysis, *Ceramics International* 40 (2014) 8397–8404
- [27] N.G. Pramod, S.N. Pandey, Influence of Sb doping on the structural, optical, electrical and acetone sensing properties of In<sub>2</sub>O<sub>3</sub> thin films, *Ceramics International* 40 (2014) 3461–3468.

- [28] Cody GD, Tiedje T, Abeles B, Brooks B, Goldstein Y (1981). Theoretical study of the optical absorption edge in Amorphous Semiconductors. *Phys. Rev. Lett.*, 47: 1480-1486 .
- [29] Kamal Baba , Claudia Lazzaroni , Mehrdad Nikravech , ZnO and Al doped ZnO thin films deposited by Spray Plasma: Effect of the growth time and Al doping on microstructural, optical and electrical properties, *Thin Solid Films* . 595 (2015) 129 – 135.
- [30] P .Thilakan , J Kumar, Studies on the preferred orientation changes and its influenced properties on ITO thin films, *Vacuum* . 48(1997) 463 - 466 .
- [31]P.Thilakan, J.Kumar, Oxidation dependent crystallization behavior of IO and ITO thin films deposited by reactive thermal deposition technique , *Materials Science and Engineering B* .55(1998)195–200.
- [32]Said Benramache, Hachemi Ben Temam, Ali Arif, Abderrazak Guettaf, Okba Belahssen, Correlation between the structural and optical properties of Co doped ZnO thin films prepared at different film thickness, *Optik*. 125 (2014) 1816–1820
- [33] W.L. Bragg, A.B. Pippard, The form birefringence of macromolecules , *Acta Crystallogr.* 6 (1953) 865.
- [34] M. Harris, H.A. Macleod, S. Ogura, The relationship between optical inhomogeneity and film structure , *Thin Solid Films* 57 (1979) 173
- [35] D. Beena, K.J. Lethy, R. Vinodkumar, V.P. Mahadevan Pillai, V.Ganesan, D.M. Phase, S.K. Sudheer, Effect of substrate temperature on structural, optical and electrical properties of pulsed laser ablated nanostructured indium oxide films ,*Appl. Surf. Sci.* 255 (2009) 8334–8342.
- [36] V. Baranauskas, M. Fontana, Z.J. Guo, H.J. Ceragioli, A.C. Peterlevitz, Field-emission properties of nanocrystalline tin oxide films , *Sens. Actuat. B Chem.* 107 (2005) 474.
- [37] P. Manjula, L. Satyanarayana, Y. Swarnalatha, Sunkara V. Manorama, Raman and MASNMR studies to support the mechanism of low temperature hydrogen sensing by Pd doped mesoporous SnO<sub>2</sub>, *Sens. Actuat. B* 138 (2009) 28.

[38] C.Chen, D.Chen, X.Jiao, C.Wang, Ultrathin corundum-type  $\text{In}_2\text{O}_3$  nanotubes derived from orthorhombic  $\text{InOOH}$ : synthesis and formation mechanism, Chem. Commun. (2006) 4632

[39] D.Chu, YP.Zeng, D.Jiang, J. Xu, Tuning the phase and morphology of  $\text{In}_2\text{O}_3$  nanocrystals via simple solution routes, Nanotechnology 18(2007)435605-436 510

[40] Guodong Liu, Synthesis,Characterization of  $\text{In}_2\text{O}_3$  Nanocrystals and Their Photoluminescence Property , International journal of electrochemical science 6 (6) (2011) 2162-2170

## **CHAPTER V**

# **INFLUENCE OF THE SUBSTRATES ON PROPERTIES OF INDIUM OXIDE THIN FILMS**

## V.1 Introduction:

Photovoltaic cell and some optoelectronic devices are based on thin films as semiconductor material to build up it. The different parameters important are used to prepare these films by ultrasonic spray, including mechanisms for nucleation and growth or film thickness which it is affected by various processing conditions such as: precursors ,concentration, substrates type , heat treatment and film thickness [1]. And also the contamination and the presence of defects on the substrate surface influence on the growth, structure and properties of thin films. In the last years ,the used interesting of flexible substrates is increased in the electronics where it is investigated in three directions [2] : Materials for substrates ; Technology for deposition of different films ; Circuit applications . The growth films is created by the conditions of deposition and the choice of the substrates because both are important factors in this growth , also the substrate chosen must present a difference in suitable lattice less than 3% to have a good growth of the crystal on the substrate [3]. It is well known a thin film is created when the atoms arrives substrate surface. A structure-zone model [4], which it has been advanced to class the common regimes of film growth behavior. Also, the nucleation and coalescence processes are based on the bonding force between the substrate and the deposited atoms as well as the size and structure of islands in the initial formation.

In order to evaluate this ,it is examined  $\text{In}_2\text{O}_3$  thin films deposited with different substrates type ; Glass (called :  $\text{In}_2\text{O}_3$ / glass) , Corning glass (called :  $\text{In}_2\text{O}_3$  / Co. glass), Indium tin oxide (called :  $\text{In}_2\text{O}_3$  / ITO) and monocrystalline silicon (called :  $\text{In}_2\text{O}_3$  / Si) ; by the ultrasonic spray method where it is optimized the conditions in order to have a good quality  $\text{In}_2\text{O}_3$  thin films with developed suitable properties for many applications such as solar cells, gas sensors, emitting diodes (LEDs), etc.

## V.2 Growth rate:

The growth rate of the thin films was calculated by dividing the thickness on the deposition time. The growth rate results of  $\text{In}_2\text{O}_3$  thin films are shown in fig .1. It is observed that a different growth rate for various substrates type back to the difference of the bonding force between the substrate and the atoms of deposition which follow the different islands in the initial formation as result the different growth is taking its

place because the substrates have not the same bonds between their atoms. The growth steps and the form of the films which have seen in the first chapter. As The activation energy of growth process is lower than the activation energy of the nucleation process. There are a lot of nucleation mechanisms which define the crystal size and orientation, which in turn determine the film's properties. During the change in the substrates, each step will be different; hence, the formed films may be diverse. It is clear that the growth rate of both the thin films of indium oxide deposited on ( $\text{In}_2\text{O}_3$  / glass) and ( $\text{In}_2\text{O}_3$  / Co. glass) are higher than the others thin films deposited on ( $\text{In}_2\text{O}_3$  / ITO) and ( $\text{In}_2\text{O}_3$  / Si) that can be explained by the various surface morphology of substrate whereas, its defects effects on the film growth process. In addition, this difference in the growth rate may be attributed to the substrate temperature because it is the main parameter that determines the film properties whereas 400 °C is optimized temperature for deposited on the glass [5]. Xuemei Cheng and al, study the properties of  $\text{TiO}_2$  thin films deposited by reactive DC sputtering on glass and Si substrate .They found ; From the structure and morphology results; more anatase nuclei are formed on crystalline Si than on amorphous glass substrates which is presented in fig 2 . Also Hayk Khachatryan and al , Who study the effect of substrate type on Al thin film formation and morphology [6] , they found difference in the fundamental of film grown between the metallic substrate , glass and Si wafer. Which have seen in the previous chapters .

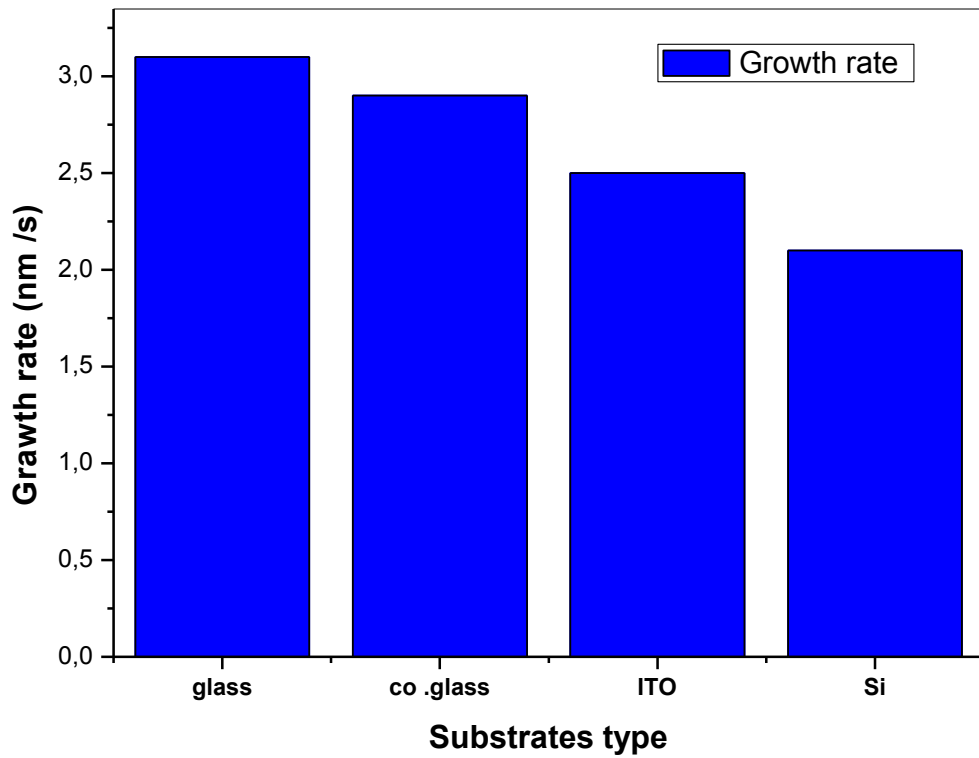


**Figure V.1:** The growth rate of  $\text{In}_2\text{O}_3$  films on different substrates.

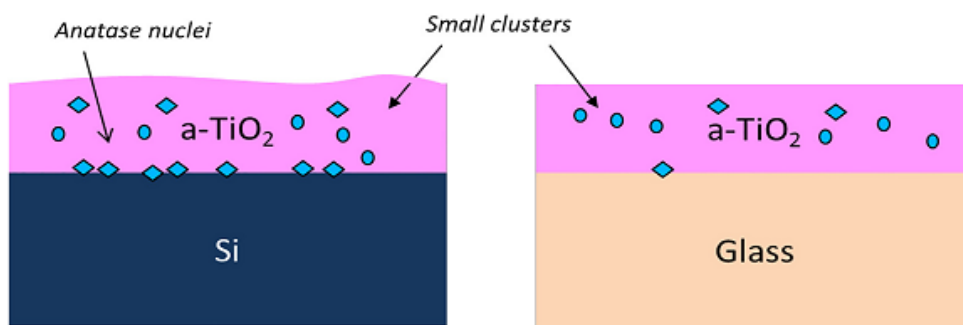


**Figure V.2:** Anatase nuclei  $\text{TiO}_2$  formed on Si (left) and glass (right) substrates [5].

### V.3 Structural properties:

Fig.3 shows XRD pattern of  $\text{In}_2\text{O}_3$  thin films deposited on a different substrates type. It is clear that the  $\text{In}_2\text{O}_3$  thin films reveal polycrystalline structure with various orientated crystalline planes such as (222), (321), (400), (411), (156),(611),(440) and (622) with all different substrates. The orientation intensity of ( $\text{In}_2\text{O}_3$  / Glass) and ( $\text{In}_2\text{O}_3$  /Co. glass) are higher than others which may be attributed to good crystallinity. The lower intensity can be explained by degradation of the crystallinity maybe for the attraction between the atoms of substrates and deposited atoms in the film ( $\text{In}_2\text{O}_3$  / ITO) following that the growth rate decreases while the film ( $\text{In}_2\text{O}_3$  / Si) has the lowest crystallinity back to mismatching ( $\text{In}_2\text{O}_3$  / Si) networks [7]. As it is observed the various the predominated orientation of growth with different substrates type used (see fig .4). The (400) orientation is the highest intensity in two films ( $\text{In}_2\text{O}_3$  / Glass) and ( $\text{In}_2\text{O}_3$  / Co.glass) but in others, the (222) is preferred orientation may be caused by the accumulation of the oxygen in the films. The highest surface free energy in the bixbyite structure in (400) orientation because of the oxygen ratio in the films which will repress in this growth [8].

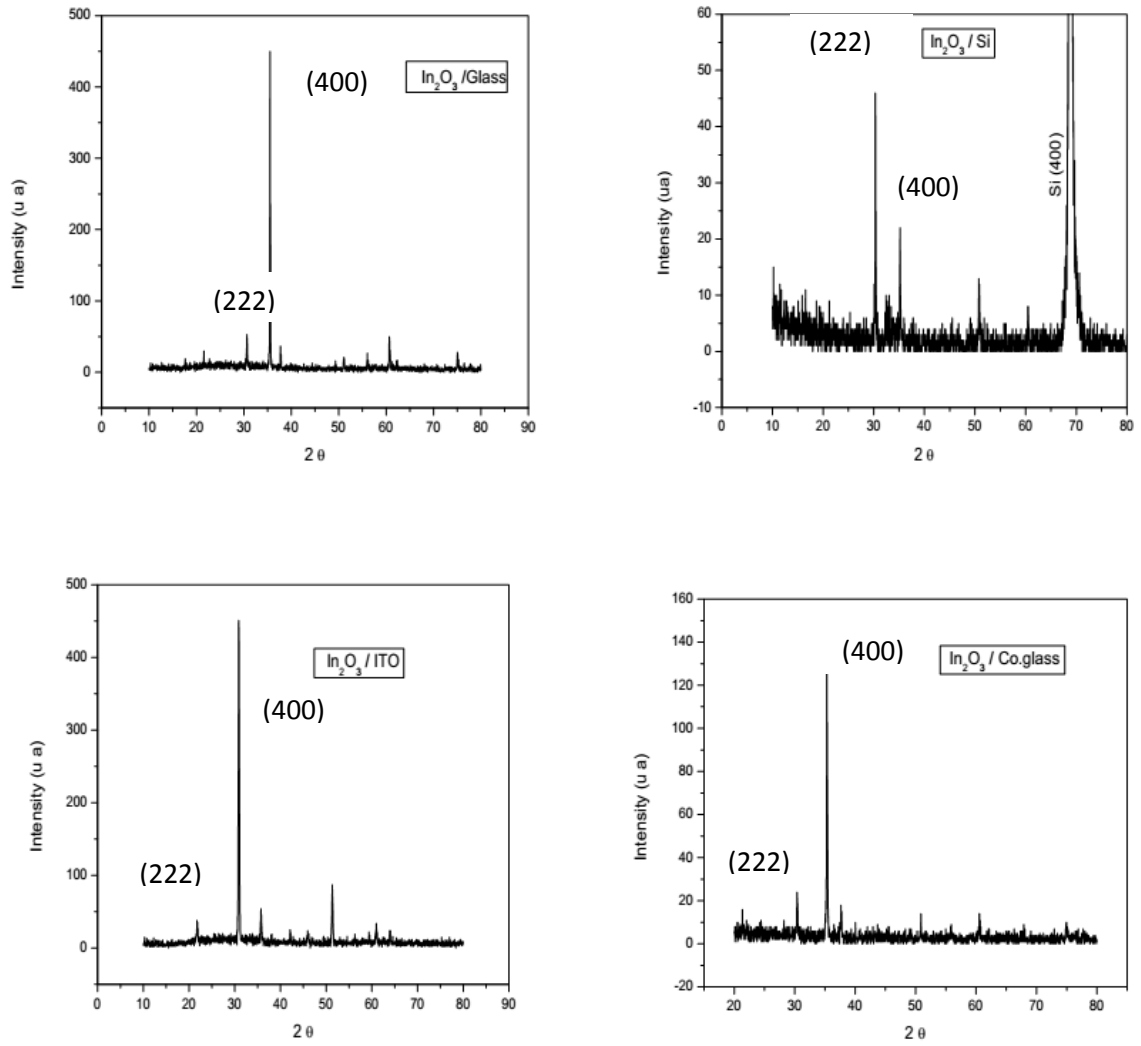


**Figure V.3:** XRD pattern of  $\text{In}_2\text{O}_3$  thin films deposited on a different substrates type.

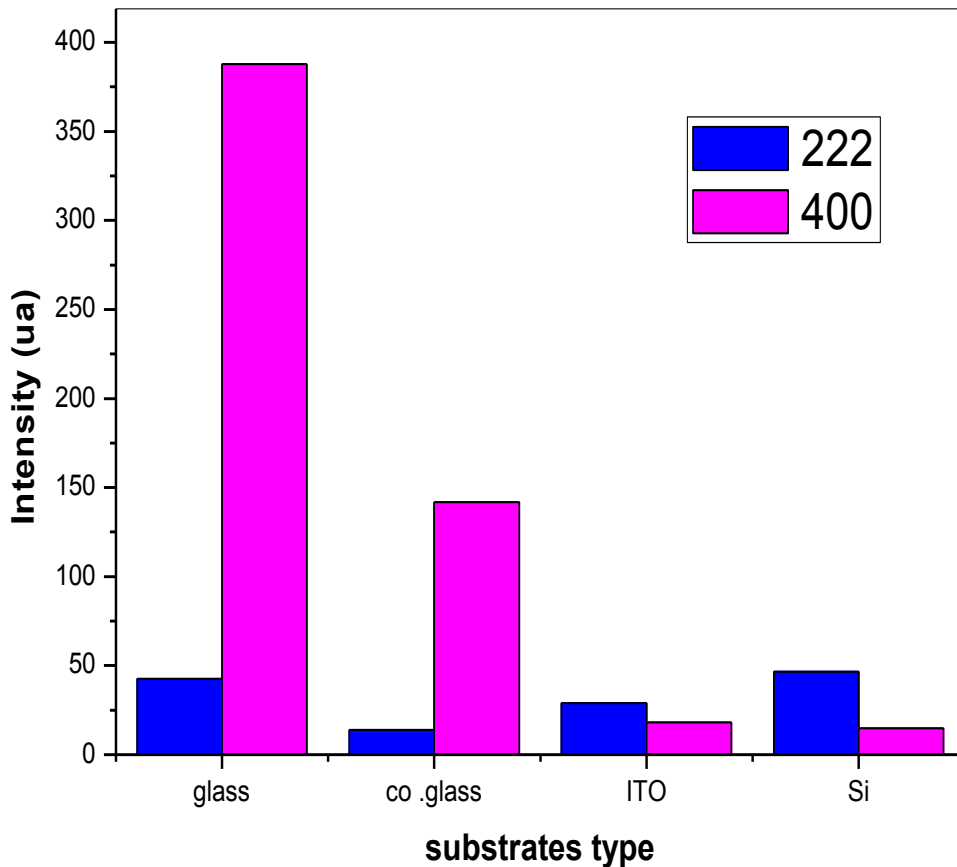


**Figure V.4 :** The preferential orientation (222) and (400) of growth with various substrates type.

The crystallite size is determined from The full width at half maximum (FWHM) of (400) and (222) peaks . The results of the crystallite size with a different substrates are represented on the fig .5. Generally in spray pyrolysis method, the starting solution sprayed onto the preheated substrate, which results in the formation of a thin film on the substrate. The grain growth is formed when the droplets of spray solution reach the hot substrate then the atoms moved on the surface, and their mobility which based on a lot of factors like substrate temperature, diffusion (bulk and surface), adsorption strength , the defects on the substrate surface and the contamination because the first atoms are located along active spots. As a result, the growth process of  $\text{In}_2\text{O}_3$  thin films are affected by the substrate. The highest crystallite size was observed in the films (  $\text{In}_2\text{O}_3$  / Glass) and ( $\text{In}_2\text{O}_3$  / Si) but the smallest crystallite size watched in (  $\text{In}_2\text{O}_3$  /ITO) and ( $\text{In}_2\text{O}_3$  /Co. glass).These can be explained that by the nucleation barrier whereas the smallest grains are observed in film with

smaller nucleation barrier relatively [6]. However, it is well known the ITO and Si substrates have a good crystallization and helps the nucleation of condensed  $\text{In}_2\text{O}_3$  atoms. While, in the glass substrates, above a specific thickness, the attraction between glass atoms and deposited material atoms is very strong and may not allow for the nucleation and the formation of cluster of crystallites. Once it overcomes this situation it can form grains in a larger size.

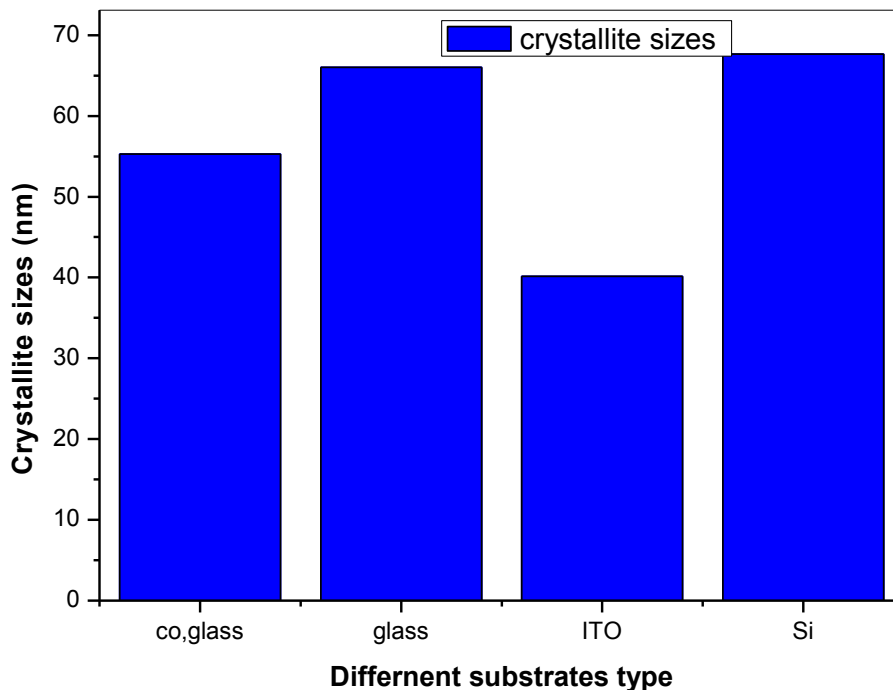


**Figure V.5 :** The crystallite size of the  $\text{In}_2\text{O}_3$  thin films deposited on various substrates.

The lattice parameter value for pure is  $10.11 \text{ \AA}$  [9]. The lattice parameter values of indium oxide ( $\text{In}_2\text{O}_3$ ) vary with the substrate used. As in the following:  $a = 10.08 \text{ \AA}$  (Glass),  $a = 10.04 \text{ \AA}$  (ITO),  $a = 10.18 \text{ \AA}$  (Si) and  $a = 10.16 \text{ \AA}$  (Corning glass). This difference is related to the substrates type because there are disagreements between the substrate and the material deposited, this disagreement induces constraints. These constraints are divided into two components type : a thermal and an

intrinsic, the first component is based on the various differences between the coefficients of thermal expansion but the second depends on differences in parameters like substrate material and the deposition parameters. Also the deviation of orientation in the film growth is affected by generation of intrinsic stress [3]. It can be observed that the higher values of tensile stress are obtained for the films deposited on Si and Corning glass. Generally, it can be explained with the interaction between the substrate surface and  $\text{In}_2\text{O}_3$  film atoms which lead to deform the dimensions of lattice in the film along the weak bond direction. The same results are observed in SnS films [10].

#### V.4 Optical properties:

The transmittance spectra of  $\text{In}_2\text{O}_3$  thin films deposited on various substrates are shown in Fig 6. It is clearly seen that all the films exhibit a transmittance about 70-85% in the visible region and the presence of the interference fringes concerning the ( $\text{In}_2\text{O}_3$  / Co. glass) and ( $\text{In}_2\text{O}_3$  / Glass) films may be due to the smooth surface of these films [11]. The higher transmittance for the films grown on ITO substrate and it decreases slightly for ( $\text{In}_2\text{O}_3$  / Corning glass) and ( $\text{In}_2\text{O}_3$  / Glass) films, respectively. This decrease is due to the varying type of the substrate and may be attributed to thickness of films and the degradation of the crystallinity of these films and these results confirm the results of DRX whereas the enhanced light transmitting due to the continuous grain growth which is considered the best crystallinity films.

Fig .7 shows the variation of the band gap energy for different substrates. It is observed that the layers are almost with the same values of indium oxide thin films of ( $\text{In}_2\text{O}_3$  / Glass) and ( $\text{In}_2\text{O}_3$  / Corning glass) but the band gap energy decreases slightly with the film of ( $\text{In}_2\text{O}_3$ /ITO) .This variation of the optical band gap values of the films grown on glass substrates and Corning glass can be explained with the variation of the different factors like lattice parameter, crystallite size, deviation from stoichiometry, carrier concentration, presence of impurities or perhaps due to the formation of band tails [12]. Similar results have been found by other researchers [13,14].

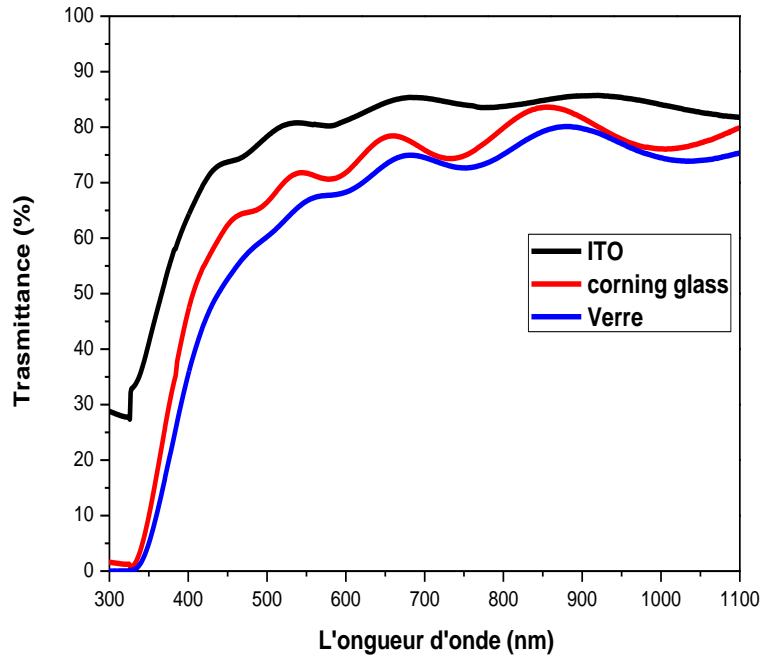


**Figure V.6:** Optical transmittance spectra of In<sub>2</sub>O<sub>3</sub> thin films as a function of different substrates type.

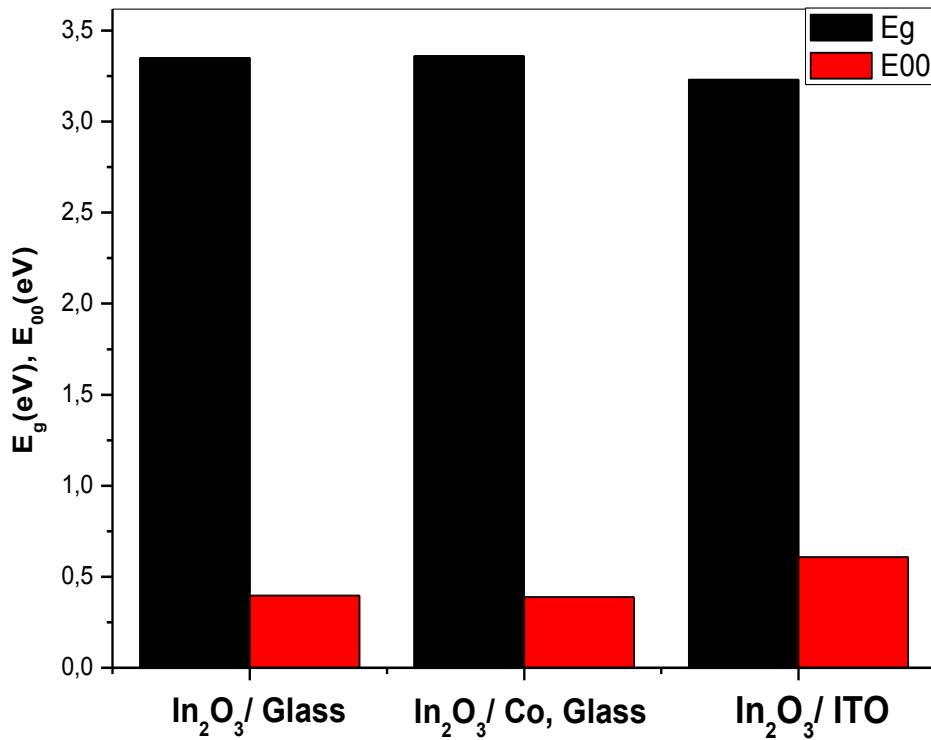


**Figure V.7:** The variation of gap energy Urbach for different substrates type.

## V .5 Electrical properties:

The four-point method for electrical measurements (conductivity and resistivity) was used. The results are shown in Table V.1. The value of electrical resistivity of the film deposited on glass is lower than the film deposited on Co.glass, and that's logical because this film had the better crystallinity.

**Table V.1:** Electrical properties of layers in different substrates.

Substrates	Glass	Corning glass	ITO	Si monocristallin
Résistivity ( $\rho$ ) ( $\Omega.cm$ )	18.063	30.48	/	/
Conductivity ( $\sigma$ ) $\times 10^{-2} (\Omega.cm)^{-1}$	5.36	3.28	/	/

## V .6 Conclusion:

The essential characteristic of thin film is whatever the procedure used for its manufacture, the thin film is always integral with a substrate. Consequently, it will be imperative to take into account this major fact in the design, namely that the support has a very strong influence on the properties of the film. Thus a thin film of the same material, of the same thickness may have substantially different physical properties because the thin film is anisotropic by construction. The influence of the substrates type (Glass, Co. glass, ITO and Si) on the structural and optical properties of thin films of indium oxide ( $In_2O_3$ ) by the ultrasonic spray technique are shown previously whereas all indium oxide films obtained are polycrystalline and the highest crystallinity in the film ( $In_2O_3$  / Glass) and also the highest crystallite size was observed for the films ( $In_2O_3$  /Glass) and ( $In_2O_3$  /Si).The interaction between the substrate surface lead to deform the dimensions of lattice in the film along the weak

bond direction. The optical study by UV-Visible spectroscopy shows that the  $\text{In}_2\text{O}_3$  films have a higher transmission in the range 70-85% in the visible region and the presence of the interference fringes concerning the ( $\text{In}_2\text{O}_3$  / Co. glass) and ( $\text{In}_2\text{O}_3$  / Glass) films and the highest transmittance for the films grown on ITO substrate. The bands gap energy for different substrates is almost with the same values of indium oxide thin films. The electrical conductivity of the film deposited on glass is higher than the film deposited on Co.glass.

## References

- [1] H. bruncková, L. medvecký, Effect of sol concentration and substrate type on microstructure formation of PZT thin films, *Ceramics Silikaty*, 55 (1) (2011) 36-42
- [2] Pavlik Rahnev, Silvija Letskovska, Dimitar Parachkevov and Kamen Seymenliyski, Sputtering of Thin Films on Flexible Substrates, Conference Paper, February 2019
- [3] M. Benhaliliba, C. E. Benouis, M. S. Aida, F. Yakuphanoglu, A. Sanchez Juarez, Indium and aluminium-doped ZnO thin films deposited onto FTO substrates: nanostructure, optical, photoluminescence and electrical properties, *J Sol-Gel Sci Technol* (2010) 55:335–342.
- [4] J.A. Thornton, Structure-zone models of thin films, *Proc. SPIE* 0821 (1988) 95 – 105
- [5] Xuemei Cheng, Kazuhiro Gotoh, Yoshihiko Nakagawa, Noritaka Usami, Effect of substrate type on the electrical and structural properties of TiO<sub>2</sub> thin films deposited by reactive DC sputtering, *Journal of Crystal Growth* 491 (2018) 120–125
- [6] Hayk Khachatryan, Sung-Nam Lee, Kyoung-Bo Kim, Han-Ki Kim, Moojin Kim, Al thin film: The effect of substrate type on Al film formation and morphology, *Journal of Physics and Chemistry of Solids* 122 (2018) 109–117
- [7] Chang, T. C., et al. "Erratum to "Extraction of electrical mechanisms of low-dielectric constant material MSZ for interconnect applications" [*Thin Solid Films* 447–448 (2004) 516–523]." *Thin Solid Films* 467.1 (2004): 342.
- [8] K.H.L. Zhang, A. Walsh, C.R.A. Catlow, V.K. Lazarov, R.G. Egdell, Surface Energies Control the Self-Organization of Oriented In<sub>2</sub>O<sub>3</sub> Nanostructures on Cubic Zirconia, *Nano Letters*. Vol. 10, (2010) 3740–3746
- [9] M. Jothibas, C. Manoharan, S. Ramalingam, S. Dhanapandian, M. Bououdina, Spectroscopic analysis, structural, microstructural, optical and electrical properties of Zn-doped In<sub>2</sub>O<sub>3</sub> thin films, *Spectrochimica Acta Part A: Molecular and Biomolecular Spectroscopy* 122 (2014) 171–178

- [10] M Devika, N Koteeswara Reddy, K Ramesh, H R Sumana, K R Gunasekhar, E S R Gopal and K T Ramakrishna Reddy, The effect of substrate surface on the physical properties of SnS films, *Semicond. Sci. Technol.*, 21 (2006) 1495–1501.
- [11] Studenikin, S. A., Nickolay Golego, and Michael Cocivera, Optical and electrical properties of undoped ZnO films grown by spray pyrolysis of zinc nitrate solution, *Journal of Applied Physics* 83.4 (1998) 2104-2111.
- [12] N.G.Pramod, S.N.Pandey, Effect of Li doping on the structural, optical and formaldehyde sensing properties of In<sub>2</sub>O<sub>3</sub> thin films, *Ceramics International*. Vol.41, (2015) 527–532
- [13] Girtan, Mihaela, and G. Folcher, Structural and optical properties of indium oxide thin films prepared by an ultrasonic spray CVD process, *Surface and Coatings Technology* 172.2 (2003) 242-250.
- [14] Cho, Shinho, Effects of rapid thermal annealing on the properties of In<sub>2</sub>O<sub>3</sub> thin films grown on glass substrate by rf reactive magnetron sputtering, *Microelectronic Engineering* 89 (2012)84-88.

## **CHAPTER VI:**

# **EFFECT OF DOPING (Sb and Mo) ON PROPERTIES OF INDIUM OXIDE THIN FILMS**

## VI .1 Introduction:

Transparent conducting oxides (TCO) films are extensively used in optoelectronic industry because of their high optical transparency and electrical conductivity and it is important for the material science because of their wide range of applications including gas sensors, photovoltaic devices, flat panel displays, touch panels and light-emitting diodes .Usually, the electrical conductivity of a TCO can be increased either by increasing carrier concentration or by enhancing carrier mobility. The carrier concentration can be increased by heavy doping or by deviating from stoichiometry [1,2]. Many of different available TCOs such as CdO, ZnO, SnO<sub>2</sub> and In<sub>2</sub>O<sub>3</sub> which is the best of TCO ; it can be used as an insulator or semiconductor or even conductor. Also doped In<sub>2</sub>O<sub>3</sub> is one of promising alternative materials are used due to their high transparency, good chemical stability, low resistivity and relatively high mobility. In addition, The optical and electrical properties of indium oxide material can be engineered by suitable doping while maintaining enviable stoichiometry. Among these TCOs , Several studies include doped to In<sub>2</sub>O<sub>3</sub> thin film with various metal ions as impurities like (Sn, Ga, Cu, Zr,Ti etc.) whereas, if impurities are added to In<sup>+3</sup>, electrons will be added to the empty 5s and 5p levels [3,4] .

In this work, I will present, the effect of antimony (Sb) and molybdenum (Mo) doping concentration on structural, optical and electrical properties of doped indium oxide thin films. we have chosen antimony as the dopant ion because there are a few reported it [5, 6] and molybdenum because Mo ([Kr]: 4d<sup>5</sup>5s<sup>1</sup>) is the more beneficial impurity to be doped into the In<sub>2</sub>O<sub>3</sub> lattice as it can be donated more than three electrons to the free carriers due to the high valence difference between Mo<sup>+6</sup> ions and substituted In<sup>+3</sup> ions. Therefore, Mo is believed to be a potential doping element in In<sub>2</sub>O<sub>3</sub> compared to other elements. Depending on the experimental conditions and the results of the work in the previous chapters. In this chapter, we will study the influence of Sb and Mo doping level on the structural, optical and electrical properties of the films which will be presented systematically later on .

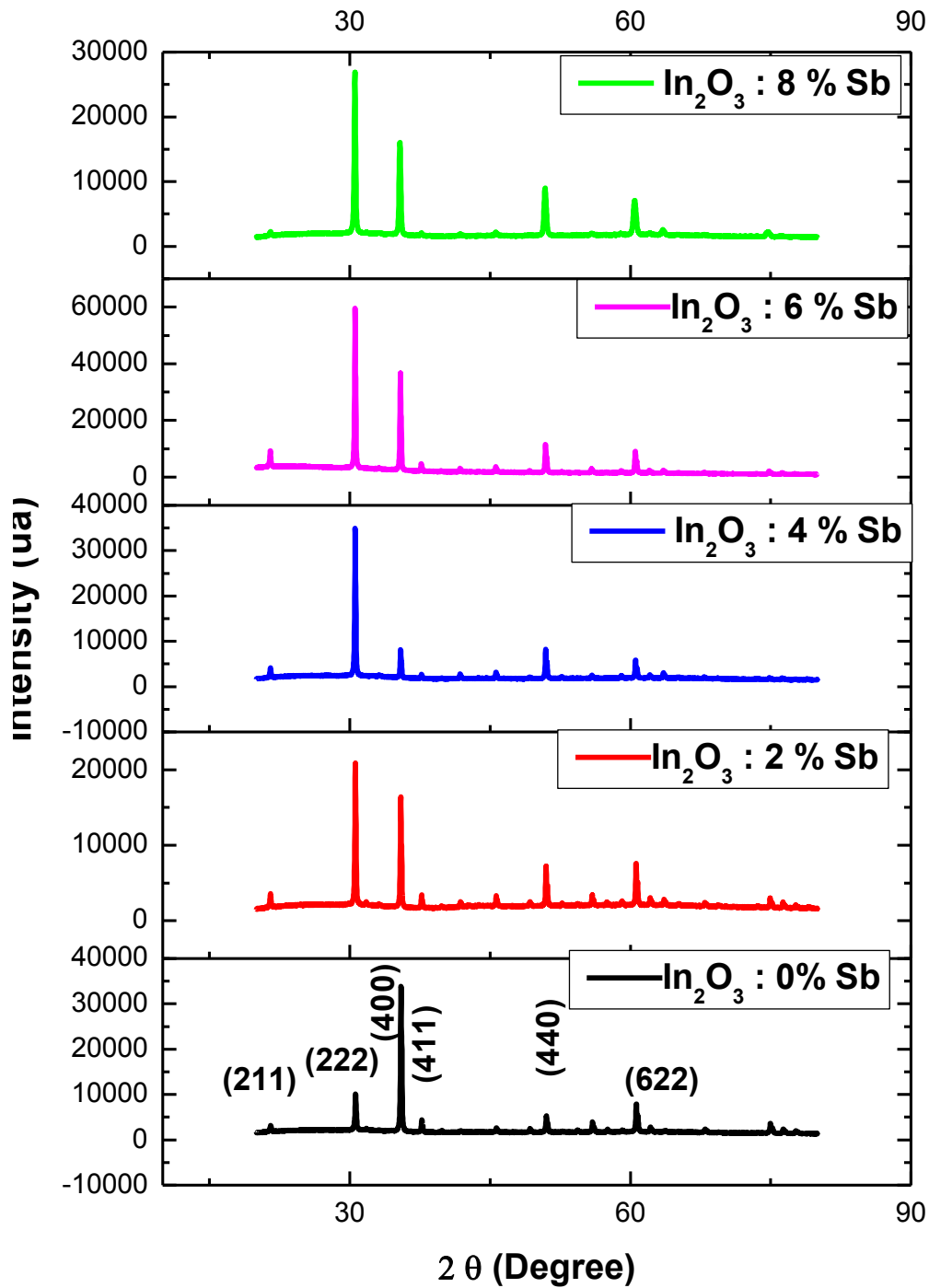
## VI.2. Antimony doping (Sb)

### VI .2.1 Structural properties :

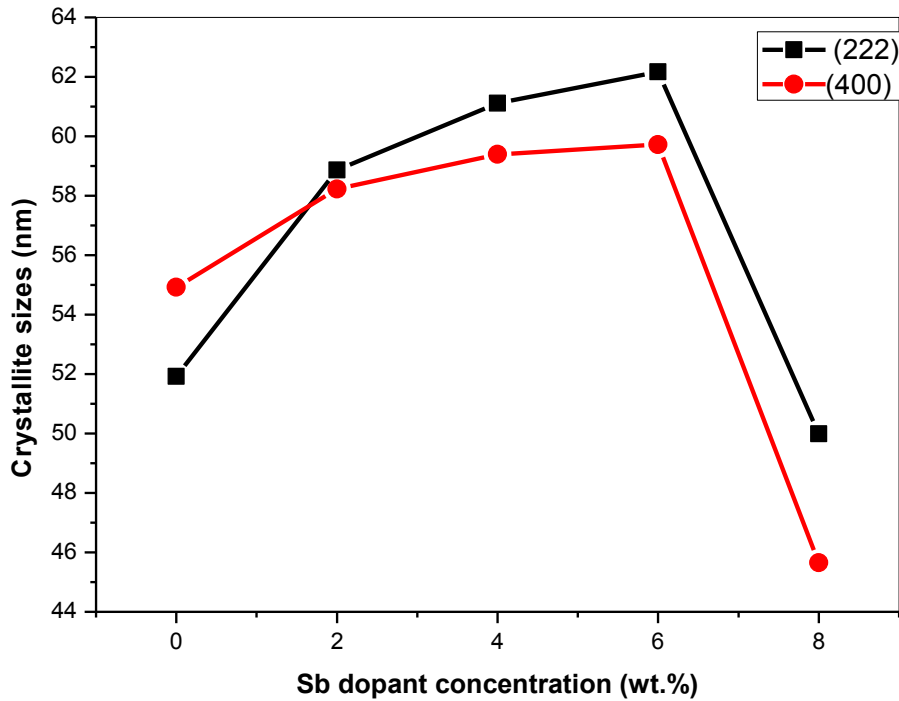
Fig. 1 displays the X-ray diffraction patterns of pure  $\text{In}_2\text{O}_3$  and  $\text{Sb-In}_2\text{O}_3$  with various Sb concentration (2,4,6 and 8 wt.%). All the films exhibit polycrystalline nature with cubic structure. It is observed that the un-doped film is not like the doped indium oxide films which grow along the preferred orientation, where (400) is the preferred orientation in the undoped film but the (222) in the doped indium oxide films. It is clear, when Sb concentration increases to 6 wt.% , the intensity of peak (2 2 2) is increased sharply because of the improvement of crystallinity, but with the increase of doping content above 6 wt.% , the decrease in intensity at higher doping level is due to structural deformation in the crystal structure [7] and it may indicate a meaningful increase of stacking defects and a loss of periodicity in the arrangement of  $\text{In}_2\text{O}_3$  lattice [8] . On the other hand , the change in the preferred orientation when adding antimony may be due to the occupancy of the indium vacancy sites in the lattice by Sb atoms [9] . Further, the lattice parameter ( $a=b=c$ ) calculated for un-doped  $\text{In}_2\text{O}_3$  thin films, a  $10.11 \text{ \AA}$  is good agreement with reported values of  $10.11 \text{ \AA}$  for pure indium oxide [10].When Sb content increases, the lattice constant was found to increase, which is slightly higher than this value . This might be due to the foundation of Sb within crystal lattice of  $\text{In}_2\text{O}_3$  films ; where the indium in this lattice are substituted by antimony atoms and other Sb atoms occupy interstitial sites in the same time [9].In addition to the difference in the ionic radius between In and Sb which creates the residual stress in the films this lead to the change position of the (222) peak to a lower angle region.

**Table VI. 1:** The structural , optical and the electrical parameters of un-doped and Sb-doped  $\text{In}_2\text{O}_3$  .

Wt% Sb	Epaisseur (nm)	Lattice parametre a ( $\text{A}^0$ )	carrier concentration n ( $10^{+20} \text{ cm}^{-3}$ )	Hall mobility $\mu$ ( $\text{cm}^2 \text{V}^{-1} \text{S}^{-1}$ )	resistivity ( $\rho$ ) $10^{-3} \Omega \cdot \text{cm}$	Rsh ( $\Omega$ )	AVT for 500-800 nm	Figure of merit $\Phi$ ( $10^{+16} \Omega^{-1}$ )
0	432,38	10,11	1,83	8,46	4,01	92,742	75	6,07
2	333,08	10.12	4,82	8,77	0,64	19,214	80	55,88
4	651,06	10.12	9,98	14	0,42	6,451	80	166
6	626,02	10.12	16,68	3,66	1,01	16,133	75	34,90
8	551,4	10.13	2,34	12,52	2,13	38,628	73	11,12



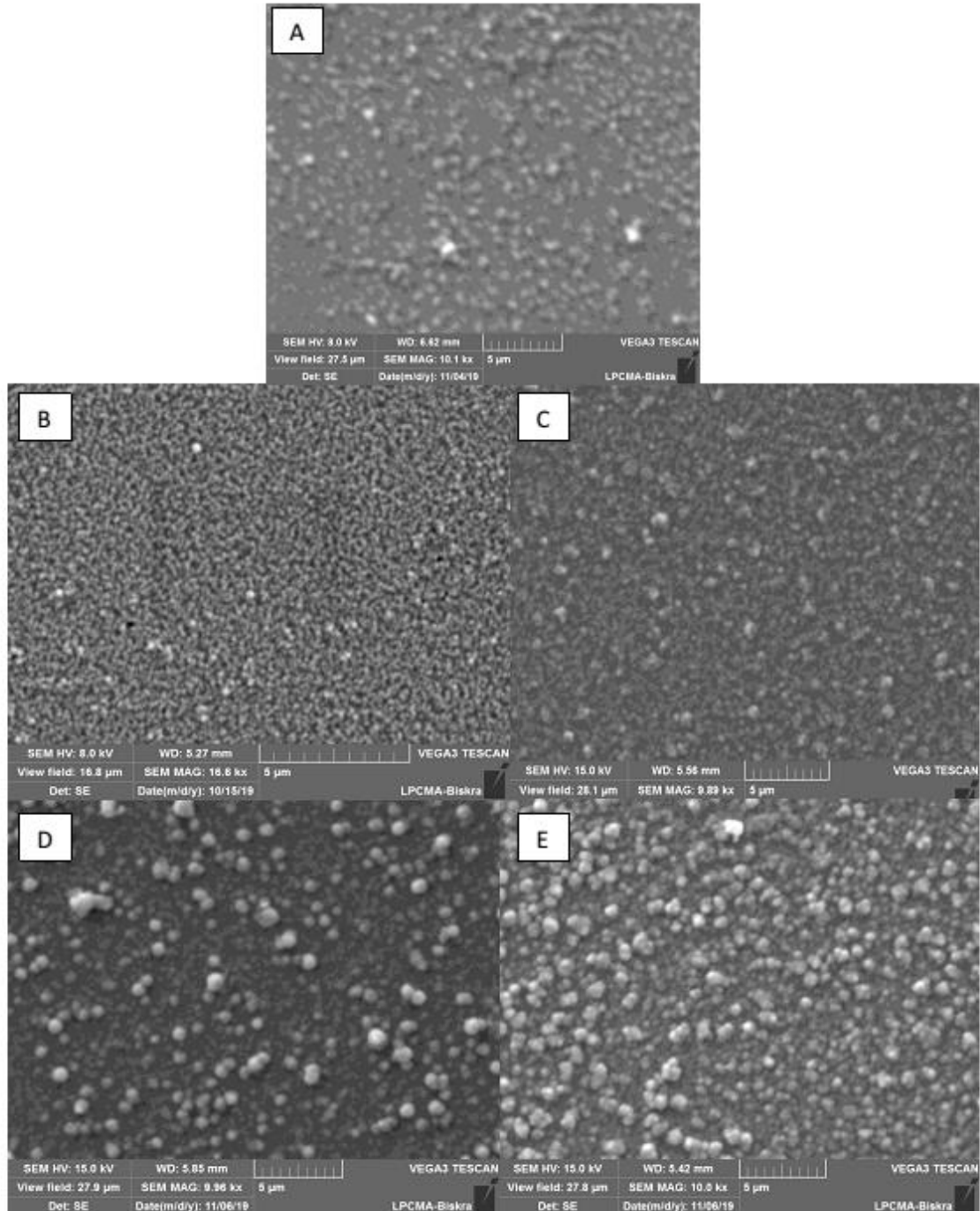
**Figure VI. 1:** XRD pattern of pure  $\text{In}_2\text{O}_3$  and Sb- $\text{In}_2\text{O}_3$  with various Sb concentration (2,4,6 and 8 Wt.%)



**Figure VI. 2:** The crystallite sizes of the two strongest peaks (2 2 2) and (4 0 0) of pure  $\text{In}_2\text{O}_3$  and  $\text{Sb-In}_2\text{O}_3$ .

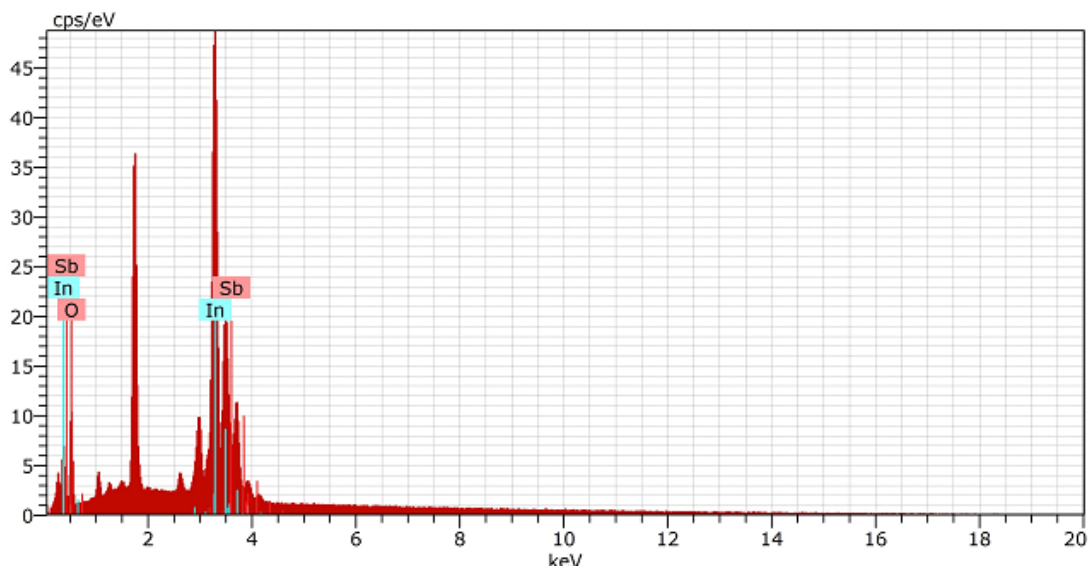
Fig .2. It is observed that the crystallite sizes of the two strongest peaks (2 2 2) and (4 0 0) of pure  $\text{In}_2\text{O}_3$  and  $\text{Sb-In}_2\text{O}_3$ . The undoped  $\text{In}_2\text{O}_3$ : the crystallite size of the (4 0 0) is greater than (2 2 2) because the (4 0 0) is the preferred orientation in this film where the more number of grains associated along that plan but, In the  $\text{Sb-In}_2\text{O}_3$  films, the values of crystallite size of the (4 0 0) become lower than (2 2 2). This is attributed to the change in the preferred orientation in  $\text{Sb-In}_2\text{O}_3$  films. Generally, the crystallite size increases with the increase in Sb doping concentration (2 to 6 wt.%), this larger crystallite size is caused by the relax of the strain between  $\text{In}_2\text{O}_3$  lattice and Sb dopants which lead to the better order structure and then decreases for further doping level 8 wt.% which may be due to the antimony (Sb) that created the more nucleation sites which inhibit the growth of crystal grains [11].

VI .2.2 Surface morphology:



**Figure VI.3:** The micrograph of SEM Sb-In<sub>2</sub>O<sub>3</sub> films (A: un-doped / B: 2 Wt% Sb / C: 4 Wt% Sb / D : 6 Wt% Sb / E: 8 Wt% Sb )

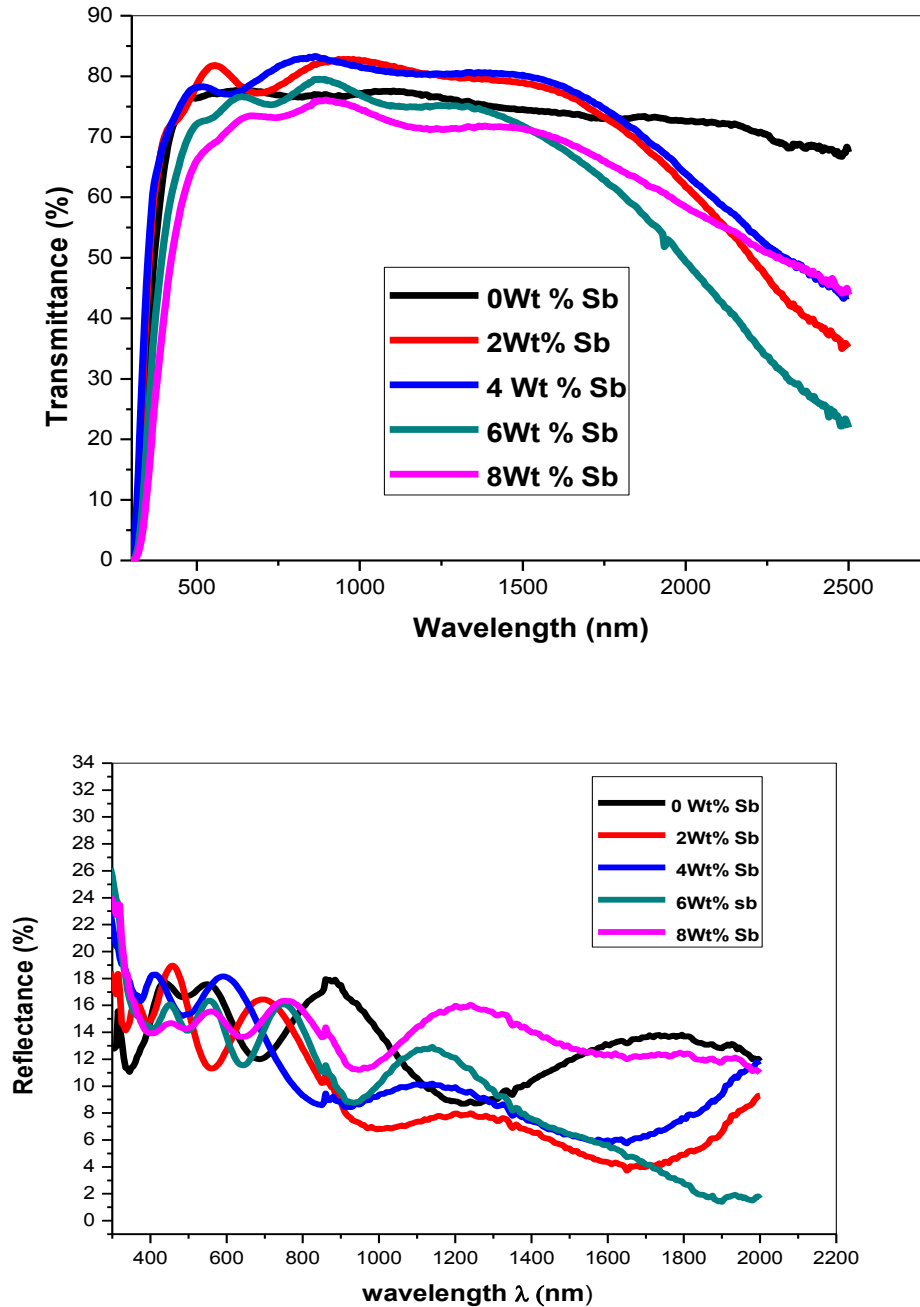
Fig.3 shows the SEM images of undoped  $\text{In}_2\text{O}_3$  film and doped with Sb thin films deposited at different of Sb Wt%. As the Sb content increases, it is observed the slightly change in the morphology. Whereas all the films has compact surfaces and covered grains with similar geometries .When the Sb is more than 4Wt% ,it is observed the formation a few of small agglomerates .As the grains size increased with the increasing of doping level which may be attributed to the combination of Sb atoms in the lattice or/and perhaps the change in the preferred orientation for doped films. EDS spectra confirm the presence of In, O and Sb elements in the films deposited with 2 Wt% Sb. This is shown in Fig.4.



**Figure VI. 4** The EDS spectra of Sb- $\text{In}_2\text{O}_3$  films (2 wt% Sb).

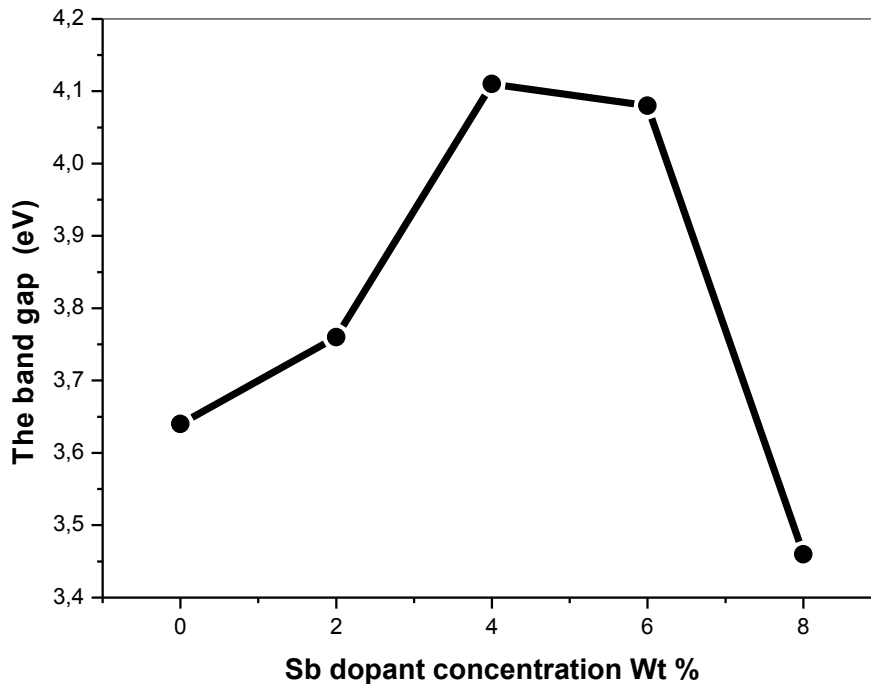
### VI .2.3 Optical properties:

Fig.5 shows the transmittance and reflectance spectra of undoped and antimony doped indium oxide films.



**Figure VI.5.** The Optical transmittance and The reflectance spectra of undoped and antimony doped indium oxide films.

The transparency of these films is high about 72-84 % in the visible range. As we have seen, the interference fringes in the visible and in the near infrared regions in all films may be attributed to homogeneity of surface and thickness uniformity. The values of the optical transmittance in the 2 and 4 Wt % Sb films are high as compared to that of the un-doped and other films, this can be caused by the low light scattering (low energy loss) or/and low micro strain in the films with comparison to other films, but above 4 Wt % Sb the decrease of transmittance at higher doping levels may be attributed to the increased scattering of photons by film defects which are created by the increase of doping. Further, it is observed that a slight shift in the absorption edge when it is decreased toward a short wavelength in 2 and 4 wt% Sb and increased toward a longer wavelength in 6 and 8 wt% Sb compared with un-doped film which indicates an increase and a decrease of the band gap energy for  $\text{In}_2\text{O}_3$  after doping, respectively. On the other hand, the cause of intense light absorption can be attributed to the transfer of electron between the different oxidation states of the element, whereas a mixed oxidation state, or the found of two different oxidation states to the element, it appears abnormally an intense coloration which was indicated by Kojima and al [12]. The doped TCOs films have an important optical characteristic where it can not transmit light after 1700 nm and strong absorption in the near-IR region. This variation is because the absorption of the free-carrier. As it is noted in the near IR region the decreasing of the transmission and increasing of the reflection, it may reach about 30-40 % at the wavelength of 2500 nm. This estimated the Sb- $\text{In}_2\text{O}_3$  thin films of interest such as IR reflectors, window coating or heat reflector. The optical phenomenon near the infrared region is explained by the classical theory of Drude free-electron, this model indicates that the drop of transmittance in the near infrared region is coordinated with the plasma frequency. It showed the reflection at longer wavelengths due to the edge of plasma, we also found that the light cannot be transmitted. In the actuality, The cut-off wavelength shifts toward lower wavelength due to the increase in carrier concentration and the electron mobility [13,14].



**Figure VI.6:** The band gap as function of Sb dopant concentration .

It is common that, the variation of the band gap values can be changed by differences factors like carrier concentration, deviation from stoichiometry of the films, presence of impurities, lattice constants and grain size [10]. In this work, the change can be explained as follows: The band gap ( $E_g$ ) increases from 3.64 eV for un-doped  $\text{In}_2\text{O}_3$  film to 4.11 eV for  $\text{In}_2\text{O}_3:\text{Sb}$  with increasing Sb concentration to 4Wt.% , the increase in the band gap values may be due to quantum reservation effects because of the enhancement in the band gap energy in nanostructured materials which caused the localization of charges in individual nanocrystals , which is formed by the quantum dots with a very small dimension [15] . Also, this results corresponds to the Burstein–Moss hypothesis [6] which shows the relation linear between the carrier concentration ( $n$ ) and band gap energy ( $E_g$ ). But , when increasing Sb concentration above 4 Wt.% , the band gap ( $E_g$ ) decreased ,that can be explained by the defect energy level of Sb (Sb acts as donor impurity) ,which forms a donor

level inside the forbidden gap region and below the conduction band, lowering the band gap of  $\text{In}_2\text{O}_3$ . [16].

#### VI.2.4 FTIR Analysis :

Fig.7 shows the spectrum of fourier transform infrared (FTIR) of  $\text{In}_2\text{O}_3$  films doped with Sb deposited on glass substrate .It is observed that the stretching vibrations of In-O and In-In are found in the region  $800\text{--}300\text{ cm}^{-1}$  [17,18]. The In-O stretching is usually observed in the region  $700\text{--}300\text{ cm}^{-1}$  [19]. In this spectrum, it is observed that the bands absorptions around ( $565, 820\text{ cm}^{-1}$ ) are due to the In-O vibrations, moreover, but the bands absorptions at ( $1260\text{--}1270\text{ cm}^{-1}$ ) are attributed to the typical of vibrations in the boron-oxygen groups with trigonally coordinated boron (boron-oxygen triangles  $\text{BO}_3$ ) [20].

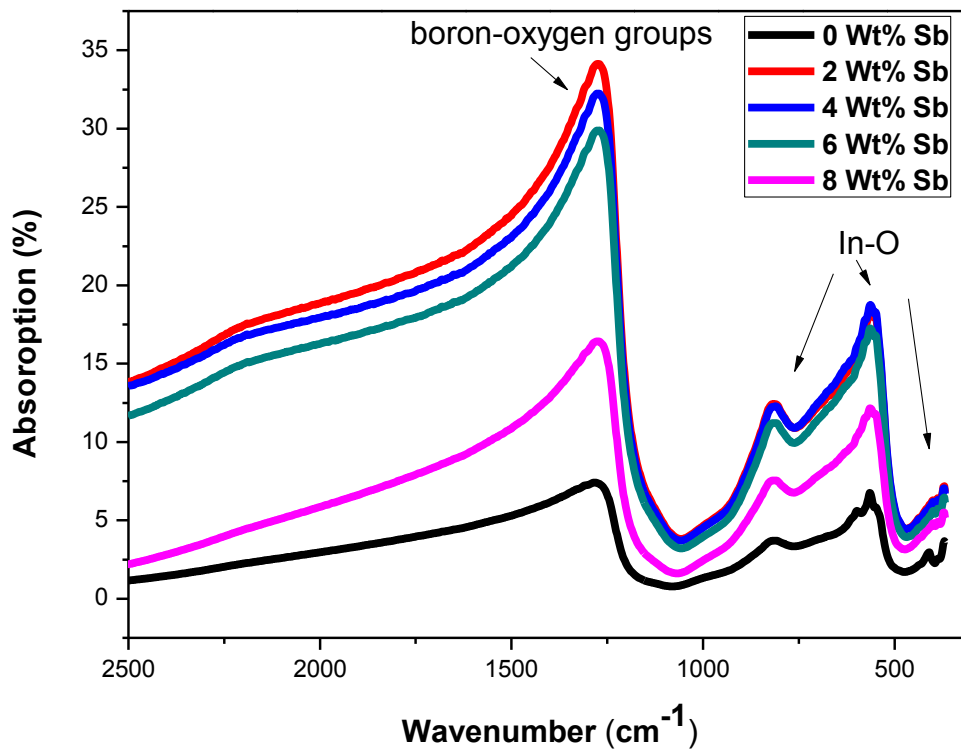


**Figure VI.7 :** The Fourier transform infrared (FTIR) spectrum of undoped and antimony doped indium oxide films deposited on glass substrate

### VI .2.5 Photoluminescence properties:

The property of luminescence of the films generally has relation with the crystallinity of the films where the increase of this latter was caused by the reduction in the density of defects. Fig.8. shows Photoluminescence spectra of un-doped and antimony doped indium oxide films in the wavelength range from 280 to 700 nm. The intensity of the PL emission peaks are decreased with the increase of quantum of Sb. Many emission peaks were observed for un-doped indium oxide and Sb-doped indium oxide films with various concentration are centered at about 312, 364, 400, 460, 480, 530 and 620 nm .The un-doped  $\text{In}_2\text{O}_3$  thin film has a strong emission intense violet bands at 364 and 400 nm .In addition, in the other emission, blue band centered at 480 nm . This latter peak may be attributed to the O, In and/or In/O vacancies centers, as well as reported [21,22].Also, the peaks located in the green and red emission centered at 530 and 620 nm respectively .The broad peak of the red emission is attributed to the O interstitial defects in the films. It is known that the oxygen vacancies can produce a new energy levels in the band gap and the cubic  $\text{In}_2\text{O}_3$  which has oxygen-deficient structure [23].The same observation of emission peaks watched in the Sb-doped indium oxide films with the 2 Wt% Sb but with a less intensity, plus that emission blue band at 460 nm .The emission peaks intensity decreased with an increase of Sb doping concentration. This decreasing may be attributed to the rise in Sb content in the films .The same result observed that in the IMO films [24] and Zn-doped  $\text{In}_2\text{O}_3$  thin films [10].

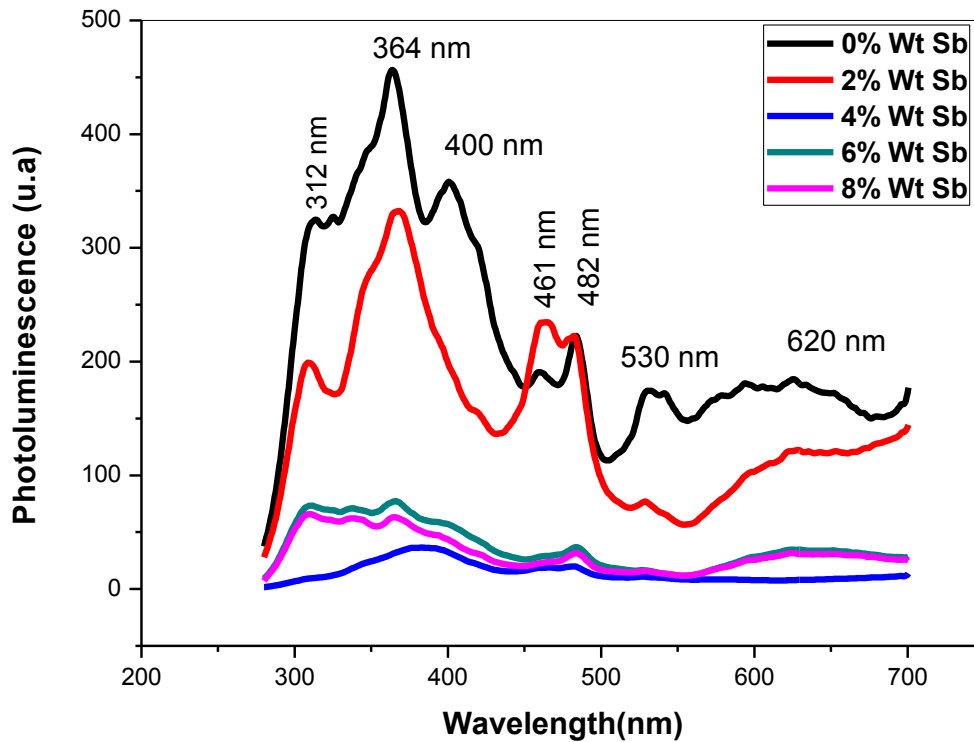


**Figure VI.8 :** Photoluminescence spectra of undoped and antimony doped indium oxide films deposited on glass substrate

The energy corresponds all the observed emission peaks 312 (3.97 eV), 364(3.41 eV), 400(3.10 eV), 460(2.69 eV), 480(2.58 eV), 530(2.34 eV), and 620 nm (2.00 eV) . Generally, It is observed that there are two cases: in the first case, the energy corresponds to emission peaks (364, 400, 460, 480, 530, and 620 nm) is lower than the band gap energy of the films, they cannot be assigned to the direct recombination between electrons in the conduction band and holes in the valence band [ 25,26] .In the second case , it is the inverse ; the band gap is lower than the energy corresponding to emission peak 312 nm in the un-doped and doped with 2 and 8 Wt% Sb indium oxide films , it is may be attributed to the radiative recombination of bound excitons . This explained the luminescence process in two steps : At the first step , a hole captures an electron in donor level so that a hole on an acceptor to form a trapped exciton and in the second step the trapped exciton recombines radiatively to produce the observed emission [27,28]. Several reports observed that the

photoluminescence emission peaks are centered at 480 and 520 nm from  $\text{In}_2\text{O}_3$  nanoparticles. Lee and al reported a peak at 637 nm for pure  $\text{In}_2\text{O}_3$  films. Commonly, these emission peaks are indicated as the deep level or trap state emissions because of the oxygen deficiencies [27].

### **VI .2.6 Electrical properties:**

The electrical resistivity ( $\rho$ ), Hall mobility ( $\mu$ ) and carrier concentration (n) of un-doped and Sb-doped  $\text{In}_2\text{O}_3$  (2,4,6 and 8 Wt.%) films are shown in the Table 1. The resistivity which decreases after the add of antimony concentrations compared with un-doped film. This reduce can be attributed to an enhancement of the carrier concentration after doping which are resulted by the electron donor of Sb ions. In addition, the improved grain growth lead to the decreasing in the grain boundary scattering. But , at 8Wt % Sb-doping the carrier concentration decreases may be caused by the disorder and/or the oxidation states of Sb ; the activation energy of donor becomes higher when the disorder increase in the lattice because Sb concentration increases. Thus, it does not lead to sufficiently ionization of Sb high doping level. However, it finds two oxidations of Sb ( $\text{Sb}^{5+}$  and  $\text{Sb}^{3+}$ ) [29] which its role is to cause an increase in resistivity. The Same result observed in  $\text{SnO}_2$  doped 7% Sb [30]. Further, the resistivity related to the defect structures as the interstitial solid solution of Sb which would trap electrons. It is usually attributed to the increase of the grain boundary scattering. Similar result obtained in the Zn-doped  $\text{In}_2\text{O}_3$  thin films [10] . The minimum values of electrical resistivity are found for indium oxide films doped with 2 and 4 Wt % Sb.

### VI. 3. Molybdenum doping (Mo)

#### VI .3.1 Structural properties:

Fig.9. shows the XRD patterns for un-doped and doped  $\text{In}_2\text{O}_3$  thin films with Mo dopants deposited by spray ultrasonic on glass substrate. The observed XRD patterns which is found in all the films have polycrystalline structure regardless of the doping with preferred growth along the (400) direction in the pure  $\text{In}_2\text{O}_3$  thin films but the (222) direction is preferred in all the dopant films, together with low intensity of the other peaks having (211), (411), (431), (440), (611), and (622) orientations. The intensity of (222) orientation is increased with increasing of Mo dopants to 4 Wt % Mo. It is attributed to the improvement of crystallinity but more than this value which is decreased of the (222) intensity may be to deformate the structure of film. There is one new peak observed in the two films deposited with 3 and 4 Wt% Mo. This can be related to  $\text{MoO}_3$  phase (110) located at  $2\theta = 24.2^\circ$  [31]. Further, in the un-doped  $\text{In}_2\text{O}_3$  and doped films the (400) and (222) positions; respectively; slightly shifts towards higher  $2\theta$  angles as compared with that of standard positions, this is back to the Mo ions occupy In sites within  $\text{In}_2\text{O}_3$  crystal network [10] and it is also attributed to the residual stress because there is a difference in the ionic radius between  $\text{In}^{+3}$  and  $\text{Mo}^{+3}$  [7]. The structural parameters of  $\text{In}_2\text{O}_3:\text{Mo}$  films are organized in Table 2. The lattice constant of un-doped film is  $10.1108 \text{ \AA}$  which is in agreement with the standard data of  $\text{In}_2\text{O}_3$  film [10] But if Mo concentration is added, the lattice constant will be decreased to be lower than the standard value which due to the difference between ionic radius and when  $\text{Mo}^{+3}$  ( $0.83 \text{ \AA}$ ) is slightly smaller than  $\text{In}^{+3}$  ( $0.94 \text{ \AA}$ ) because molybdenum atoms substitute indium atoms [32] except the ones deposited at 2 Wt% Mo, the lattice constant of this film is bigger than standard value which may be attributed to the indium atoms that are substituted by some molybdenum atoms in the lattice and the last quantity of molybdenum atoms occupy interstitial sites [33] this variation lead to a clear expansion of the crystal network.

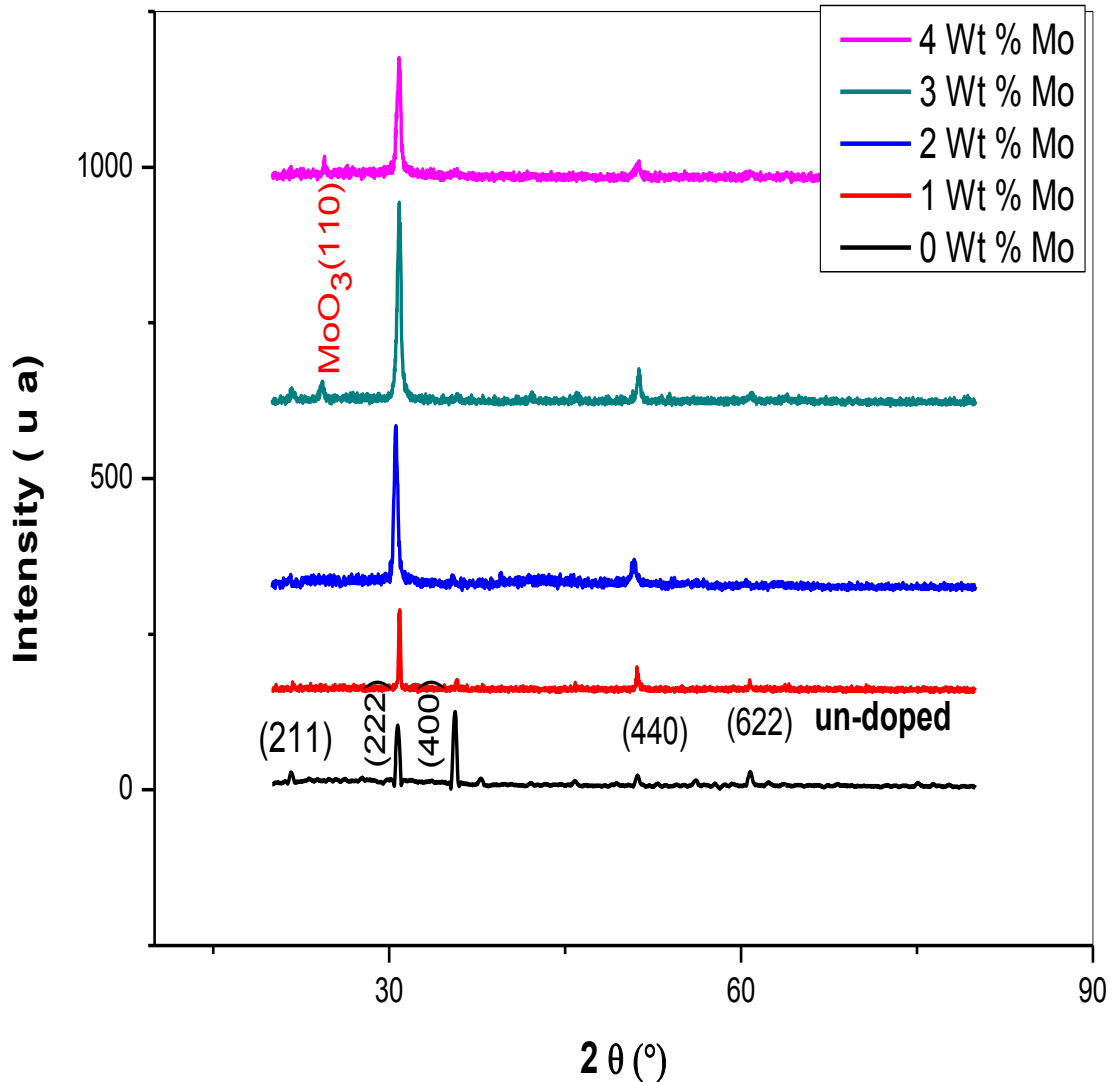


**Figure VI.9:** XRD pattern of un-doped  $\text{In}_2\text{O}_3$  and  $\text{Mo-In}_2\text{O}_3$  with various Mo concentration (1,2,3 and 4 wt.%)

The microstrain and dislocation density of crystal structure are increased with the increasing of Mo concentration. This variation is an inverse relationship with crystallite size because of the enhancement of Mo concentration which is leading to increase the nucleation centers densities that lead to small crystallites (see fig 10).

Table VI. 2 The structural parameters of  $\text{In}_2\text{O}_3:\text{Mo}$  films .

Mo concentration (Wt%)	Epaisseur (nm)	hkl	$\theta_{\text{stand}}(^{\circ})$	$\theta_{\text{exp}}(^{\circ})$	$d_{\text{hkl}}$	a ( $\text{A}^{\circ}$ )	$\delta$ ( $\cdot 10^{+14}$ lin /m <sup>2</sup> )	$\epsilon$ ( $\cdot 10^{-3}$ )
0	432	400	35.45	35,63	2,52	10,1108	9,74	7,10897
1	389	222	30.58	30,9	2,89	10,0309	3,15	4,64449
2	411	222	30.58	30,54	2,98	10,14	13,98	9,79469
3	474	222	30.58	30,9	2,89	10,0368	17,86	11,08957
4	240	222	30.58	30,83	2,9	10,0479	17,81	11,06525

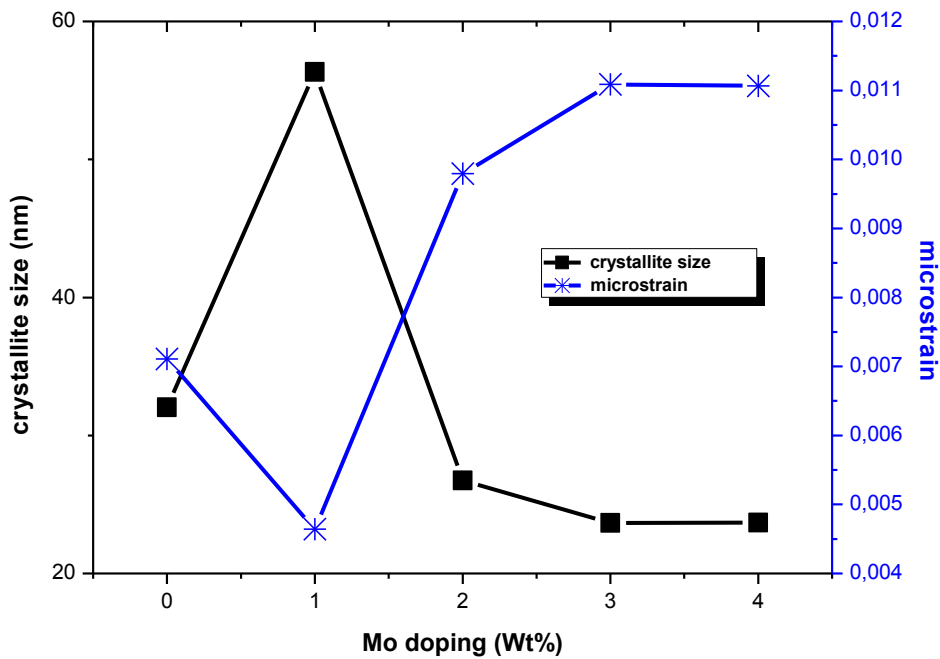


Figure VI.10: The crystallite sizes of and microstrain of un-doped  $\text{In}_2\text{O}_3$  and  $\text{Mo-In}_2\text{O}_3$ .

VI .3.2 Surface morphology:

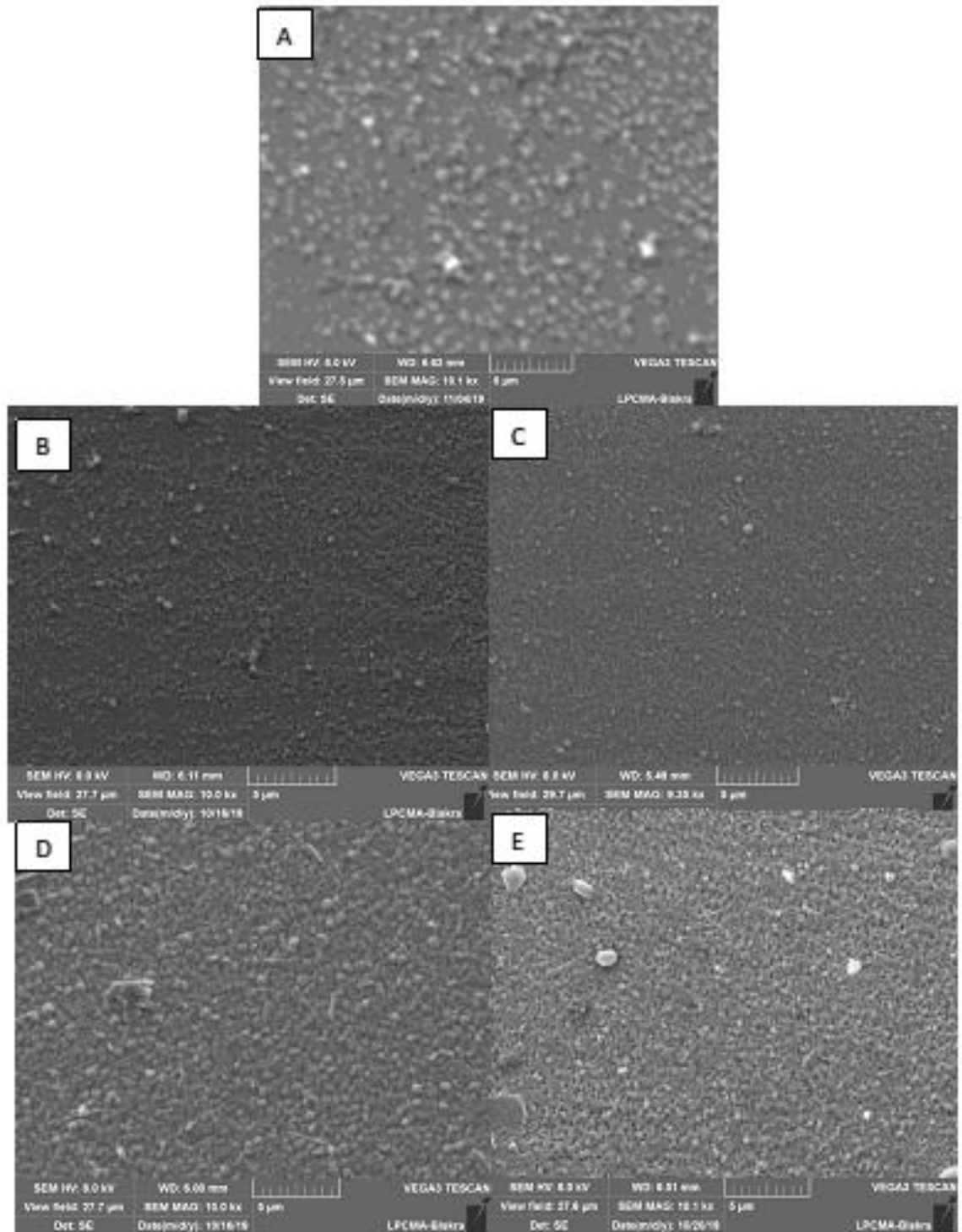
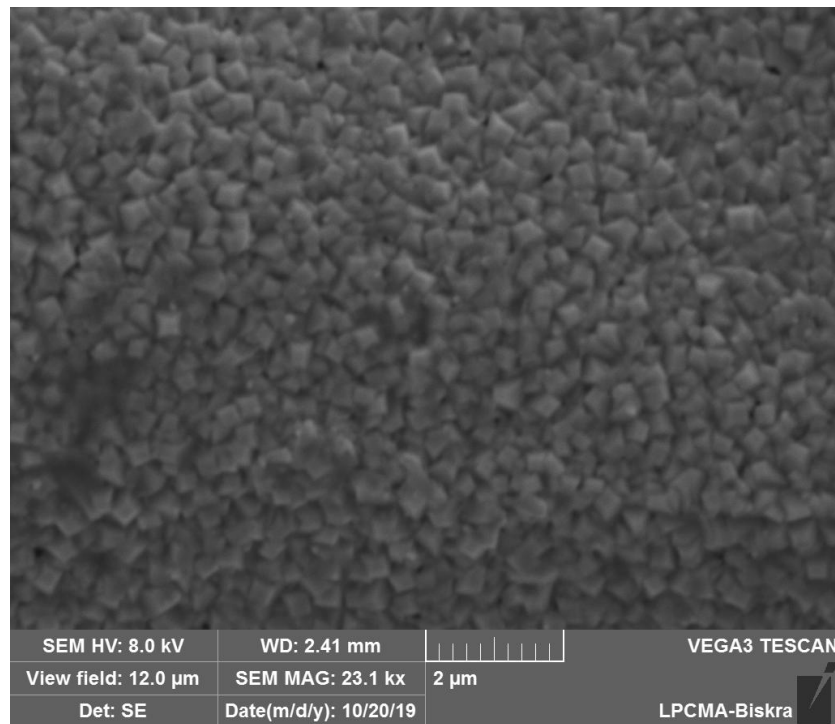
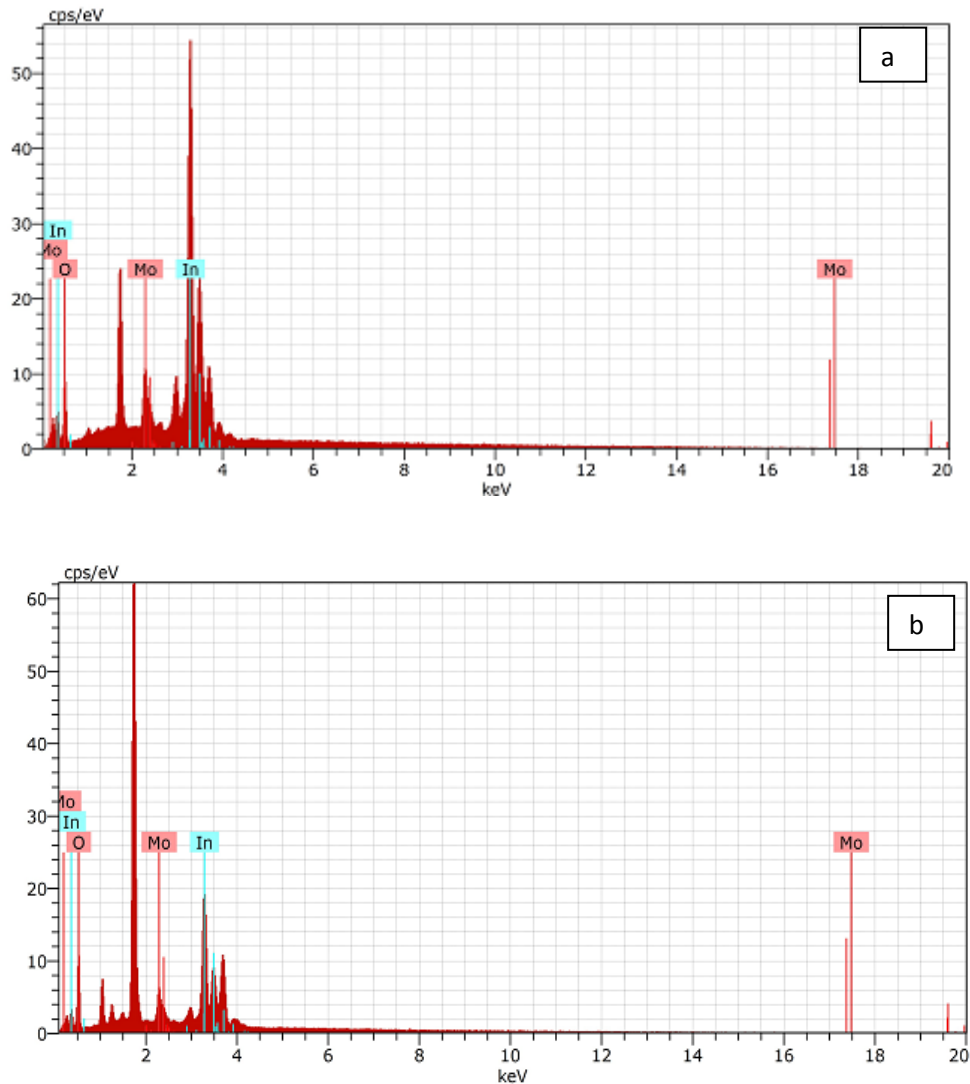


Figure VI.11: The micrograph of SEM Mo-In<sub>2</sub>O<sub>3</sub> films (A: un-doped /B: 1 Wt% Mo / C: 2 Wt% Mo / D : 3 Wt% Mo / E: 4 Wt% Mo )

Fig.11 shows the micrograph of SEM doped indium oxide films with different Mo-doping contents. All the nanostructure thin films have smooth, homogeneous and continuous surface. When the Mo-doping contents increased at 3 wt % Mo the grain size increased with almost uniform size, this result is according to the XRD pattern which it takes the best crystallization, But more than this value which shows smooth surface covered with uniformly spread grains, few agglomerates and the free voids on the surface lead to a high porosity, this latter affects the optical transmittance where it takes a higher transmittance than film with 3 Wt% Mo. Fig 12 shows the micrograph of SEM indium oxide films doped with 1% Mo which is obtained with rotation of the film  $45^\circ$  on the stage of device scanning electron microscopy (See from another angle). It is very clear, the granules of the film are similar to each other. The EDS spectra obtained from the films deposited with 2 Wt % Mo doping and 4 Wt % Mo. It is observed that the composition of the constituents in this films are Mo, In and O with a different atomic data. It is also observed that the Mo ratio increased from a to b (see Fig 13).



**Figure VI.12 :** The micrograph of SEM Mo-In<sub>2</sub>O<sub>3</sub> films (1 Wt% Mo )**Figure VI.13** The EDS spectra of Mo-In<sub>2</sub>O<sub>3</sub> films (a: 2 Wt% Mo /b: 4 Wt% Mo).

### VI .3.3 Transmittance Analysis:

Fig.14 shows the optical transmittance spectrum of the un-doped In<sub>2</sub>O<sub>3</sub> film and doped In<sub>2</sub>O<sub>3</sub> films with different Mo concentration as a function of the wavelength . The average optical transmittance of the films varies between 55 and 82 % in the visible range. The interference fringes are observed in the visible region in all films which may be indicated to homogeneity of surface and thickness uniformity. As we have seen, a slight shift in the absorption edge increase toward to a longer wavelength compared with un-doped film which indicates decreasing in the band gap energy for

$\text{In}_2\text{O}_3$  after doping with Mo. Generally, the transmittance decreases slightly after doping, this back to many effects like : the thickness, homogeneity of surface and crystallinity with it . Enhance with films has more homogeneity and lower thickness and decline with higher thickness or heterogeneous because it leads to increase scattering of photons. Also, The oxygen concentration affects the transmittance of thin films where there is a direct proportion between them [34]

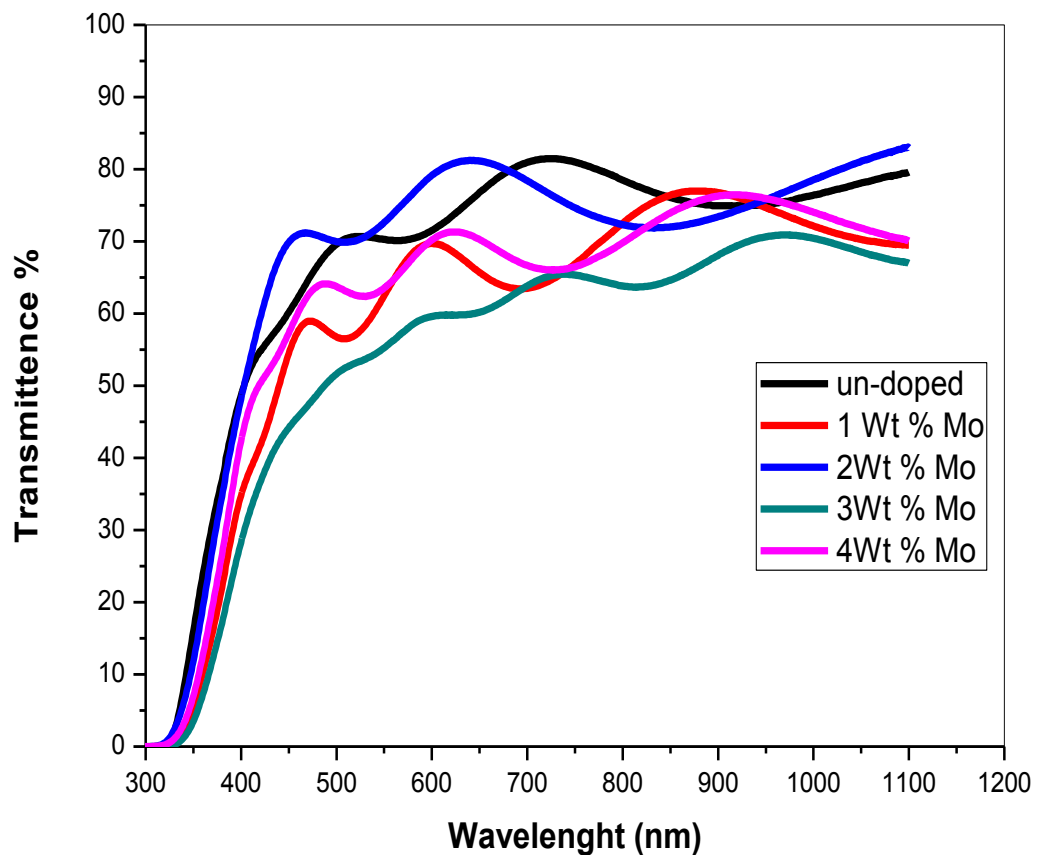


**Figure VI.14:** . Optical transmittance spectra of undoped and Mo doped indium oxide films

The band gap energy decreases after doping with the different Mo concentration. It is attributed to Mo atoms located at donor level [35]. The band gap is also related to the oxidation of the components due to the oxygen concentration of the films in oxide semiconductors [36 ].

### VI .3.4 The resistivity:

**Table VI. 3:** The electrical and optical parameters values  $\text{In}_2\text{O}_3$  thin films doped with various Mo concentration.

Mo (Wt%)	$\rho(10^{-2} \Omega\text{Cm})$	$R_{\text{sh}} (\Omega)$	$E_g$	$E_{00}$
0	0,48	111	3.64	0.32
1	66,97	17219	2.69	0.37
2	33,54	8156	2.66	0.37
3	60,14	12687	2.73	0.36
4	35,83	14952	2.78	0.35

The resistivity ( $\rho$ ) and sheet resistance ( $R_{\text{sh}}$ ) of the  $\text{In}_2\text{O}_3:\text{Mo}$  thin films are summarized in Table 3. It is observed that the both values of un-doped film are lower than the doped films with various Mo. This observation is not common to previous authors. When Mo content increases it may do not occupy proper lattice sites in the  $\text{In}_2\text{O}_3$  network. In addition, the ionic radius of In is bigger than that of Mo and some of these later may occupy interstitial positions which lead to the increase in the deformation in crystal structure by dispersion of impurities, defect, grain boundaries. All these occur when Mo concentrations increases. This latter lead to the decrease of the carriers' mobility in the  $\text{In}_2\text{O}_3:\text{Mo}$  thin films. Further, The decrease in the electrical resistivity may be due to the increase of the oxygen vacancies or the new phases of  $\text{MoO}_3$ . Generally, the electrical resistivity TCO can be decreased to cause the increase of oxygen vacancies [37].

## VI .4 Conclusion:

Through this study of un-doped , antimony doped indium oxide films and molybdenum doped indium oxide films deposited on glass substrates by spray ultrasonic, it is concluded that all the films exhibit polycrystalline nature with a change in the preferred orientation (222) for un-doped films to (400) with the adding antimony or molybdenum as dopant . Also, the crystallite size increases with the increase of sb doping concentration (2 to 6 wt.%) and decreases with the adding of Mo doping concentration (1 to 4 Wt.%) . The average optical transparency of all the films in visible spectra about 55-85 % with the interference fringes in the visible and near infrared regions in all films which are attributed to homogeneity of surface and thickness uniformity. The band gap ( $E_g$ ) increases from 3.64 eV for un-doped  $In_2O_3$  film to 4.11 eV for  $In_2O_3:Sb$  with increasing Sb concentration to 4 Wt.% Sb but with the increasing of Mo concentration which was decreased .The intensity of the PL emission peaks are decreased with the increase of quantum of Sb. The resistivity decreases with Mo doping as the resistivity and the mobility of the electrons decreases after the adding antimony concentrations. The two films deposited with 2 and 4 Wt % Sb have a minimum values of electrical resistivity and high optical transmittance (about 84%). According to these results, these two films can be developed as a capable material for a sensor element in sensing devices like acetone sensing devices and as various optoelectronic applications.

## References

- [1] Chopra KL, Major S, Pandya DK, Transparent conductors—a status review, *Thin Solid Films* 1983;102:1
- [2] Pankratz JM, Characteristics of  $\text{In}_2\text{O}_3:\text{Sn}$  films prepared by reactive rf sputtering, *J Electron Mater* 1972;1:182
- [3] N. Ito, Y. Sato, P.K. Song, A. Kaijio, K. Inoue, Y. Shigesato, Electrical and optical properties of amorphous indium zinc oxide films, *Thin Solid Films* 496(2006) 99–103.
- [4] A.V. Moholkar, S.M. Pawar, K.Y. Rajpure, V. Ganesan, C.H. Bhosale, Effect of precursor concentration on the properties of ITO thin films, *J. Alloys Compd.* 464 (2008) 387–392.
- [5] M.V. Vinokurova, L.E. Derlyukova, A.A. Vinokurov, Sorptive Properties of Antimony-Doped  $\text{In}_2\text{O}_3$ , *Inorganic Materials* 43 (2007) 1085–1092.
- [6] N.G. Pramod, S.N. Pandey, Influence of Sb doping on the structural, optical, electrical and acetone sensing properties of  $\text{In}_2\text{O}_3$  thin films, *Ceramics International* 40 (2014) 3461–3468
- [7] C. Manoharan , M. Jothibas , S. Johnson Jeyakumar , S. Dhanapandian , Structural, optical and electrical properties of Zr-doped  $\text{In}_2\text{O}_3$  thin films, *Spectrochimica Acta Part A: Molecular and Biomolecular Spectroscopy* 145 (2015) 47–53
- [8] K. Santhosh Kumar , C. Manoharan, S. Dhanapandian, A. Gowri Manohari, Effect of Sb dopant on the structural, optical and electrical properties of SnS thin films by spray pyrolysis technique, *Spectrochimica Acta Part A: Molecular and Biomolecular Spectroscopy* 115 (2013) 840–844
- [9] Nasreddine Beji , Mehdi Souli , Mejda Ajili , Sonia Azzaza , Safia Alleg , Najoua Kamoun Turki , Effect of iron doping on structural, optical and electrical properties of sprayed  $\text{In}_2\text{O}_3$  thin films, *Superlattices and Microstructures* 81 (2015) 114–128
- [10] M. Jothibas , C. Manoharan , S. Ramalingam , S. Dhanapandian , M. Bououdina , Spectroscopic analysis, structural, microstructural, optical and electrical

properties of Zn-doped  $\text{In}_2\text{O}_3$  thin films, *Spectrochimica Acta Part A: Molecular and Biomolecular Spectroscopy* 122 (2014) 171–178

[11] C.S. Prajapati , Ajay Kushwaha , P.P. Sahay , Effect of Al dopants on the structural, optical and gas sensing properties of spray-deposited ZnO thin films, *Materials Chemistry and Physics* 142 (2013) 276-285

[12] Sushant Gupta , B.C. Yadav , Prabhat K. Dwivedi , B. Das , Microstructural, optical and electrical investigations of Sb-SnO<sub>2</sub> thin films deposited by spray pyrolysis, *Materials Research Bulletin* 48 (2013) 3315–3322

[13] T. Minami, H. Nanto, S. Takata, Optical properties of aluminum doped zinc oxide thin films prepared by RF magnetron sputtering, *Jpn. J. Appl. Phys.* 24 (1985) L605–L607.

[14] S.Y. Lee, B.O. Park, Structural, electrical and optical characteristics of SnO<sub>2</sub>:Sb thin films by ultrasonic spray pyrolysis, *Thin Solid Films* 510 (2006) 154–158.

[15] D. Beena, K.J. Lethy, R. Vinodkumar, V.P. Mahadevan Pillai, V. Ganesan, D.M. Phase, S.K. Sudheer, *Applied Surface Science* 255 (2009) 8334–8342.

[16] A . Bouaoud , A. Rmili , F. Ouachtari , A. Louardi , T. Chtouki , B. Elidrissi , H. Erguig , Transparent conducting properties of Ni doped zinc oxide thin films prepared by a facile spray pyrolysis technique using perfume atomizer, *Materials Chemistry and Physics* 137 (2013) 843-847

[17] V. Baranauskas, M. Fontana, Z.J. Guo, H.J. Ceragioli, A.C. Peterlevitz, Field-emission properties of nanocrystalline tin oxide films , *Sens. Actuat. B Chem.* 107 (2005) 474.

[18] P. Manjula, L. Satyanarayana, Y. Swarnalatha, Sunkara V. Manorama, Raman and MASNMR studies to support the mechanism of low temperature hydrogen sensing by Pd doped mesoporous SnO<sub>2</sub>, *Sens. Actuat. B* 138 (2009) 28.

[19] S. Yang, L. Gao, Facile and Surfactant-Free Route to Nanocrystalline Mesoporous Tin Oxide ,*J. Am. Ceram. Soc.* 89 (5) (2006) 1742.

- [20] S.V. Stefanovsky, K.M. Fox, J.C. Marra, Infrared and Raman Spectroscopic Study of Glasses in the  $\text{Al}_2\text{O}_3\text{-B}_2\text{O}_3\text{-Fe}_2\text{O}_3\text{-Na}_2\text{O-SiO}_2$  System, Mater. Res. Soc. Symp. Proc.. 1518 (2013)53-58
- [21] Zhiwen Liang, Xiang Yu, Bingfu Lei, Pengyi Liu, Wenjie Mai, J. Alloy. Compd. 509 (2011) 5437–5440.
- [22] S. Kaleemulla, A. Sivasankar reddy, S. Uthanna, P. Sreedhara reddy, Optoelectron. Adv. Mater. – Rapid Commun. 2 (12) (2008) 782–787
- [23] H. Cao, X. Qiu, Y. Liang, Q. Zhu, M. Zhao, Room-temperature ultraviolet-emitting nanowires, Appl. Phys. Lett. 83 (2003) 761–763
- [24] D.J. Seo, S.H. Park, Structural, electrical and optical properties of  $\text{In}_2\text{O}_3$ : Mo films deposited by spray pyrolysis, Physica B 357 (2005) 420–427
- [25] S. Bansal, D.K. Pandya, S.C. Kashyap, D. Haranath, Growth ambient dependence of defects, structural disorder and photoluminescence in  $\text{SnO}_2$  films deposited by reactive magnetron sputtering, J. Alloys Compd. 583 (2014) 186–190
- [26] M. Fang, L. Zhang, X. Tan, X. Hu, W. Yan, P. Liu, Fabrication and photoluminescence property of  $\text{SnO}_2$  microtowers with interstitial tin ions, J. Phys. Chem. C 113 (2009) 9676–9680.
- [27] S. Kaleemulla , A. Sivasankar Reddy , S. Uthanna , P. Sreedhara Reddy , Room temperature photoluminescence property of Mo-doped  $\text{In}_2\text{O}_3$  thin films, Current Applied Physics 10 (2010) 386–390
- [28] Dong Ju Seo , Sun Hum Park, Structural, electrical and optical properties of  $\text{In}_2\text{O}_3$ :Mo films deposited by spray pyrolysis, Physica B 357 (2005) 420 – 427
- [29] E. Elangovan, S.A. Shivashankar, K. Ramanurthi, Studies on structural and electrical properties of sprayed  $\text{SnO}_2$ :Sb films , J. Cryst. Growth 276 (2005) 215
- [30] Caina Luan, Zhen Zhu, Wei Mi, Jin Ma , Effect of Sb doping on structural, electrical and optical properties of epitaxial  $\text{SnO}_2$  films grown on r-cut sapphire, Journal of Alloys and Compounds 586 (2014) 426–430

- [31] Powder Diffraction File 2005 JCPDS-International Centre for Diffraction Data-ICDD, Philadelphia, PA, Card 05-0508
- [32] R. D. Shannon (1976). "Revised effective ionic radii and systematic studies of interatomic distances in halides and chalcogenides". *Acta Cryst.* **A32**: 751–767.
- [33] S. Parthiban, V. Gokulakrishnan, K. Ramamurthi, E. Elangovan, R. Martins, E. Fortunato, R. Ganesan, *Sol. Energy Mater. Sol. Cells* 93 (2009) 92–97.
- [34] S Parthiban, E Elangovan, K Ramamurthi, D Kanjilal, K Asokan, R Martins and E Fortunato , Effect of  $\text{Li}^{3+}$  heavy ion irradiation on the Mo doped  $\text{In}_2\text{O}_3$  thin films prepared by spray pyrolysis technique, *J. Phys. D: Appl. Phys.* 44 (2011) 085404 (5pp)
- [35] Nasreddine Beji , Mehdi Souli , Mejda Ajili , Sonia Azzaza , Safia Alleg , Najoua Kamoun Turki , Effect of iron doping on structural, optical and electrical properties of sprayed  $\text{In}_2\text{O}_3$  thin films, *Superlattices and Microstructures* 81 (2015) 114–128
- [36] P.Thilakan, J.Kumar, Oxidation dependent crystallization behaviour of IO and ITO thin films deposited by reactive thermal deposition technique , *Materials Science and Engineering B. Vol.55*, (1998) 195–200
- [37] H.Y.Yeom, N. Popovich, E. Chason, D.C. Paine, A study of the effect of process oxygen on stress evolution in dc magnetron-deposited tin-doped indium oxide, *Thin Solid Films* 411 (2002) 17

# General conclusion

## General conclusion

In this thesis .We have reported the experimental results and the characterization of undoped and doped indium oxide thin films deposited by ultrasonic spray in order to explain and discuss the structural, electrical and optical properties of these oxide thin films with different parameter conditions ( flow rate , molar concentration, substrates type and the effect of doping) . These later are characterized by some techniques - X-ray diffraction, UV-visible spectrophotometry, FTIR , Photoluminescence and Four points - to be optimized for elaborating those films with good quality and competitive industry.

The experimental results and the characterization of undoped and doped indium oxide films are explained in the second part of the thesis so that , the results of undoped indium oxide films are presented in the chapters III ,IV and V with the influence of flow rate , concentration solution and substrates type respectively. Moreover, results of doped indium oxide films are presented in the chapter VI

The main results obtained during this study are as follows:

- For all parameters studies we found , that all the films obtained by D R X are polycrystalline with a a preferred growth orientation and changed between (222) and (400) orientations .
- **Influence growth rate (by changing the solution flow rate ):**
  - The crystallite size of the films slightly increases with the increase of growth rate where it is varied between 26 and 32 nm.
  - The average transmittance is about 80% in the visible region.
  - The optical band gap decreases with the increase of the growth rate from 3.93 to 3.62 eV.
  - The electrical resistivity decreases with the increase of the growth rate in the range of 20 - 5.5 ( $10^{-2}\Omega \text{ Cm}$  ).
- **Influence of indium acetate (various molar concentration):**
  - The grain size varied with different of molar concentration in the range 22.7 - 32.7 nm

- The average optical transmittance of the films varies between 73 and 87 % in the visible region .
- The optical band gap values decrease with the increasing of the molar concentration.
- The Fourier transform infrared (FTIR) spectrum indicated that these films are  $\text{In}_2\text{O}_3$  films.
- The low resistivity obtained at 0.1 M .
- **Influence of substrates type :**
  - The highest crystallite size was observed in the films (  $\text{In}_2\text{O}_3$  / Glass) and ( $\text{In}_2\text{O}_3$  / Si) but the smallest crystallite size watched in (  $\text{In}_2\text{O}_3$  /ITO) and ( $\text{In}_2\text{O}_3$  /Co. glass)
  - The higher transmission in the ITO substrate reaches up to 85% in the visible range with a gap's energy of 3.25 eV with a disorder value about 0.60 eV. The result of the ITO Substrate shows the best optical transmittance.
  - The resistivity of the  $\text{In}_2\text{O}_3$  films deposited on glass substrate is the arrange of [18.06  $\Omega$ .cm].
- **Influence of doping of indium oxide thin films.**
  - When we add antimony or molybdenum, the preferred orientation is changed due to the occupancy of the indium vacancy sites in the lattice by Sb or Mo atoms.
  - The lattice parameters calculated for un-doped  $\text{In}_2\text{O}_3$  thin films is 10.11  $\text{\AA}$ . It is good agreement with reported values of 10.11  $\text{\AA}$  for pure indium oxide .Nevertheless for doped  $\text{In}_2\text{O}_3$  thin films. It is decreased to be lower than the standard value that due to the difference between ionic radius.
  - The crystallite size increases with the increase of Sb doping concentration (2 to 6 wt.%) and it decreases with Mo doping concentration.
  - The resistivity and the mobility of the electrons decrease after adding antimony concentrations. The two films which deposited with 2 and 4 Wt % Sb have a minimum values of electrical resistivity and high optical transmittance (about 84%) and it is increasing with the adding Mo.

According to the results obtained during the various characterization carried out , we can say that optimal conditions of indium oxide film deposition which lead to obtain a material with good optoelectronic and photovoltaic properties are :

- flow rate is 40 or 50 ml / h ,
- The initial material is  $\text{InCl}_3$  with molar concentration is 0.1 mol/ L .
- Glass substrate and 2 or 4 wt.% Sb but with Mo dopant ; Unsatisfactory results that is common , in which we try to improve it , perhaps due to a change in the source of molybdenum and other factors, We will investigate in the coming research.

As conclusion, we can say that a continuation of this work is necessary and must be made to optimize the performance of this promising material, and to improve the properties of indium oxide thin films which are more suitable for application of optoelectronic, photovoltaic especially in a sensor element in sensing devices.

## Growth rate influence on indium oxide thin films grown by an ultrasonic spray technique

R. Azizi<sup>a</sup>, A. Attaf<sup>a</sup>, H. Saidi<sup>a</sup>, Y. Benkhetta<sup>a</sup>, I. B. Kherkhachi<sup>a</sup>, N. Attaf<sup>b</sup>, M. Dahnoun<sup>a</sup> and A. Bouhdjer<sup>a</sup>

<sup>a</sup> Physics of thin films and applications laboratory, University of biskra, BP 145 RP, 07000 Biskra, Algeria.

<sup>b</sup>Unité de Recherche "Sciences des Matériaux et Applications", Université Mentouri, Constantine, 25000, Algérie

e-mail address of the corresponding author: ab\_attaf@univ-biskra.dz

Received date: Feb. 20, 2019 ; accepted date: May 21, 2019

---

### Abstract

Indium oxide ( $\text{In}_2\text{O}_3$ ) thin films have been grown prosperously on glass substrates by an ultrasonic spray CVD process. The structural, morphological, optical and electrical studies of the films with controlled growth rate induced during elaboration by changing the solution flow rate from 20 to 60 mL/h. The X-ray diffraction (XRD) exhibit that the films are polycrystalline with centered cubic structure, whereas the predominant plane in the films change from (222) to (400) plane. The crystallite size of the films slightly increases with the increase of growth rate where it is varied between 26 and 32 nm. UV-Visible spectroscopy show that the average transmittance is about 80% in the visible region. The optical band gap decreases with an increase of the growth rate from 3.93 to 3.62 eV. Where the high value of band gap can be correlated with the preferential orientation of the (222) plane. The electrical resistivity decreases with the increase of the growth rate in the range of 20 - 5.5 ( $10^4 \Omega \text{ Cm}$ ). From these results we can say that the indium oxide thin films have a promising properties which make them applicable in the photovoltaic field.

**Keywords:** Thin films, Indium oxide, Ultrasonic Spray, Growth rate, Electrical properties.

---

**Abstract**

Our study talks about the deposition and characterization of the thin films of un-doped and doped indium oxide films obtained by ultrasonic spray technology with a view to obtaining suitable properties for optoelectronic applications, where:

Firstly, we have studied the un-doped indium oxide films with different parameters such as: flow rate solution, molar concentration solution and effect of substrates type.

Secondly, we have studied the effect of doping by antimony and molybdenum on indium oxide films, then we have characterized it by different techniques such as: X-RD, SEM, EDS analysis, UV spectroscopy, FTIR spectroscopy, luminous spectroscopy and Four-point technique. The main results obtained are:

Indium oxide crystallizes with polycrystalline structure by a cubic structure and it is a semiconductor of type n with a band gap  $E_g$ . It has a width between 3.25-4.1 eV for all the films which have a high transmittance up to 85% with disparate electrical conductivity, these properties are allowed to be used in many applications in the optoelectronic and photovoltaic fields.

**Keywords :** Thin films, Indium oxide, doping, Ultrasonic spray, Optoelectronic Properties.

**L'effet du dopage sur les propriétés couches minces d'oxyde d'indium ( $\text{In}_2\text{O}_3$ ) déposé par spray ultrasonique en vue d'applications optoélectronique**

**Résumé**

Notre étude a porté sur la déposition et la caractérisation des films minces de d'oxyde d'indium non dopés et dopés obtenus par technologie de spray ultrasonique en vue d'obtenir des propriétés adaptées aux applications optoélectroniques, où:

Premièrement, nous avons étudié les films d'oxyde d'indium non dopés avec différents paramètres tels que: débit de la solution, concentration molaire de la solution et effet du type de substrats.

Deuxièmement, nous avons étudié l'effet du dopage par l'antimoine et le molybdène sur l'oxyde d'indium, puis nous l'avons caractérisé par différentes techniques telles que: DRX, MEB, EDS, spectroscopie UV, spectroscopie FTIR, spectroscopie lumineuse et technique à quatre points. Les principaux résultats obtenus sont:

L'oxyde d'indium cristallise avec une structure polycrystalline par une structure cubique et c'est un semi-conducteur de type n avec une bande interdite  $E_g$ . Il a une largeur entre 3,25-4,1 eV pour tous les films qui ont une transmittance élevée jusqu'à 85% avec une conductivité électrique disparate, ces propriétés peuvent être utilisées dans de nombreuses applications dans les domaines optoélectroniques et photovoltaïques.

**Mots-clés :** Couches minces, L'oxyde d'indium, dopage, Spray ultrasonique, Les propriétés optoélectroniques.

**تأثير التطعيم على خصائص الشرائح الرقيقة لأكسيد الإنديوم المحضرة بواسطة الرش فوق صوتي للتطبيقات الالكتروضوئية ملخص**

تمحور دراستنا حول ترسيب و تشخيص الطبقات الرقيقة لأكسيد الإنديوم غير المطعم والمطعم المتحصل عليها بواسطة تقنية الرش فوق صوتي بهدف الحصول على خصائص مناسبة للتطبيق الالكتروضوئي حيث :

أولاً ، قمنا بدراسة الطبقات الرقيقة لأكسيد الإنديوم غير المطعم و ذلك بوساطة مختلفة مثل : نسبة تدفق المحلول ، التركيز المولي للمحلول و تأثير الركائز . ثانياً، قمنا بدراسة تأثير التطعيم بواسطة الأنتيمون و الموليبيديوم على أكسيد الإنديوم ، بعد ذلك قمنا بتشخيصها بواسطة تقنيات مختلفة مثل : انعراج الاشعة السينية ، المجهر الالكتروني الماسح ، التحليل الكيميائي ، المطيافية فوق البنفسجية و المرئية ، مطيافية تحويل الأشعة تحت الحمراء ، مطيافية المعان الضوئي و تقنية أربع نقاط. وكانت أهم النتائج المتحصل عليها :

يتبلور أكسيد الإنديوم ببنية متعددة البلورات ذو هيكل مكعب و هو نصف ناقل من نوع n له نطاق ممنوع  $E_g$  ذو عرض يتراوح بين 3.25-4.1 eV لجميع العينات التي تتمتع بنفاذية عالية تصل الى 85% مع ناقلية كهربائية متفاوتة و هذه الخصائص يُسمح باستخدامها في تطبيقات عديدة في المجالات الكهروضوئية و الالكتروضوئية .

**الكلمات المفتاحية :** الأغشية الرقيقة ، أكسيد الإنديوم ، التطعيم ، الرش بالموجات فوق الصوتية ، الخصائص الإلكترونية البصرية.